

AUG 25 1947



# RESEARCH MEMORANDUM

HIGH-SPEED LOAD DISTRIBUTION ON THE WING OF A  
3/16-SCALE MODEL OF A SCOUT-BOMBER  
AIRPLANE WITH FLAPS DEFLECTED

By

Robert H. Barnes

Ames Aeronautical Laboratory  
Moffett Field, Calif.

NATIONAL ADVISORY COMMITTEE  
FOR AERONAUTICS

WASHINGTON

August 21, 1947

N A C A LIBRARY  
LANGLEY MEMORIAL AERONAUTICAL  
LABORATORY  
Langley Field, Va.



## NATIONAL ADVISORY COMMITTEE FOR AERONAUTICS

RESEARCH MEMORANDUMHIGH-SPEED LOAD DISTRIBUTION ON THE WING OF A  
3/16-SCALE MODEL OF A SCOUT-BOMBER  
AIRPLANE WITH FLAPS DEFLECTED

By Robert H. Barnes

## SUMMARY

The tests reported herein were made for the purpose of determining the high-speed load distribution on the wing of a 3/16-scale model of a scout-bomber airplane. Comparisons are made between the root bending-moment and section torsional-moment coefficients as obtained experimentally and derived analytically. The results show good correlation for the bending-moment coefficients but considerable disagreement for the torsional-moment coefficients, the measured moments being greater than the analytical moments. The effects of Mach number on both the bending-moment and torsional-moment coefficients were small.

## INTRODUCTION

In order to determine the spanwise loading at high speeds with landing flaps deflected, a series of tests of a 3/16-scale model of a scout-bomber airplane was made in the Ames 16-foot high-speed wind tunnel at the request of the Bureau of Aeronautics, Navy Department.

In order to compare the experimental results with those that would be calculated according to current design specifications, the spanwise load distribution was calculated by the method of reference 1.

## MODEL AND APPARATUS

A three-view drawing of the airplane is given in figure 1. The wing of the model was equipped with plain flaps having a chord of 0.21 times the wing chord. The geometry of the flaps is given in figure 2. Pressure orifices were provided at seven spanwise stations as shown in figure 3. At

each of these stations there were 45 orifices spaced at intervals of 5 percent of the chord except on the forward 10 percent where the spacing was closer.

The airfoil section at wing station 40.102, the coordinates of which are given in table I, is a modified NACA 65-series section. The section at the point of dihedral reversal is an NACA 65,2-2518,  $a = 0.5$ ,  $b = 1$  section, and at the tip the section is an NACA 65,2-2515,  $a = 0.5$ ,  $b = 1$  section.

The model was mounted on the three-strut support system shown in figure 4. The front struts were 5 percent thick; the rear strut was 7 percent thick.

Forces were measured by automatic balancing scales. The pressures were measured on multiple-tube manometers, the data being recorded photographically. Tests were made with the flaps deflected  $0^\circ$ ,  $10^\circ$ , and  $40^\circ$ . The Mach number range of the tests was 0.296 to 0.778.

#### COEFFICIENTS AND SYMBOLS

The following standard NACA coefficients and symbols are used in this report:

$C_L$	lift coefficient ( $L/qS$ )
$C_N$	normal-force coefficient ( $N/qS$ )
$c_l$	section lift coefficient ( $l/qc$ )
$c_n$	section normal-force coefficient ( $n/qc$ )
$c_m$	section pitching-moment coefficient ( $m/qc^2$ )
$L$	lift, pounds
$N$	normal force, pounds
$l$	section lift, pounds per foot
$n$	section normal force, pounds per foot
$m$	section pitching moment, foot-pounds per foot
$S$	wing area, square feet
$q$	dynamic pressure ( $\frac{1}{2}\rho V^2$ ), pounds per square foot
$\rho$	mass density, slugs per cubic foot
$V$	velocity, feet per second

c	section chord, feet
$\alpha_u$	uncorrected angle of attack, degrees
$\alpha$	angle of attack, degrees
x	distance along chord from leading edge, feet
y	spanwise distance from center of model, feet
b	span, feet
M	Mach number
P	pressure coefficient ( $\frac{p_l - p}{q}$ )
$p_l$	local static pressure, pounds per square foot
p	free-stream static pressure, pounds per square foot

In addition to the standard NACA coefficients and symbols the following are used:

$C_{BM}$	root bending-moment coefficient ( $BM/qb^2C_S$ )
BM	root bending moment ( $q \int_0^{b/2} c_n c_y dy$ ), foot-pounds
$C_S$	root chord, feet
$C_{TM}$	root torsional-moment coefficient ( $TM/q\bar{c}^2b$ )
TM	root torsional moment ( $q \int_0^{b/2} c_m dy$ ), foot-pounds
$\bar{c}$	mean aerodynamic chord, feet

The lift coefficients used in this report are those for the standard model less tail as shown in figure 4.

#### REDUCTION AND PRESENTATION OF DATA

The data were corrected for tunnel-wall effects by the method of reference 2. Corrections were also made to account for the constriction and the upflow of the air stream.

Typical chordwise pressure distributions which show the effects of angle of attack, Mach number, and landing-flap deflection are shown in figures 5, 6, and 7, respectively.

The section normal-force and pitching-moment coefficients

were obtained by integration of the pressure distributions. The axis for the pitching-moment coefficient at each station is a line normal to the center line of the model and passing through the quarter-chord point of the M.A.C. It should be noted that no consideration was taken of the chordwise component of the pressure coefficient in obtaining the pitching-moment coefficient. These coefficients were then plotted against the model lift coefficient existing when the data were taken as found in figure 8. Figures 9 to 15 show the variations at each pressure station of the section normal-force coefficient with model lift coefficient, and figures 16 to 22 show the variations of section pitching-moment coefficient with model lift coefficient.

The product of the section normal-force coefficient times the section chord is an index of the section normal-force loading and so in order to present the spanwise variations of this loading the product  $c_{n1}$  was plotted against span. Figures 23, 24, and 25 show these variations for the three flap deflections tested. Integration of these plots yielded the total normal-force coefficients and the corresponding root bending-moment coefficients which are plotted against lift coefficient in figures 26 and 27, respectively.

In a similar manner the product of the section pitching-moment coefficient times the square of the section chord ( $c^2 c_m$ ) is an index of the torsional-moment loading. From integration of spanwise plots of this quantity the root torsional-moment coefficients were obtained. They are plotted against lift coefficient in figure 28.

Figures 29, 30, and 31 present comparisons of the experimental and analytical values of root bending-moment coefficient for flap deflections of  $0^\circ$ ,  $10^\circ$ , and  $40^\circ$ , respectively.

Figures 32, 33, and 34 show a similar comparison for the section pitching-moment coefficient.

Figures 35, 36, and 37 present some typical spanwise normal-force distributions showing effects of Mach number and flap deflection, and a comparison of experimental and analytical results.

#### ANALYTICAL CALCULATIONS

Calculations were made by the method of reference 3 of the chordwise pressure distribution at station 140 for the three flap deflections tested. Station 140 was chosen since it was on the outboard panel of the wing where the sections are

standard NACA sections for which necessary basic characteristics are known. Also this position was felt to be the best compromise to avoid flow effects due to dihedral reversal, support struts, and wing tips.

Calculations were also made of the spanwise normal-force distribution for the three flap deflections by the method of reference 1. In order to use this method it is necessary to know, among other things, the profile-drag coefficient and the angle of zero lift of the wing. The profile-drag coefficients with flaps deflected were obtained by adding increments of coefficients taken from figure 66 of reference 4 to the value of the profile-drag coefficient of the wing with flaps neutral. The angle of attack for zero lift was obtained from the force data for Mach number of 0.296 by extrapolating the curves of figure 8 to zero lift coefficient.

The spanwise load distributions so obtained were integrated to obtain the wing normal-force coefficient and the corresponding root bending-moment coefficient.

No calculation was made of the analytical root torsional-moment coefficient since it would involve calculating the chordwise pressure distribution at each station, and it was felt that the comparison of the analytical and experimental characteristics at one station indicates what can be expected for the entire wing.

## DISCUSSION

### Wind-Tunnel Data

There are no unusual effects of angle of attack upon the pressure distribution. (See fig. 5.) However, it should be noted that, contrary to what is considered normal, the local pressure coefficients over the forward 10 percent of the wing decrease as the Mach number increases. Data not presented herein for the other pressure stations show the same tendency in varying degrees.

Figure 23 shows that with the flaps neutral, separation and loss of lift at the point of dihedral reversal begins to occur at about 0.6 Mach number for a lift coefficient of 0.8, the largest for which data are presented. When the Mach number is increased to 0.73, this phenomenon is seen to occur throughout the range of lift coefficients tested. However, as the Mach number is further increased to 0.778 the local lift losses extend over the adjacent portions of the wing, as evidenced by the flattening of the load distribution.

curves for constant lift coefficient. (See figs. 23(f) and 23(g).) This effect is probably due to the shock occurring on the adjacent portions of the wing.

If the flaps are deflected  $10^\circ$  or  $40^\circ$  the pattern of events is similar to that previously described except that at the maximum Mach number of the tests there is no spreading of the local lift losses.

The following table summarizes the results:

Flap Deflection	Mach number at which separation is first noted at $C_L = 0.8$	Mach number at which separation is noted for all positive $C_L$ 's tested
$0^\circ$	0.591	0.73
$10^\circ$	.591	.685
$40^\circ$	.638	.778

Figure 28 indicates that the root torsional-moment coefficient remains practically constant for all positive lift coefficients up to 0.8. This is especially true at Mach numbers less than 0.685. It is to be noted also that the coefficients for each flap deflection remain approximately constant for all the test Mach numbers.

#### Comparison of Experimental and Analytical Results

The comparisons given in figures 29, 30, and 31 show that the calculated and experimental root bending-moment coefficients are in good agreement and in some cases in practically exact agreement.

Figures 32, 33, and 34 show that the experimental section pitching-moment coefficients are more negative than the analytical values. That is, the analytical method underestimates the loads. It will be seen that the amount of error is approximately constant at each Mach number and tends to increase with Mach number. Also, the percentage error based on the analytical value is greatest for the condition of flaps neutral or deflected  $40^\circ$  and least with flaps deflected  $10^\circ$ . For example, with neutral flaps the error varies from 30 percent at 0.296 Mach number to 100 percent at 0.778 Mach number. Also,

at 0.296 Mach number the error is 30 percent with neutral flaps, 19 percent with flaps deflected 10°, and 30 percent with flaps deflected 40°.

#### CONCLUDING REMARKS

It has been seen that the dihedral reversal of the wing affects the spanwise normal-force distribution. Therefore, the results of these tests should be considered applicable only to similar wings.

The correlation between experimental and analytical variation of root bending-moment coefficient with wing normal-force coefficient is good.

The root torsional-moment coefficient for each flap deflection remains approximately constant throughout the lift-coefficient and Mach number range of the tests.

The experimental value of the section pitching-moment coefficient was in all cases greater than the analytical value. The discrepancy varied from 20 to 100 percent of the analytical value.

Ames Aeronautical Laboratory,  
National Advisory Committee for Aeronautics,  
Moffett Field, Calif.

#### REFERENCES

1. Anon: Spanwise Air-Load Distribution, ANC-1(1). Army-Navy-Commerce Committee on Aircraft Requirements. April 1938.
2. Silverstein, Abe and White, James A.: Wind-Tunnel Interference with Particular Reference to Off-Center Positions of the Wing and to the Downwash at the Tail. NACA Rep. No. 547, 1935.
3. Anon: Chordwise Air-Load Distribution, ANC-1(2). Army-Navy-Commerce Committee on Aircraft Requirements. Oct. 28, 1942.
4. Diehl, Walter Stuart: Engineering Aerodynamics. The Ronald Press Co., N.Y. 1936.

TABLE I  
ORDINATES FOR STATION 40.102

STATION	UPPER SURFACE	LOWER SURFACE
0	0	0
1.25	2.530	-2.123
2.5	3.527	-2.874
5	4.912	-3.947
7.5	5.92	-4.72
10	6.74	-5.36
15	8.07	-6.37
20	9.05	-7.06
30	10.08	-7.68
40	10.34	-7.68
50	9.935	-7.165
60	8.67	-6.01
70	6.72	-4.355
80	4.33	-2.424
90	1.78	- .837
95	.665	- .300
100	0	0

ALL COORDINATES ARE IN PERCENT CHORD

Fig. 1

NACA RM No. A7D23

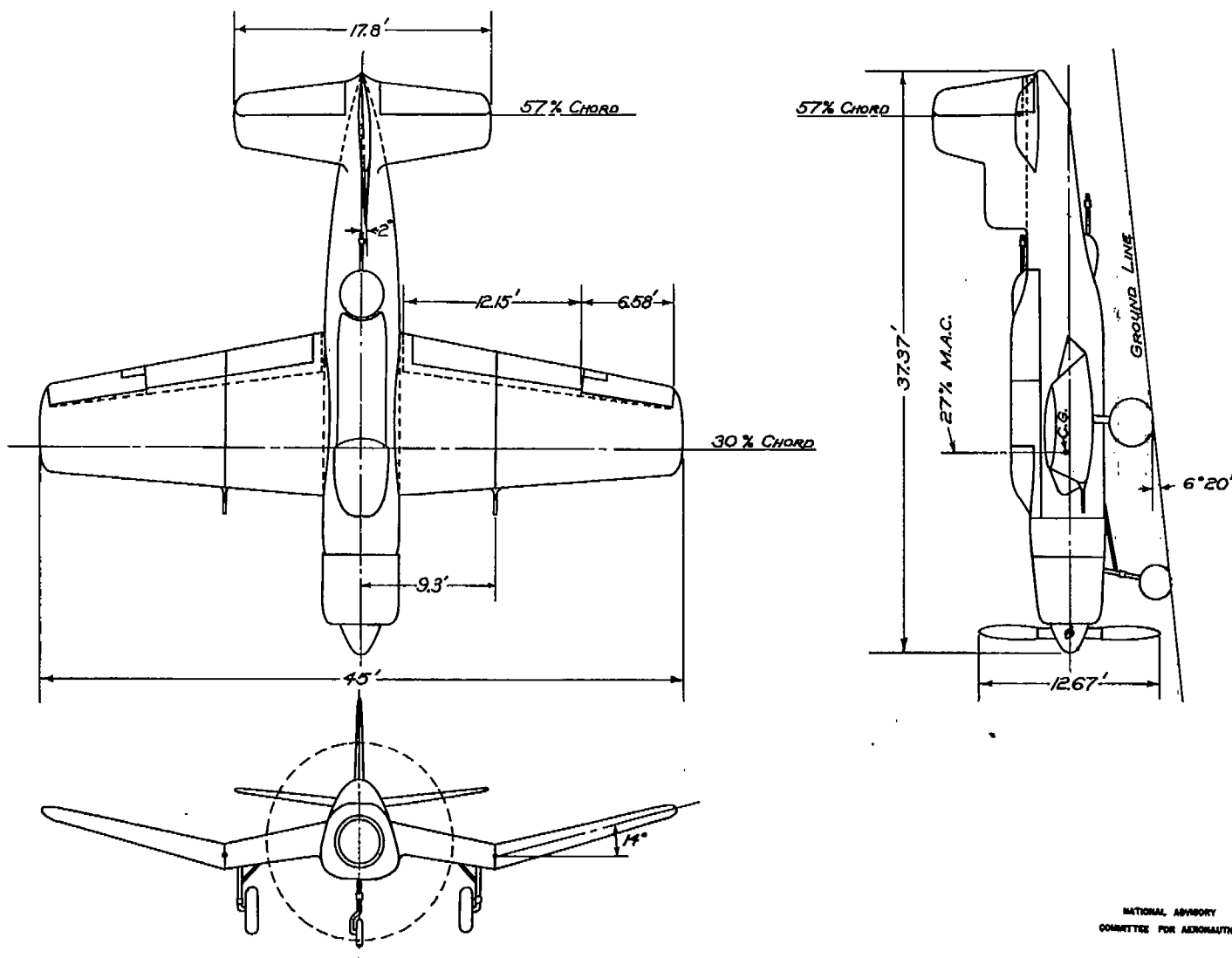
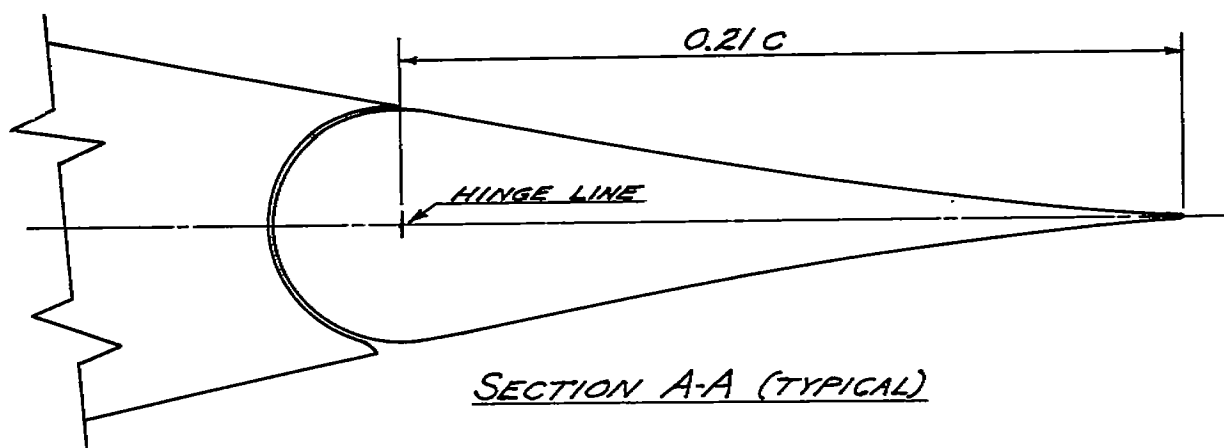
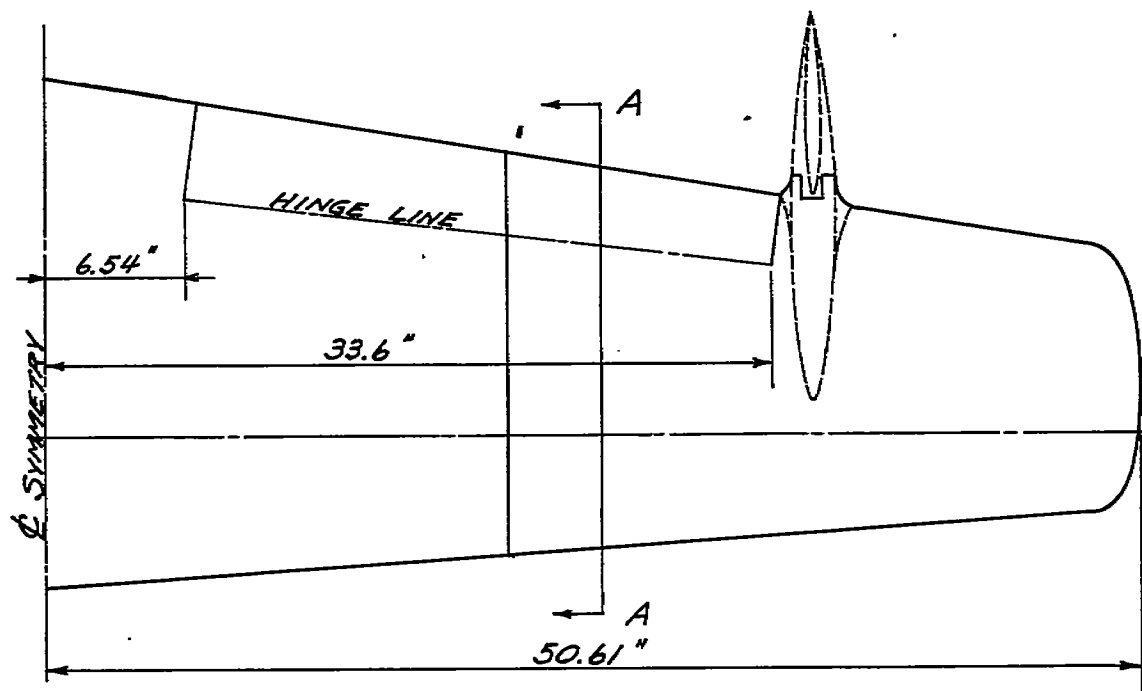


FIGURE 1. THREE VIEW DRAWING OF THE SCOUT-BOMBER AIRPLANE.

NATIONAL ADVISORY  
COMMITTEE FOR AERONAUTICS



NATIONAL ADVISORY  
COMMITTEE FOR AERONAUTICS

FIGURE 2.- GEOMETRY OF THE LANDING FLAPS ON THE MODEL.

Fig. 3

NACA RM No. A7D23

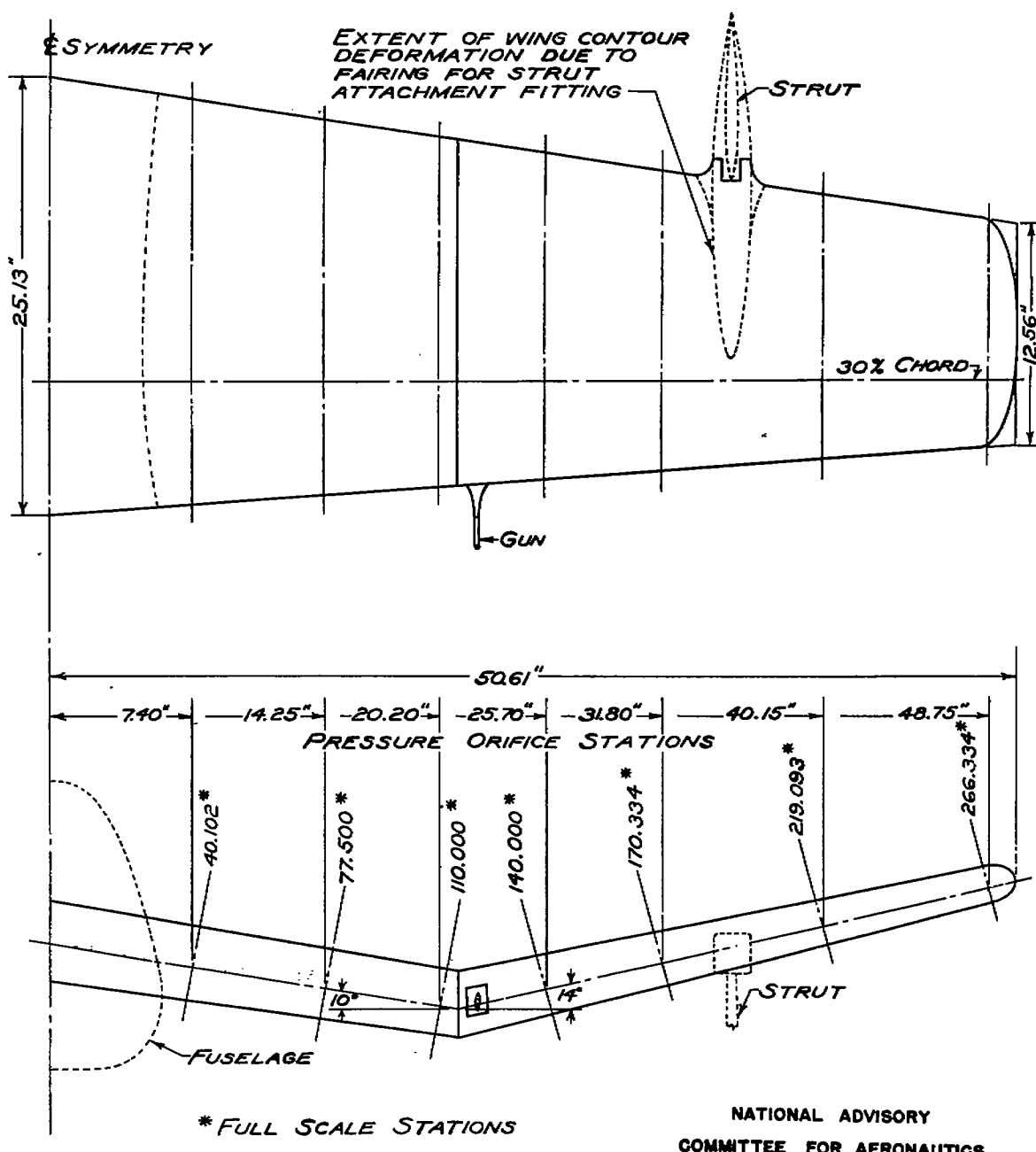


FIGURE 3. - WING GEOMETRY AND PRESSURE ORIFICE STATIONS.

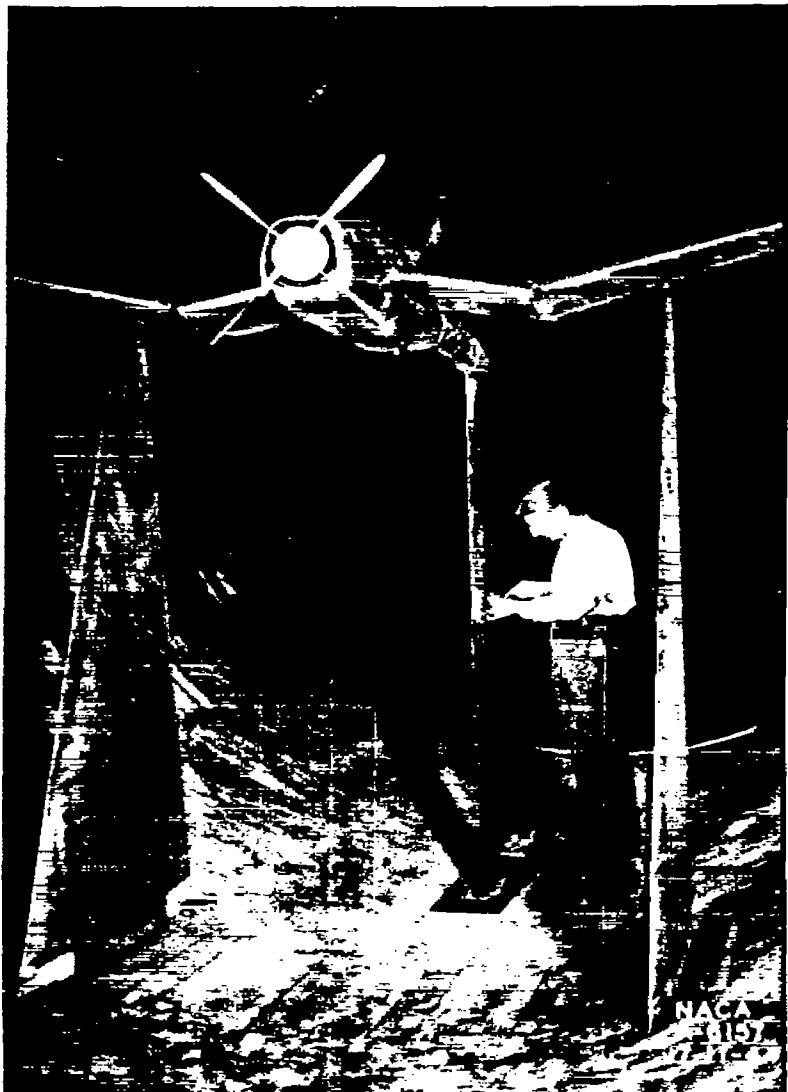


Figure 4.- The model mounted in the 16-foot wind tunnel. For these tests the propeller was replaced by a dummy spinner.

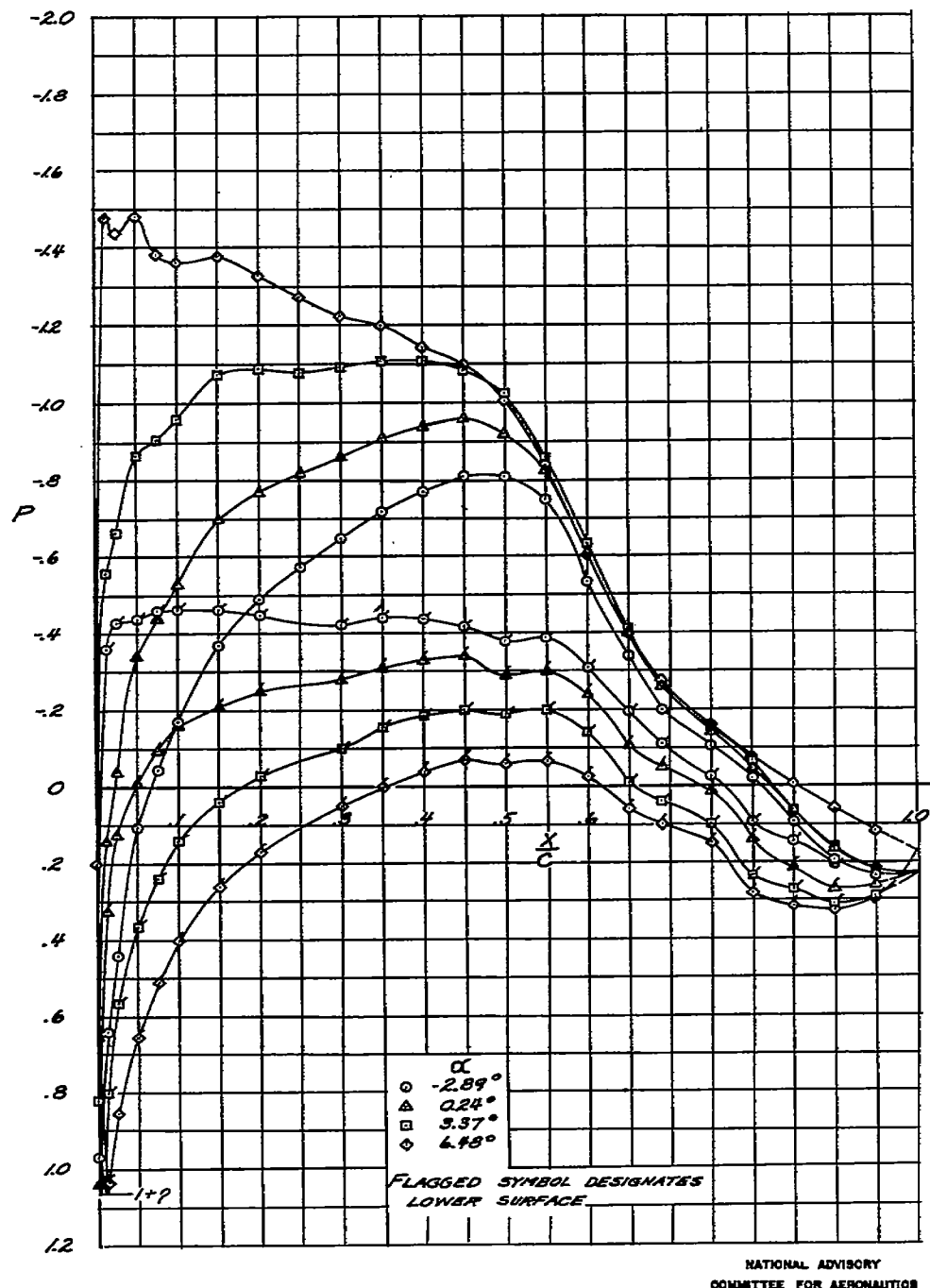


FIGURE 5.—EFFECTS OF ANGLE OF ATTACK ON THE CHORDWISE PRESSURE DISTRIBUTION AT STATION 140,000 WITH FLAPS NEUTRAL.  $M = 0.494$

Fig. 6

NACA RM No. A7D23

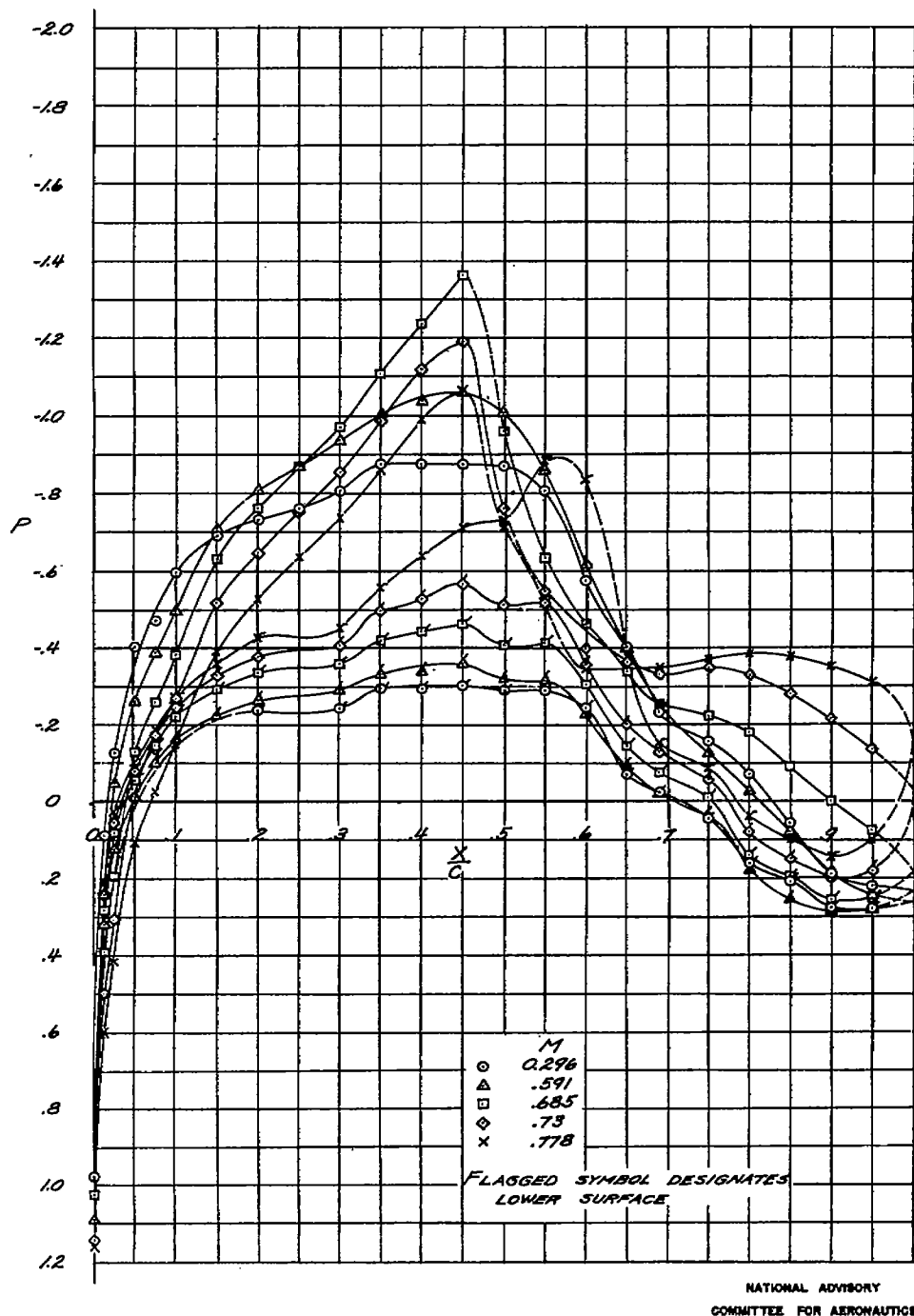


FIGURE 6.-EFFECTS OF MACH NUMBER ON THE CHORDWISE PRESSURE DISTRIBUTION AT STATION 140,000 WITH FLAPS NEUTRAL.  $\alpha = 0.2$

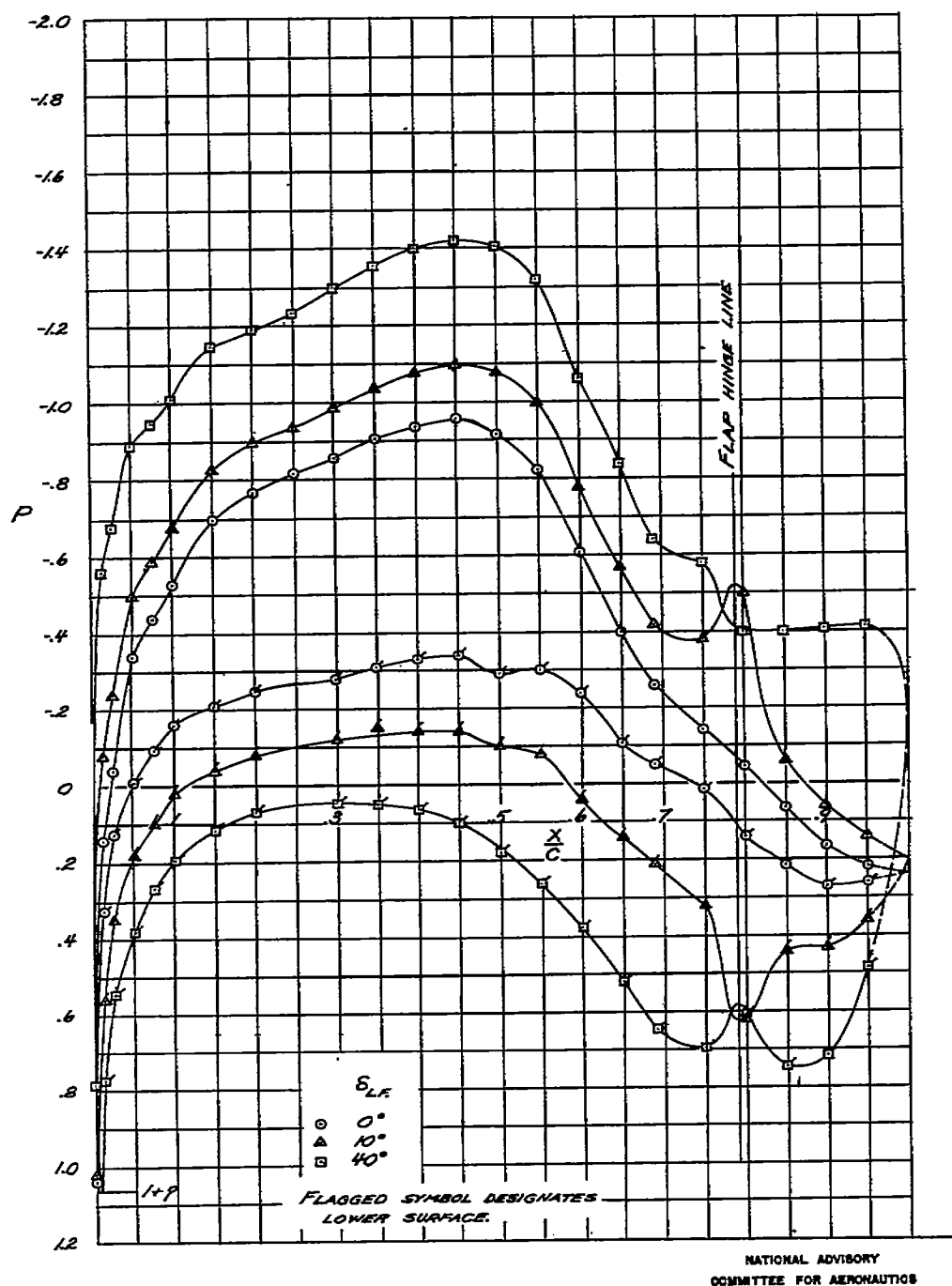
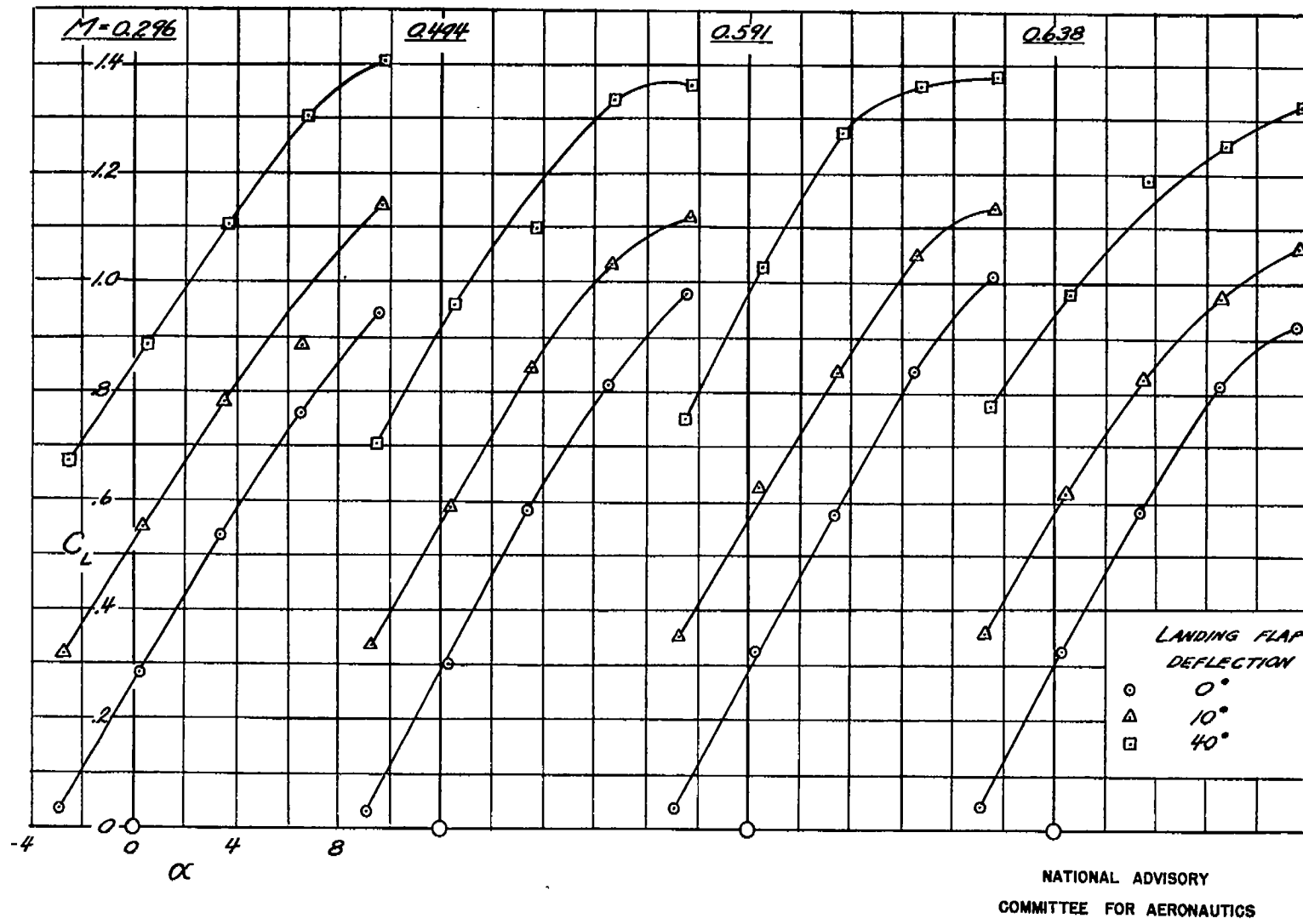


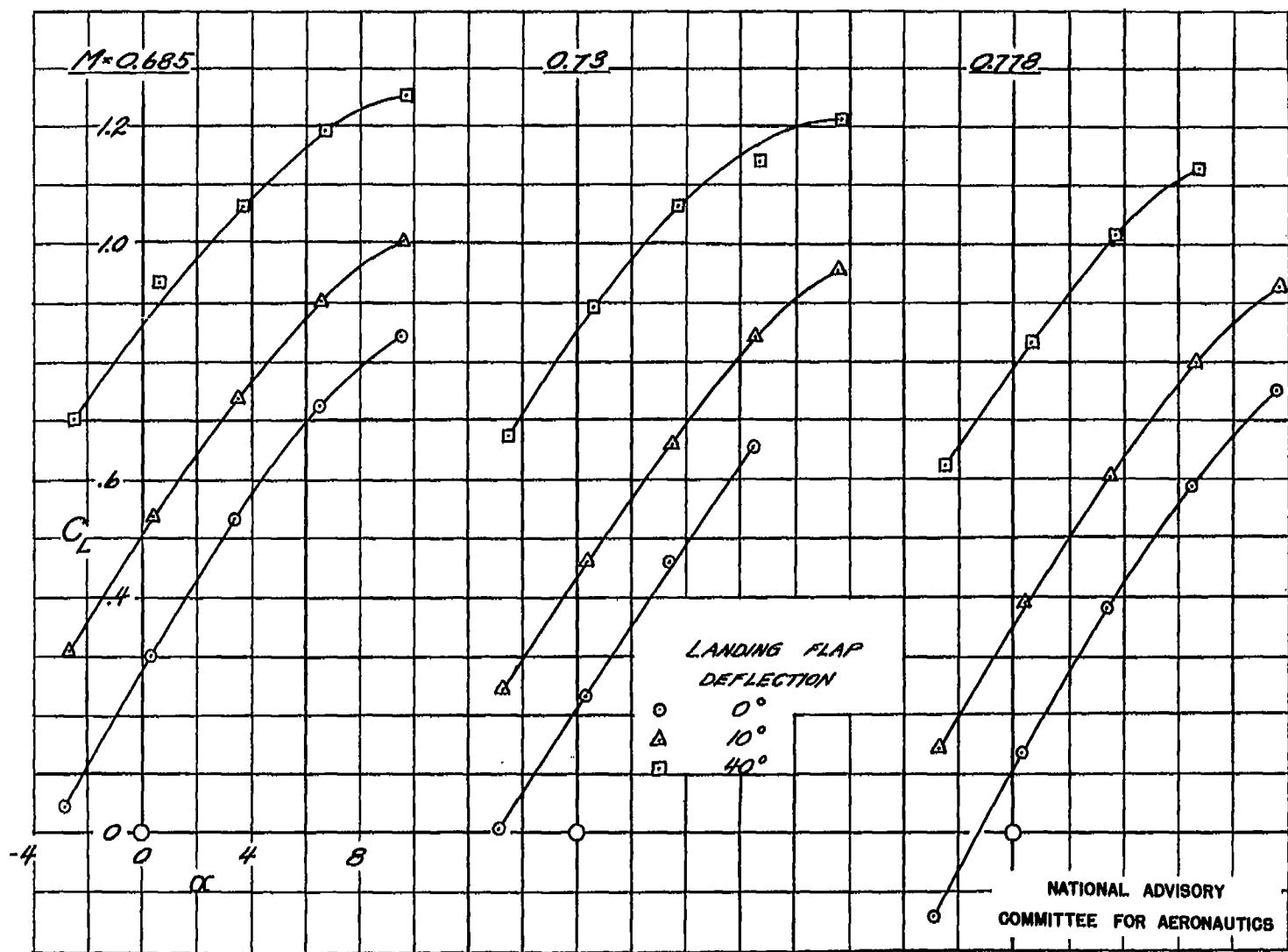
FIGURE 7.-EFFECTS OF FLAP DEFLECTION ON THE CHORDWISE PRESSURE DISTRIBUTION AT STATION 140,000.  $M=0.494$ ;  $\alpha_0 = 0^\circ$

Fig. 8a

NACA RM No. A7D23



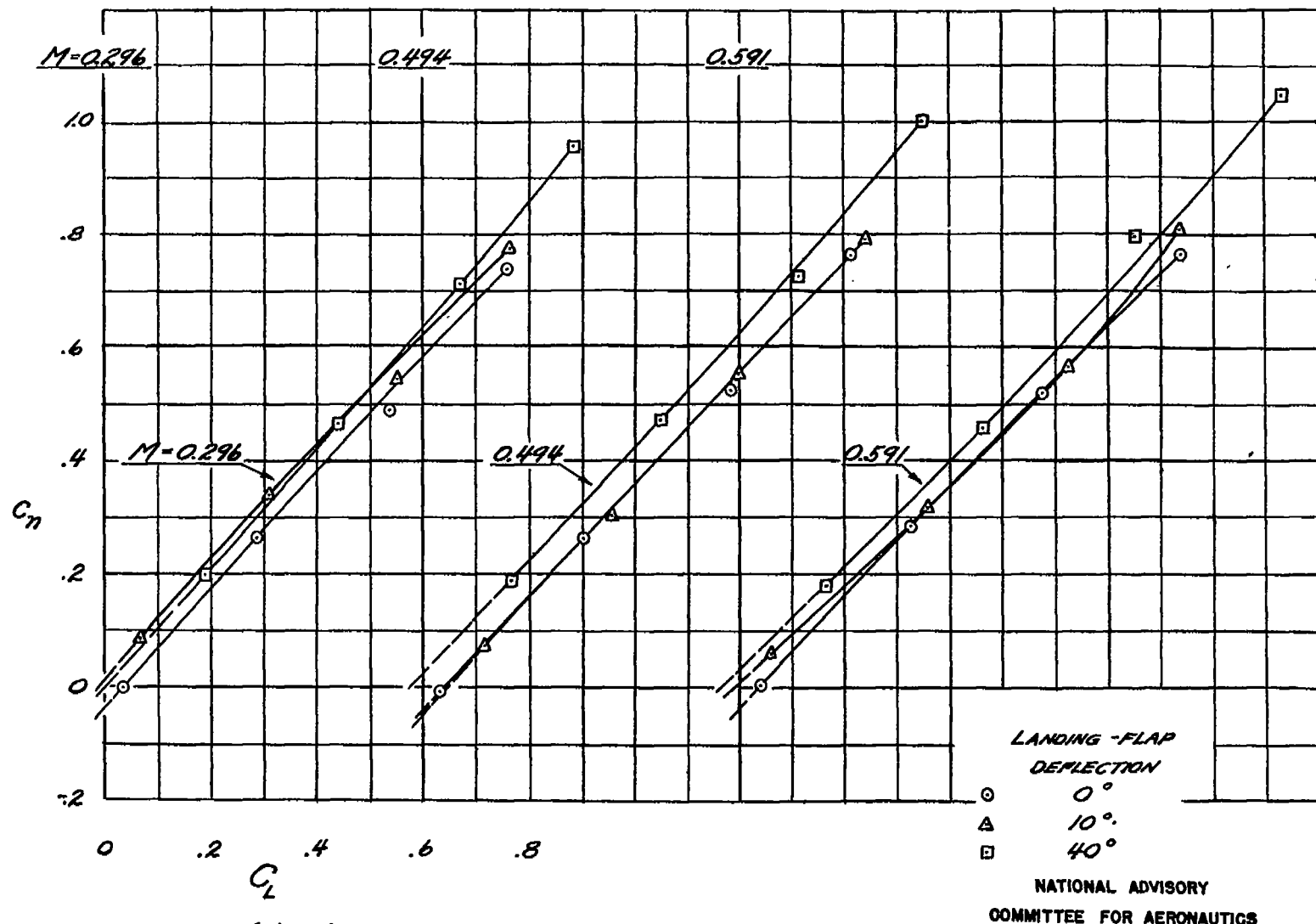
(a)  $M = 0.296, 0.494, 0.591$ , AND  $0.638$   
 FIGURE 8.- VARIATION OF THE LIFT COEFFICIENT WITH ANGLE OF ATTACK AT  
 SEVERAL MACH NUMBERS. TAIL OFF.



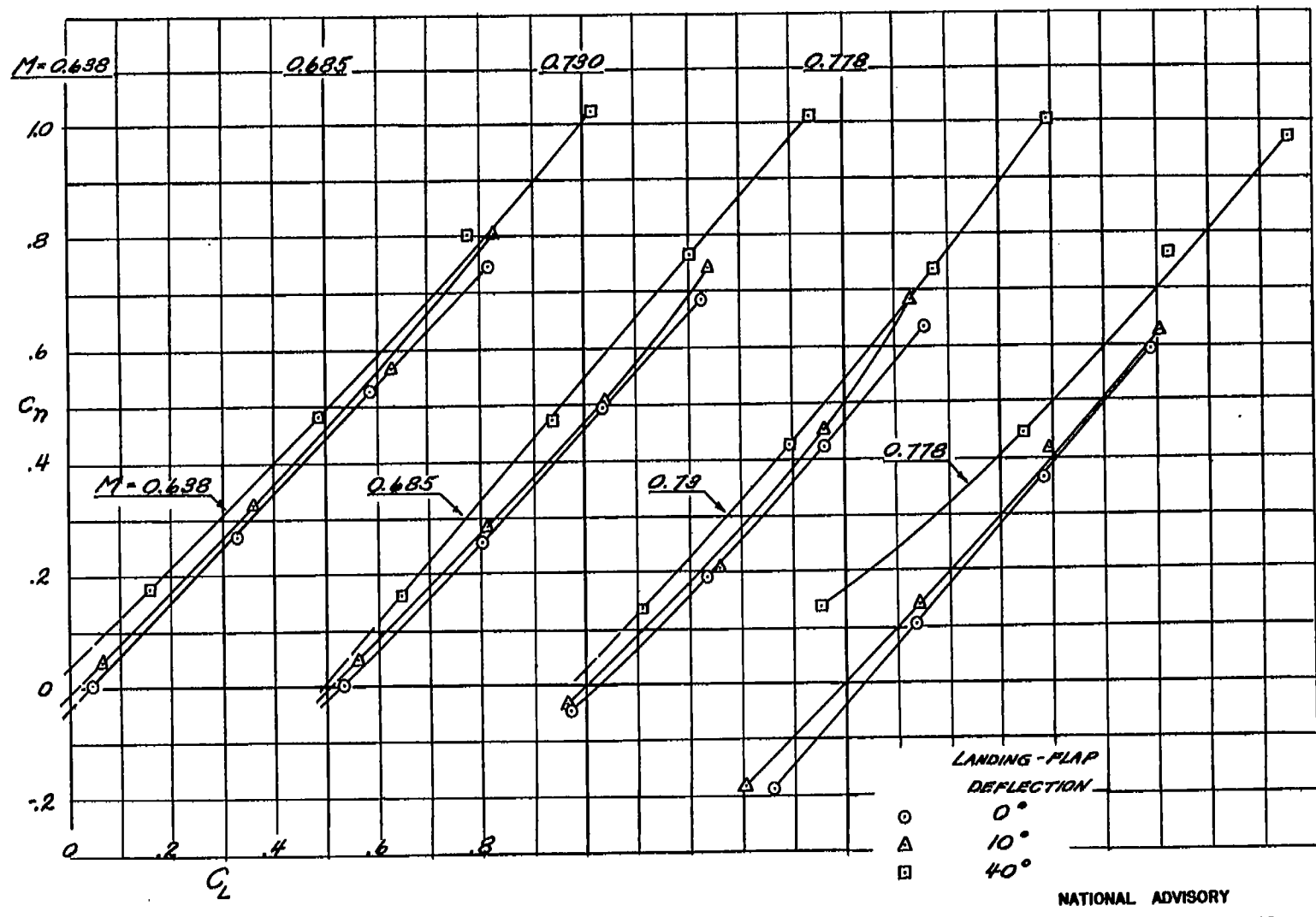
(b)  $M = 0.685, 0.73$ , AND  $0.778$   
FIGURE 8.- CONCLUDED

Fig. 9a

NACA RM NO. ATD23



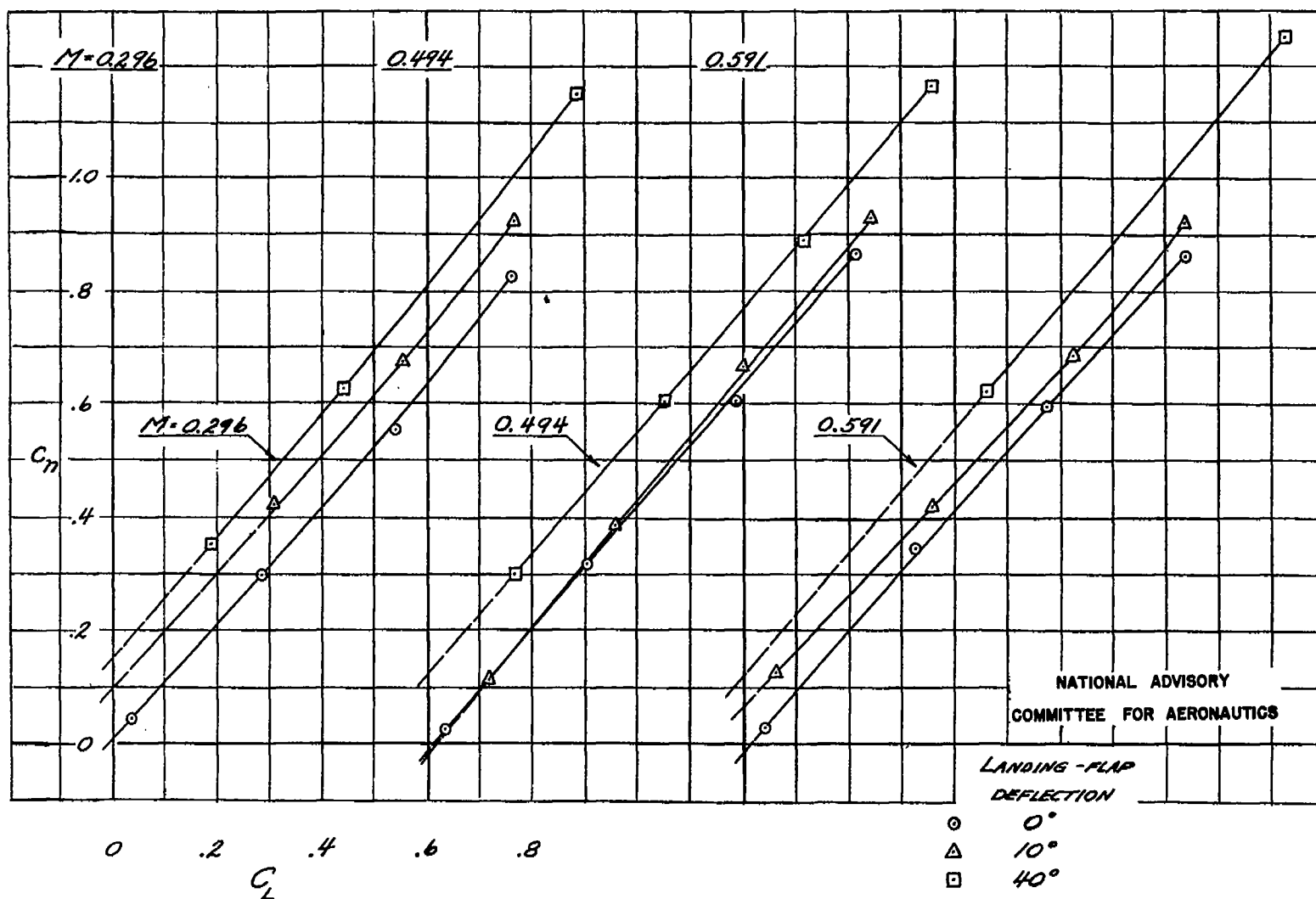
(a)  $M = 0.296, 0.494$ , AND  $0.591$   
 FIGURE 9.- VARIATION OF THE SECTION NORMAL-FORCE COEFFICIENT AT STATION 40.102 WITH TAIL-OFF LIFT COEFFICIENT.



(b)  $M = 0.638, 0.685, 0.730,$  AND  $0.778$   
FIGURE 9.- CONCLUDED

Fig. 10a

NACA RM No. A7D23

(a)  $M = 0.296, 0.494$ , AND  $0.591$ FIGURE 10.- VARIATION OF THE SECTION NORMAL-FORCE COEFFICIENT AT STATION 77.500  
WITH TAIL-OFF LIFT COEFFICIENT.

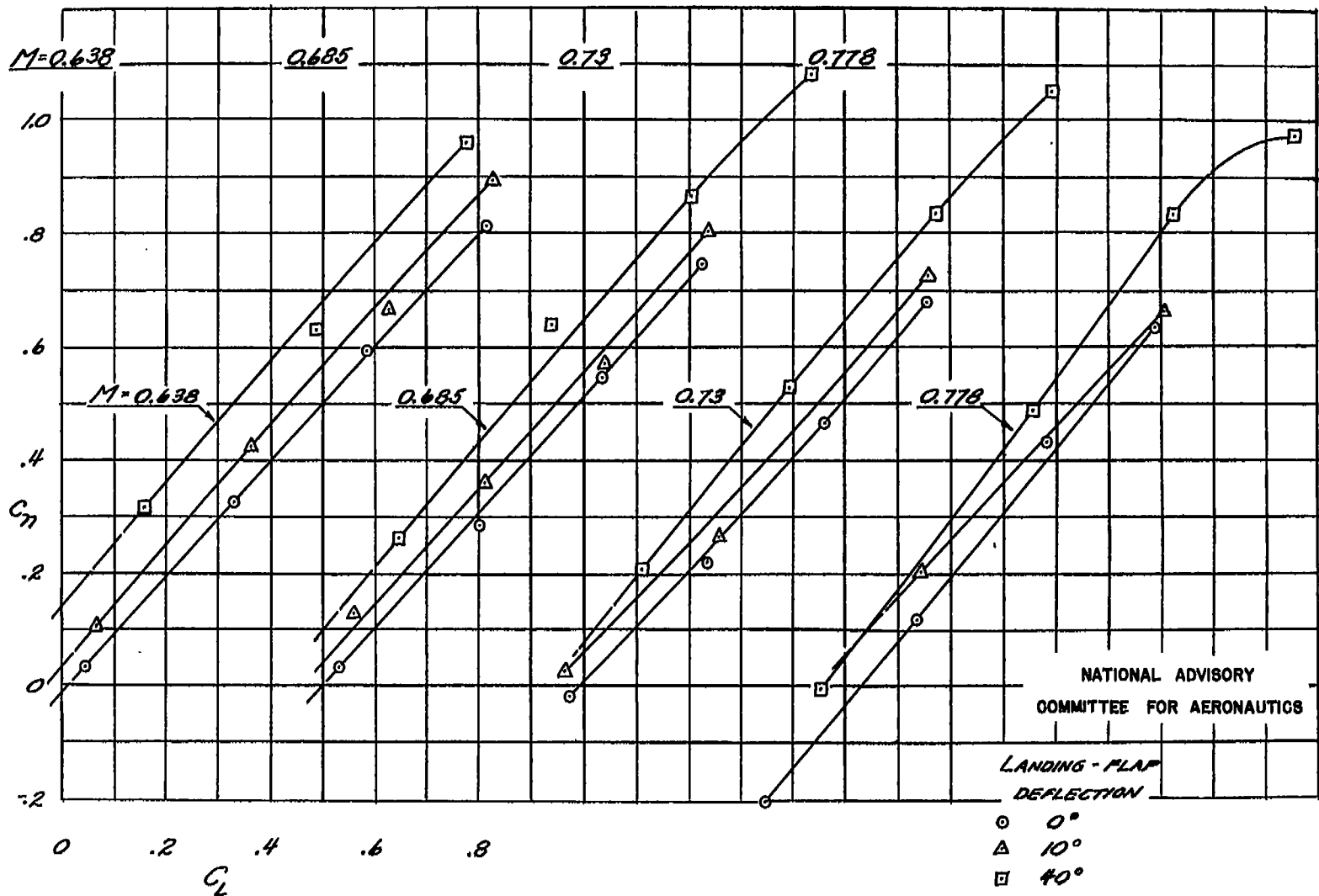
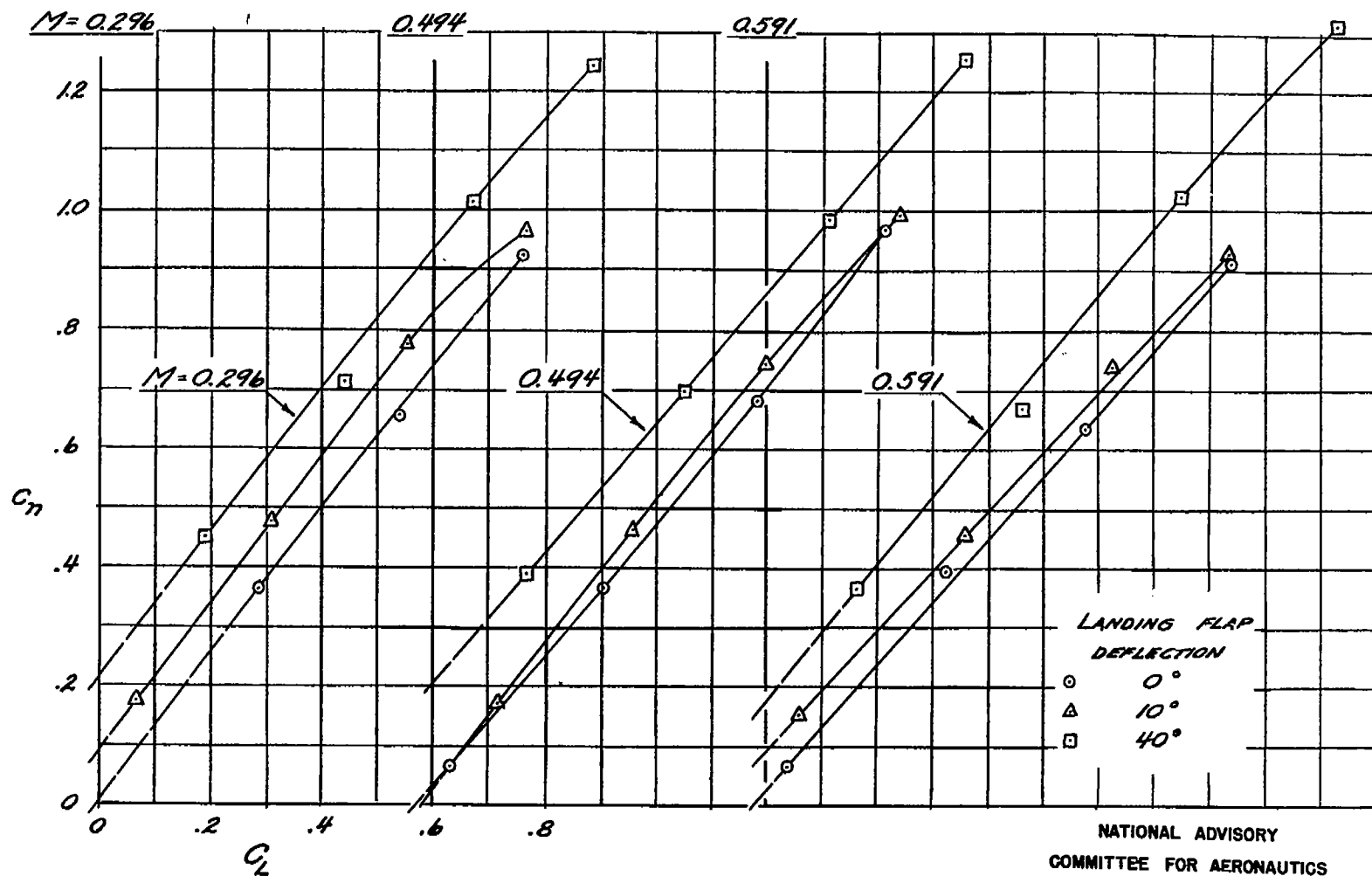
(B)  $M = 0.638, 0.685, 0.73$ , AND  $0.778$ 

FIGURE 10. - CONCLUDED

Fig. 11a

NACA RM No. A7D23



(a)  $M=0.296$ ,  $0.494$ , AND  $0.591$   
 FIGURE 11.- VARIATION OF THE SECTION NORMAL-FORCE COEFFICIENT AT STATION 110.000  
 WITH TAIL-OFF LIFT COEFFICIENT.

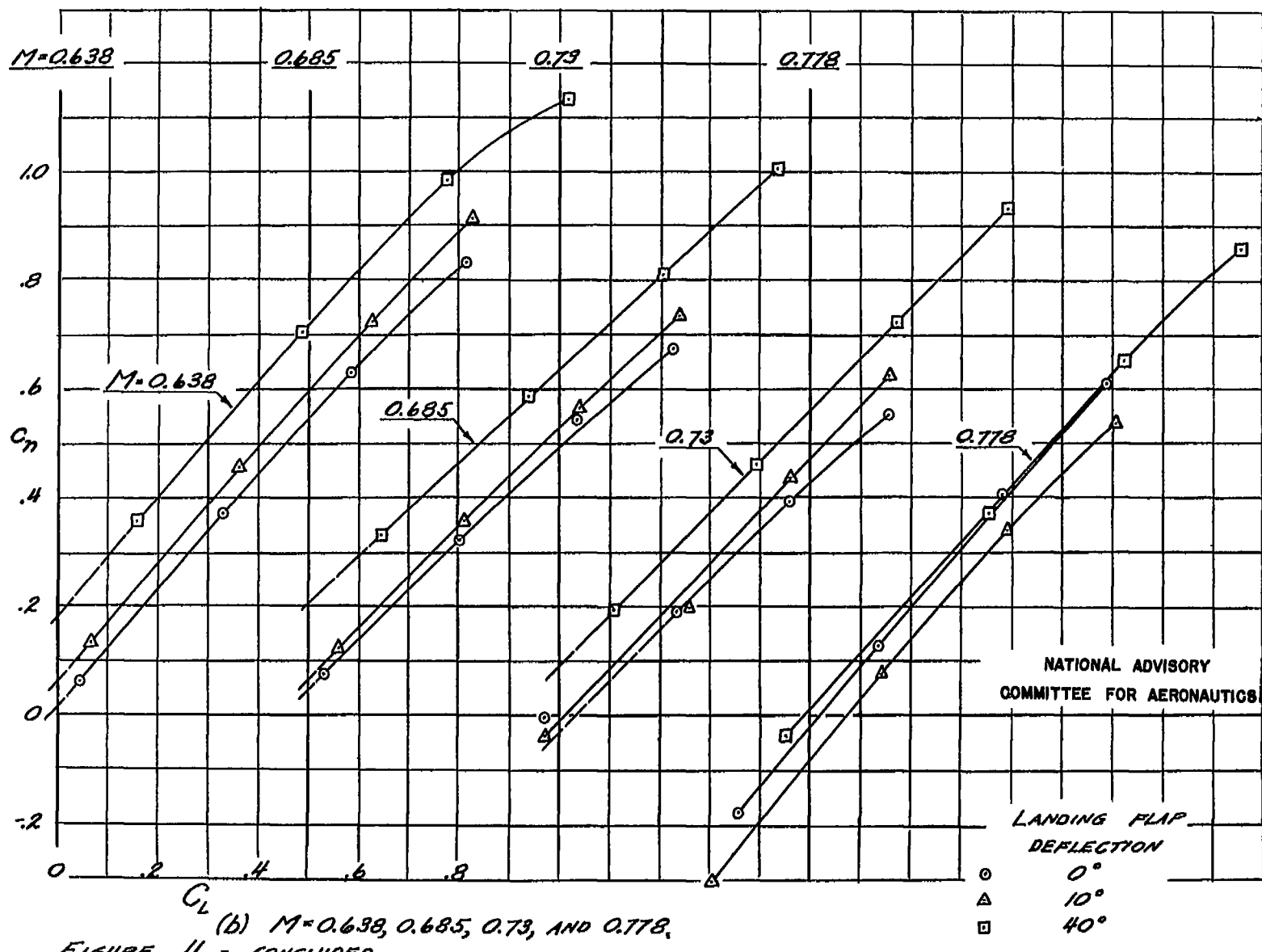
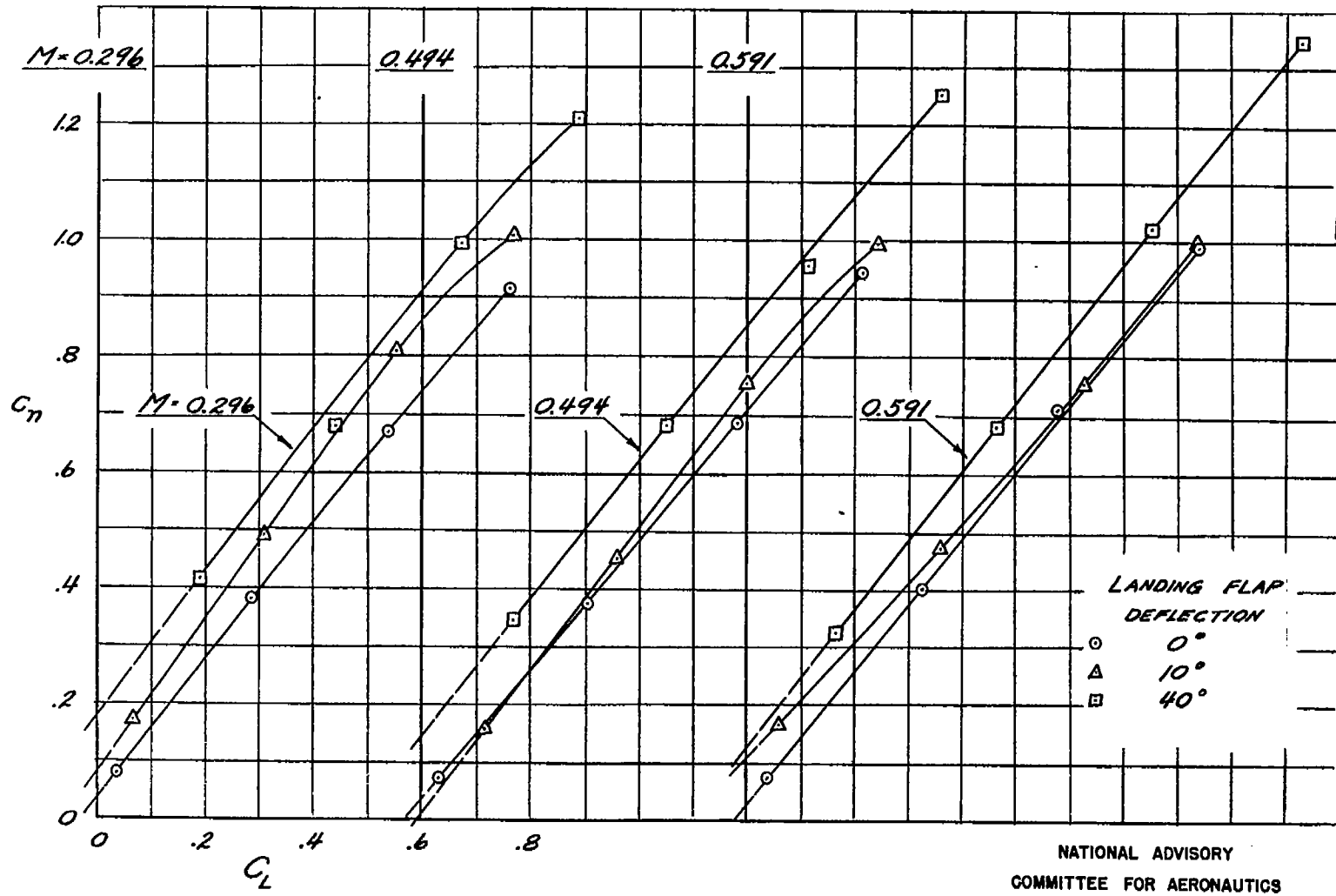


Fig. 12a

NACA RM No. A7D23



(a)  $M = 0.296, 0.494$ , AND  $0.591$   
 FIGURE 12.- VARIATION OF THE SECTION NORMAL-FORCE COEFFICIENT AT STATION 140.000 WITH TAIL-OFF LIFT COEFFICIENT.

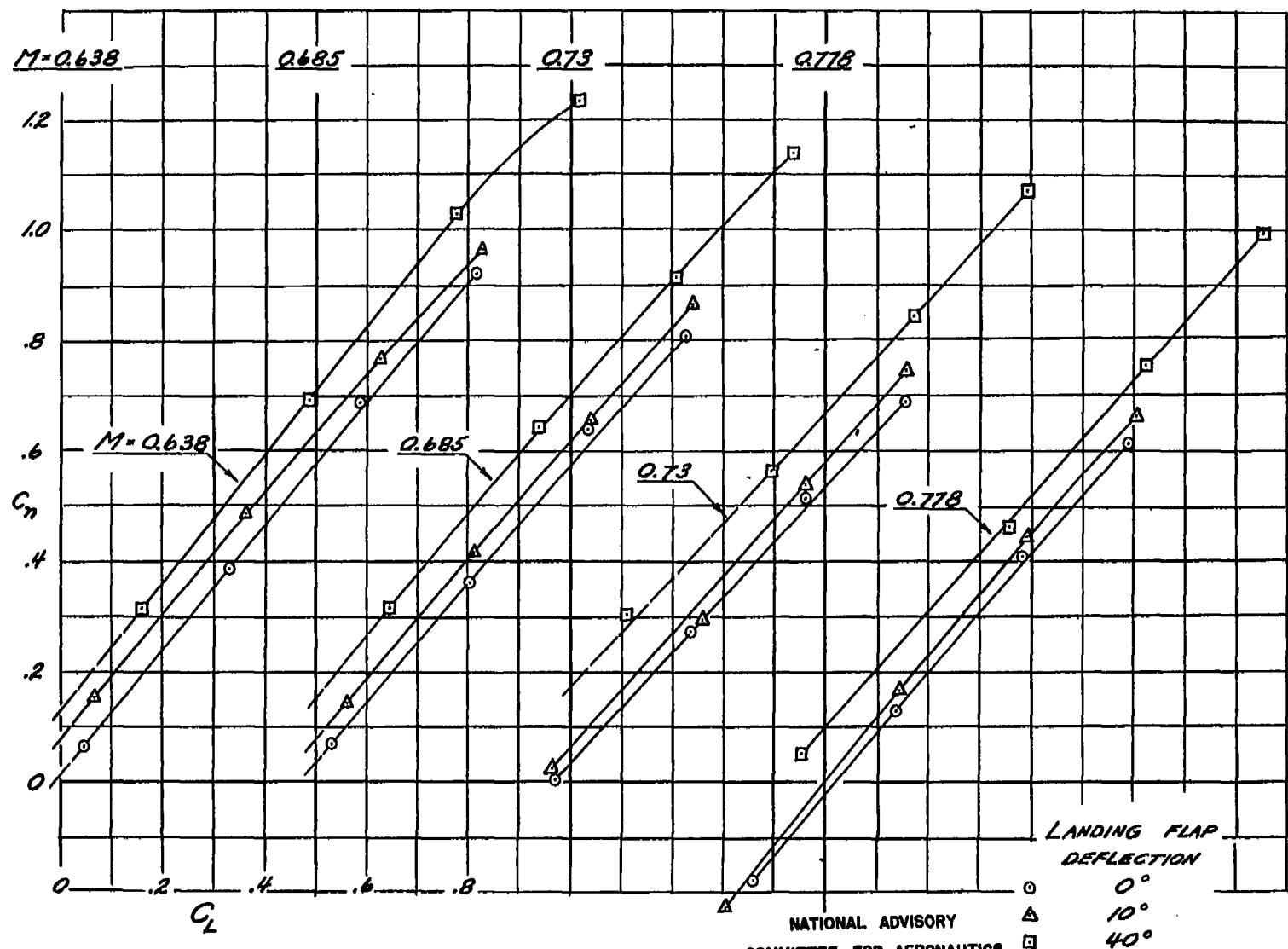
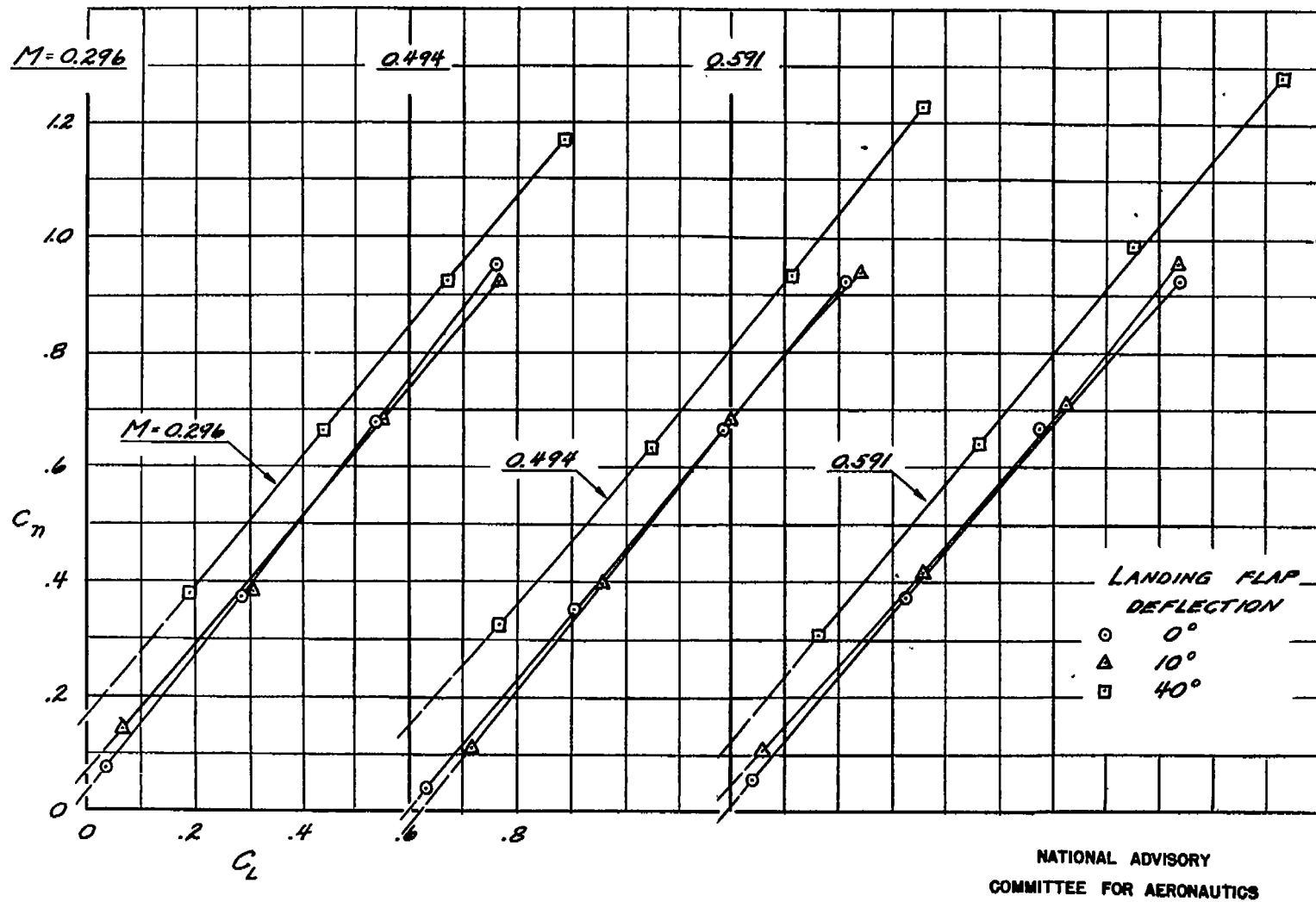
(b)  $M = 0.638, 0.685, 0.73$ , AND  $0.778$ 

FIGURE 12. - CONCLUDED

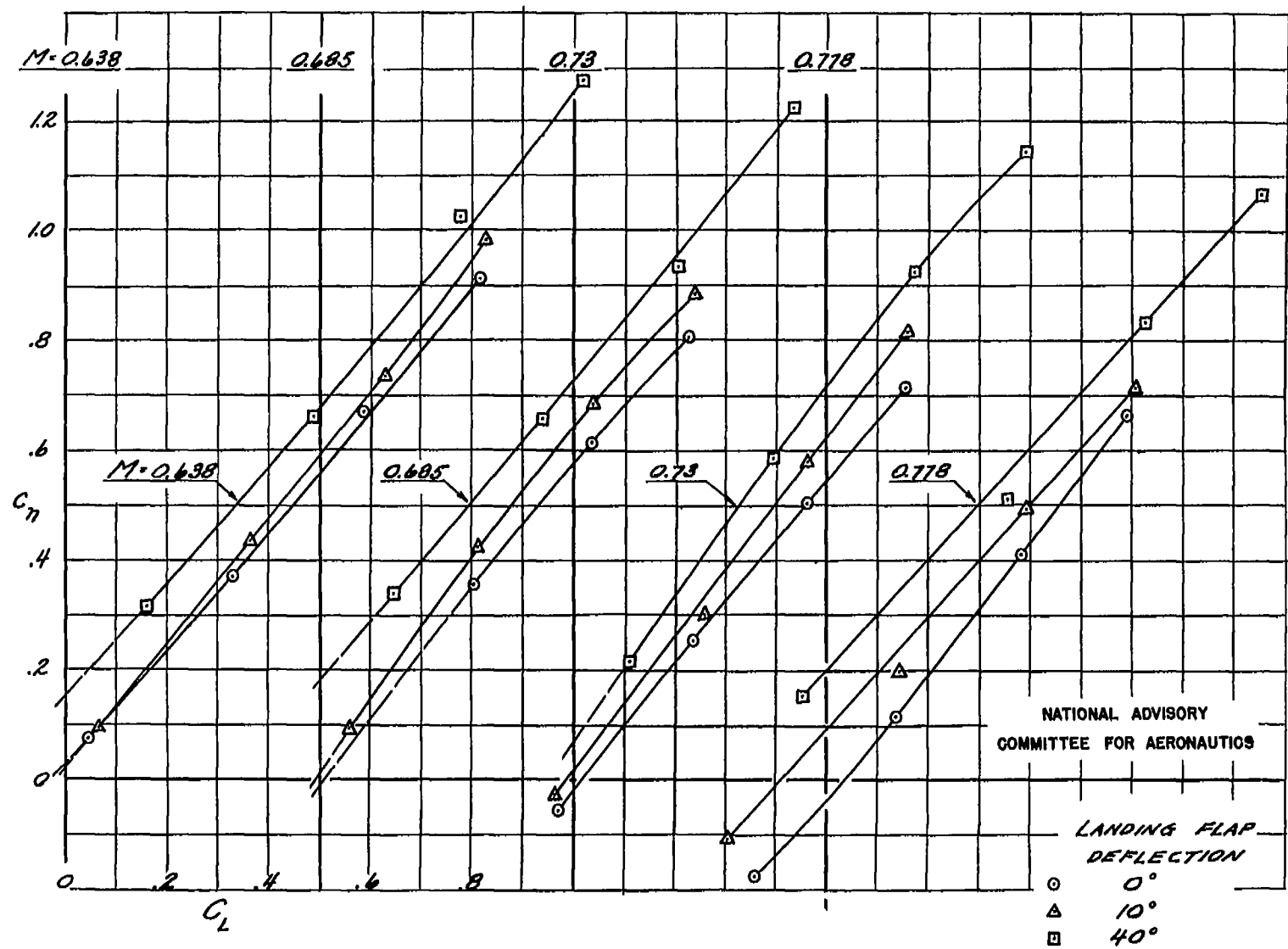
Fig. 13a

NACA RM No. A7D23



(a)  $M = 0.296, 0.494$ , AND  $0.591$   
FIGURE 13.- VARIATION OF THE SECTION NORMAL-FORCE COEFFICIENT AT STATION  
170.334 WITH TAIL-OFF LIFT COEFFICIENT.

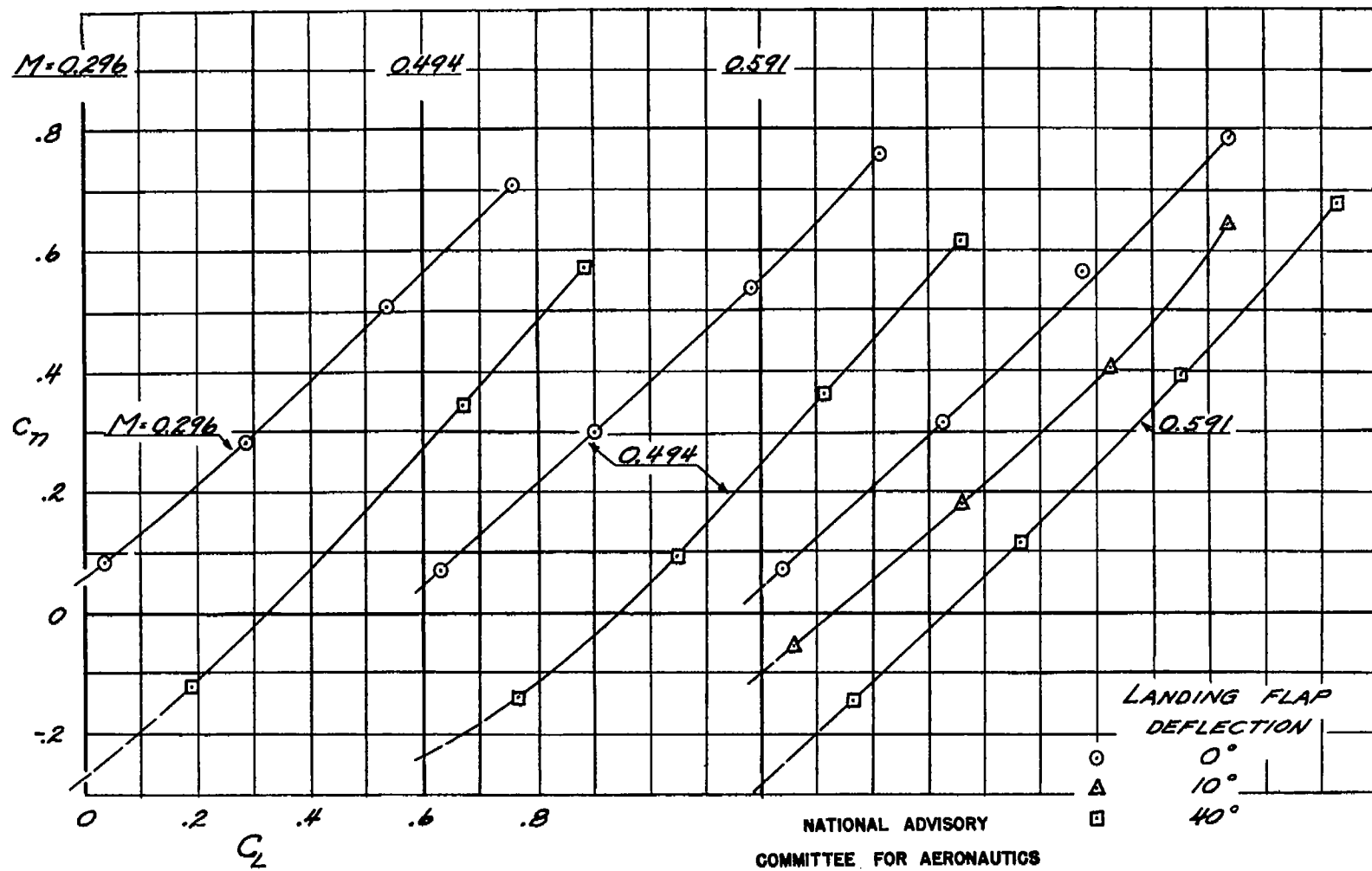
Fig. 13b



(b)  $M = 0.638, 0.685, 0.73$ , AND  $0.778$   
FIGURE 13.- CONCLUDED

Fig. 14a

NACA RM No. A7D23



(a)  $M = 0.296, 0.494$ , AND  $0.591$   
FIGURE 14.- VARIATION OF THE SECTION NORMAL-FORCE COEFFICIENT AT STATION  
219.093 WITH TAIL-OFF LIFT COEFFICIENT.

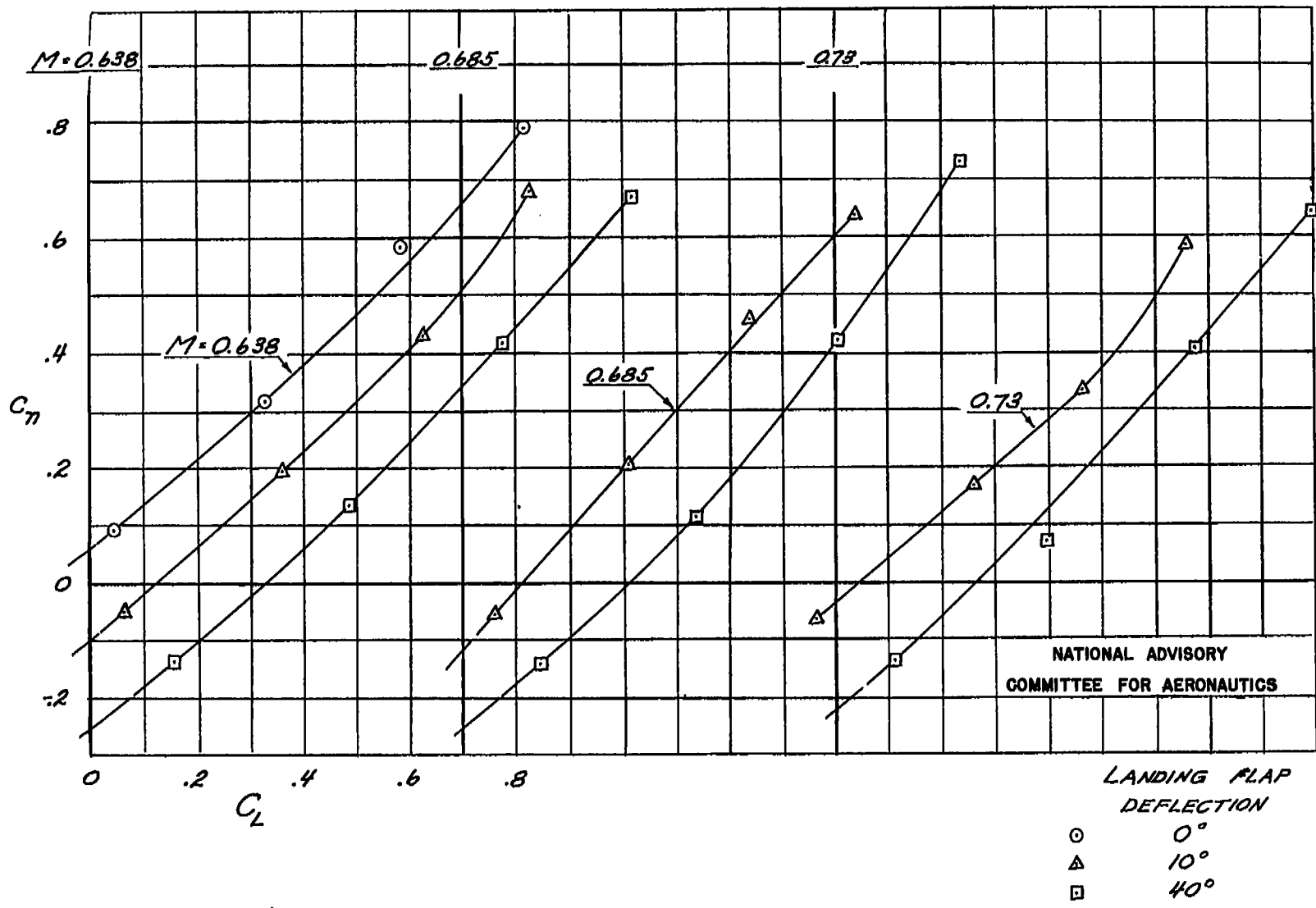
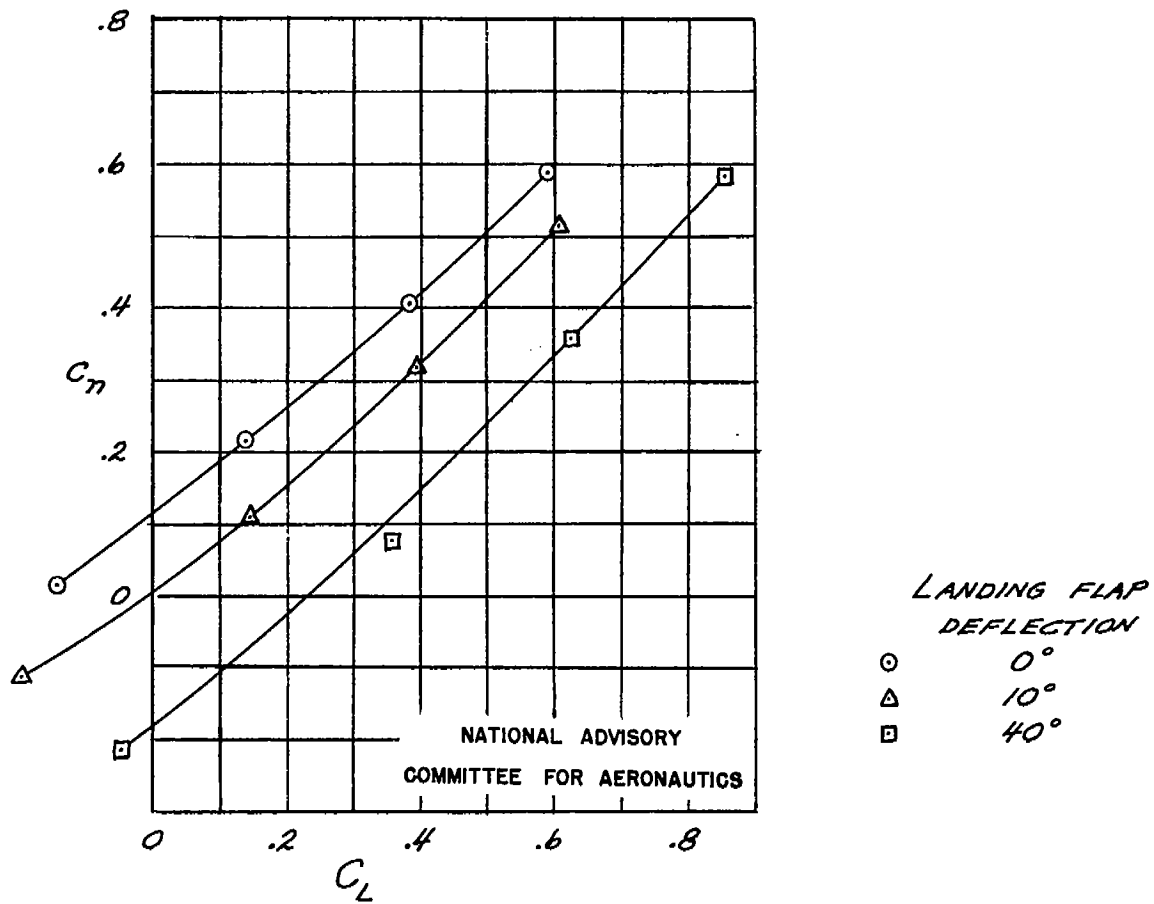
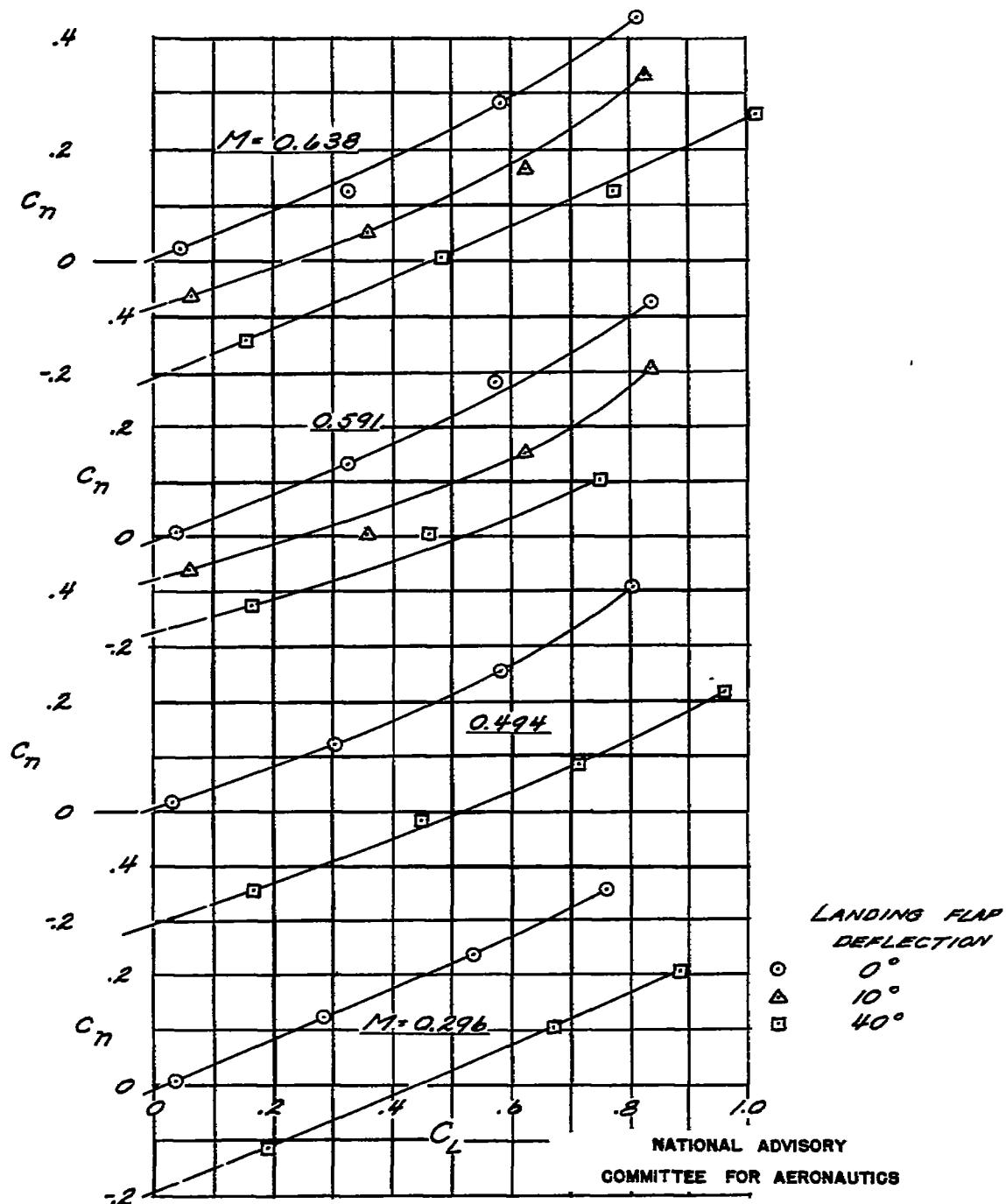
(b)  $M = 0.638, 0.685$ , AND  $0.73$ 

FIGURE 14.- CONTINUED

Fig. 14c

NACA RM No. A7D23

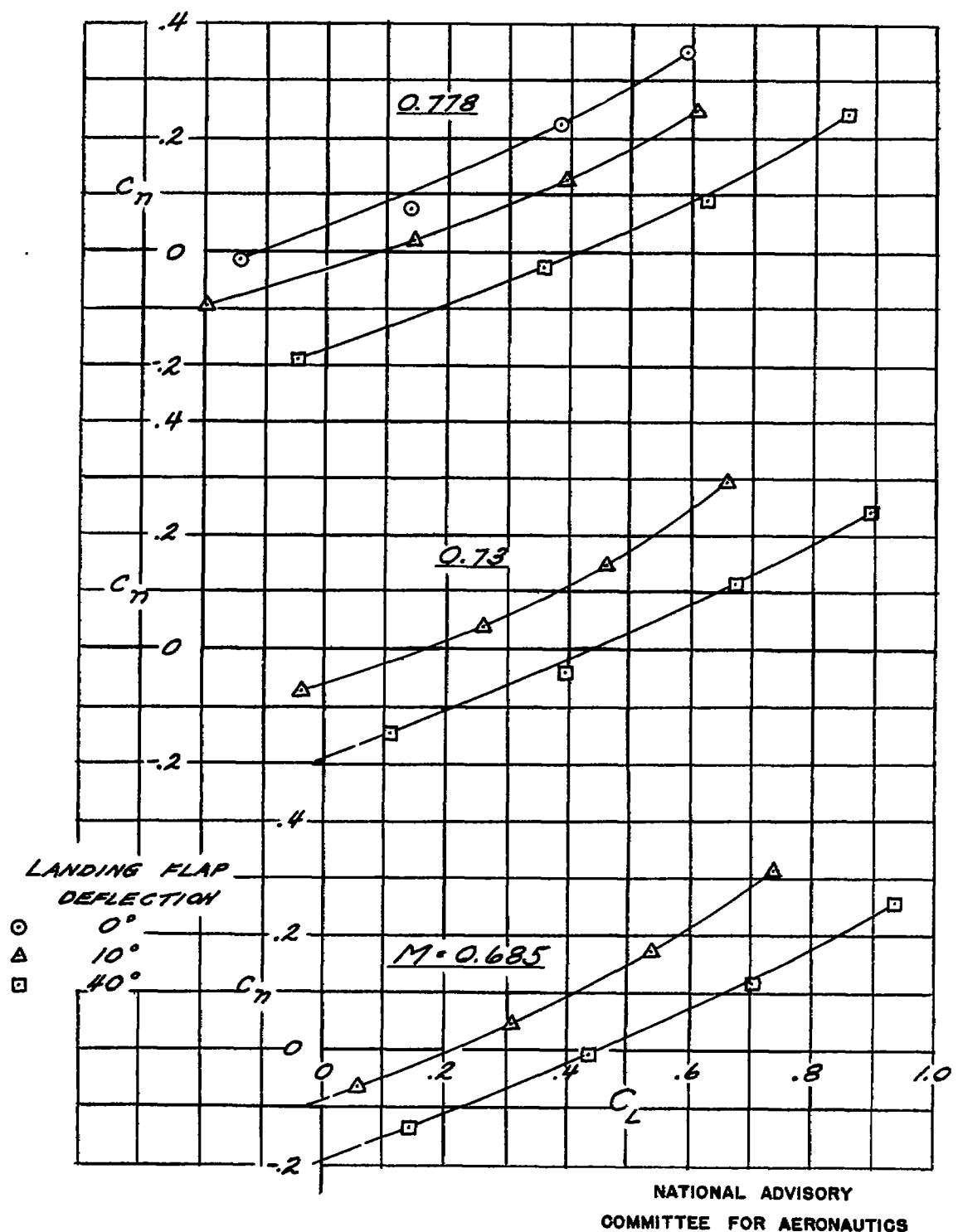




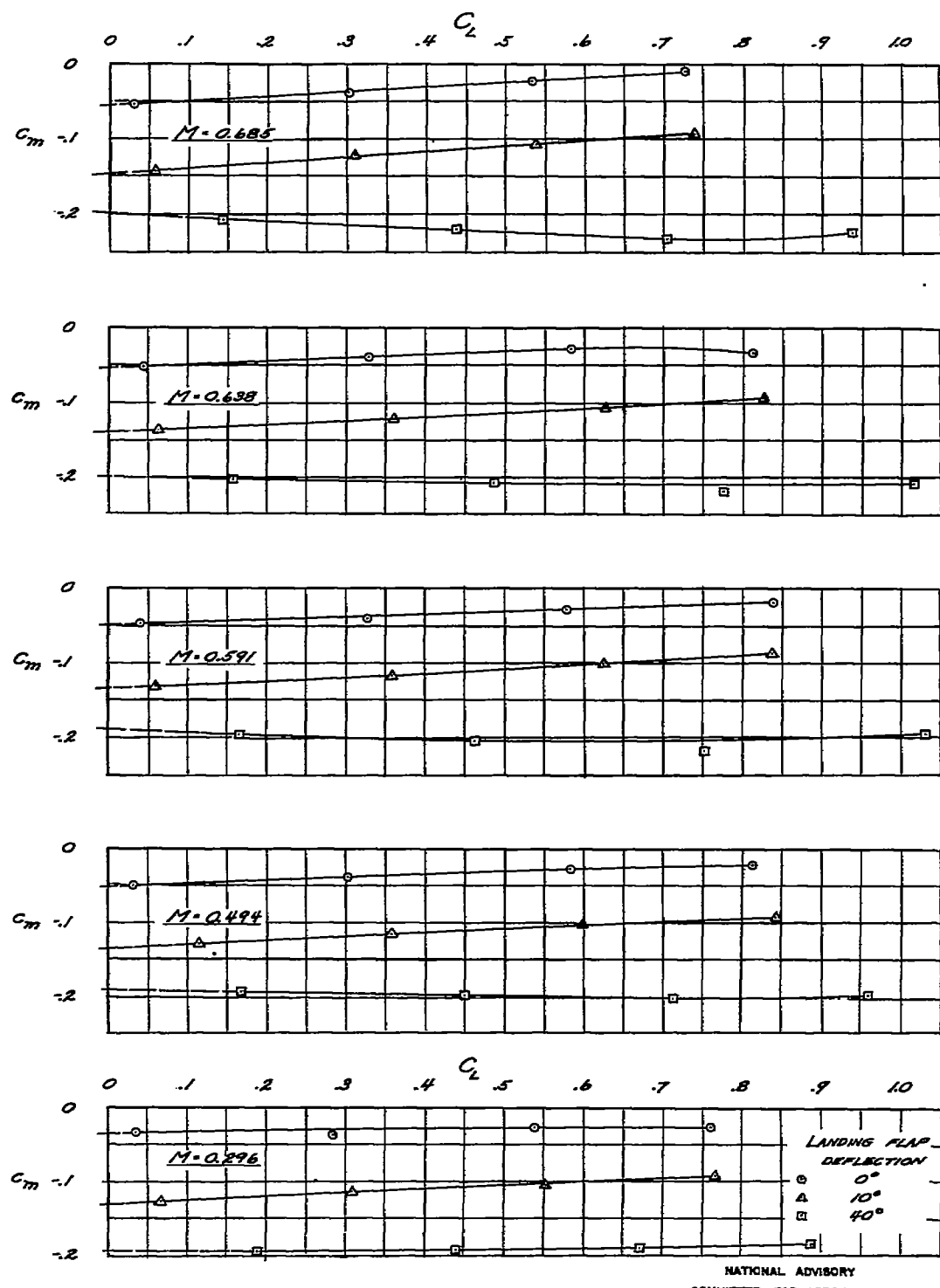
(a)  $M=0.296, 0.494, 0.591$ , AND  $0.638$   
 FIGURE 15.- VARIATION OF THE SECTION NORMAL-FORCE COEFFICIENT AT STATION 266.934 WITH TAIL-OFF LIFT COEFFICIENT.

Fig. 15b

NACA RM No. A7D23



(b)  $M = 0.685, 0.730,$  AND  $0.778$   
FIGURE 15.- CONCLUDED

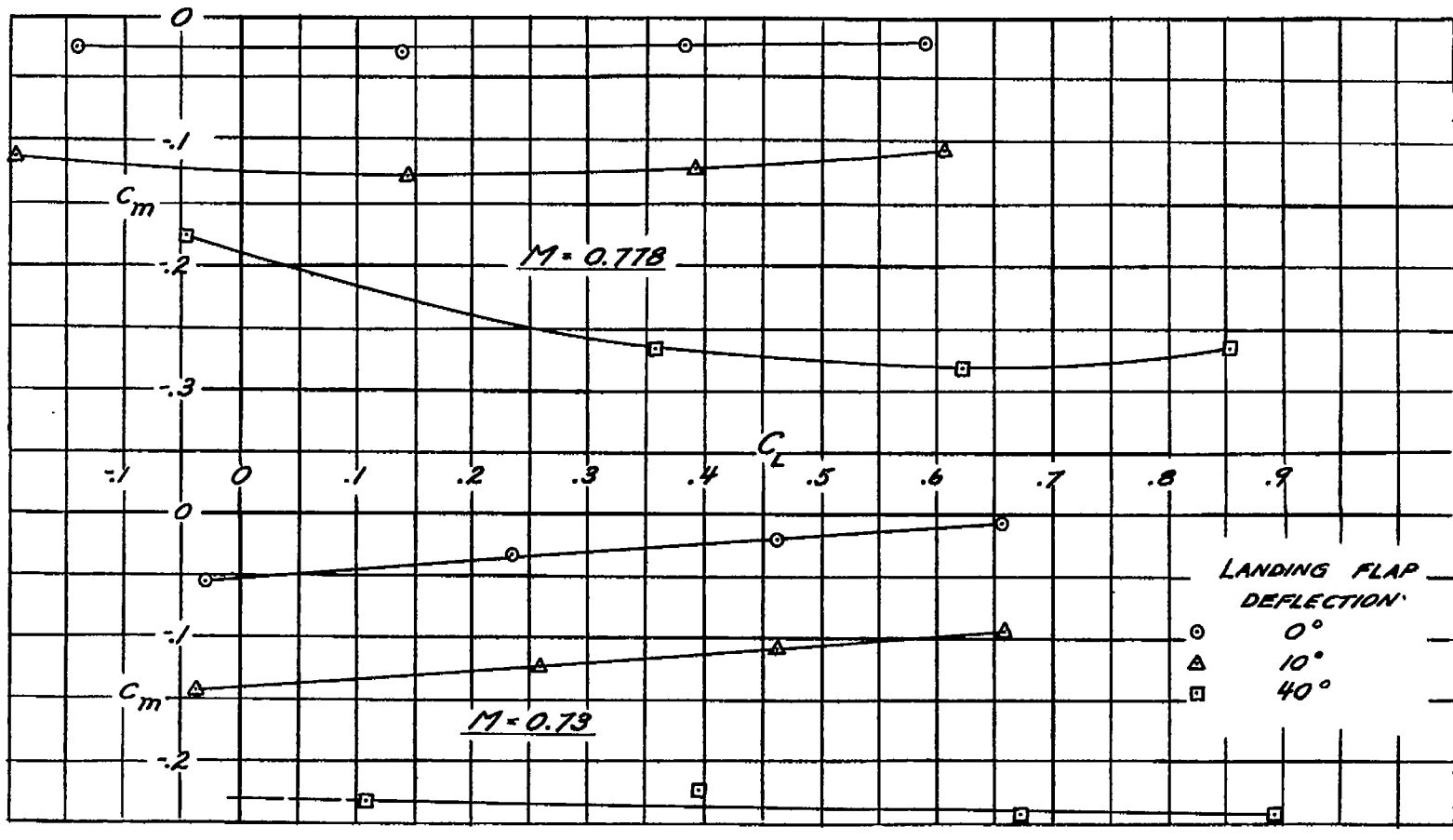


(a)  $M = 0.296, 0.494, 0.591, 0.638$ , AND  $0.685$   
 FIGURE 16.-VARIATION OF SECTION PITCHING-MOMENT COEFFICIENT AT STATION  
 40.102 WITH TAIL-OFF LIFT COEFFICIENT. MOMENT AXIS AT 25.75 PERCENT CHORD.

NATIONAL ADVISORY  
COMMITTEE FOR AERONAUTICS

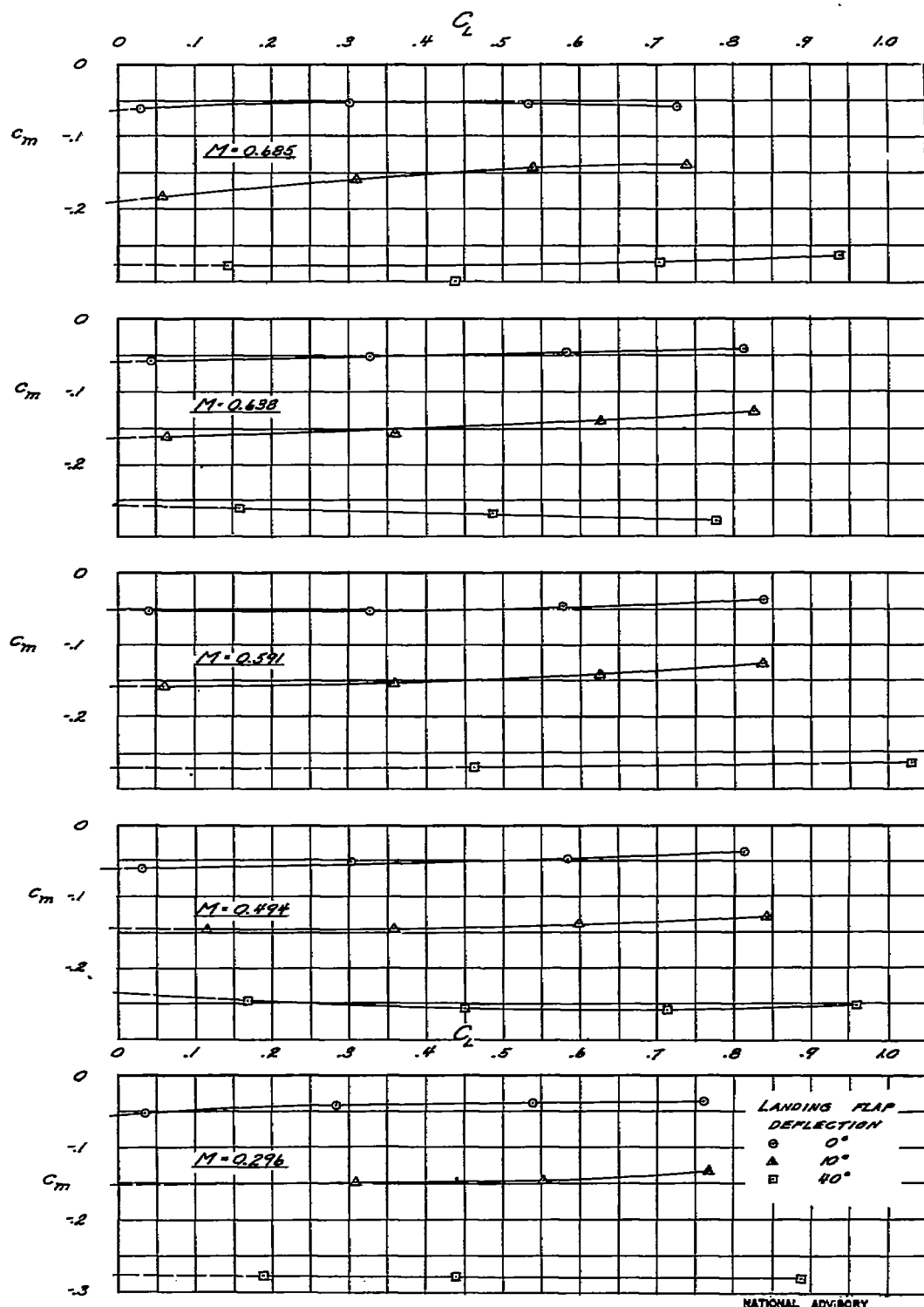
Fig. 16b

NACA RM NO. A7D23



(b)  $M = 0.73$  AND  $0.778$   
FIGURE 16.- CONCLUDED

NATIONAL ADVISORY  
COMMITTEE FOR AERONAUTICS



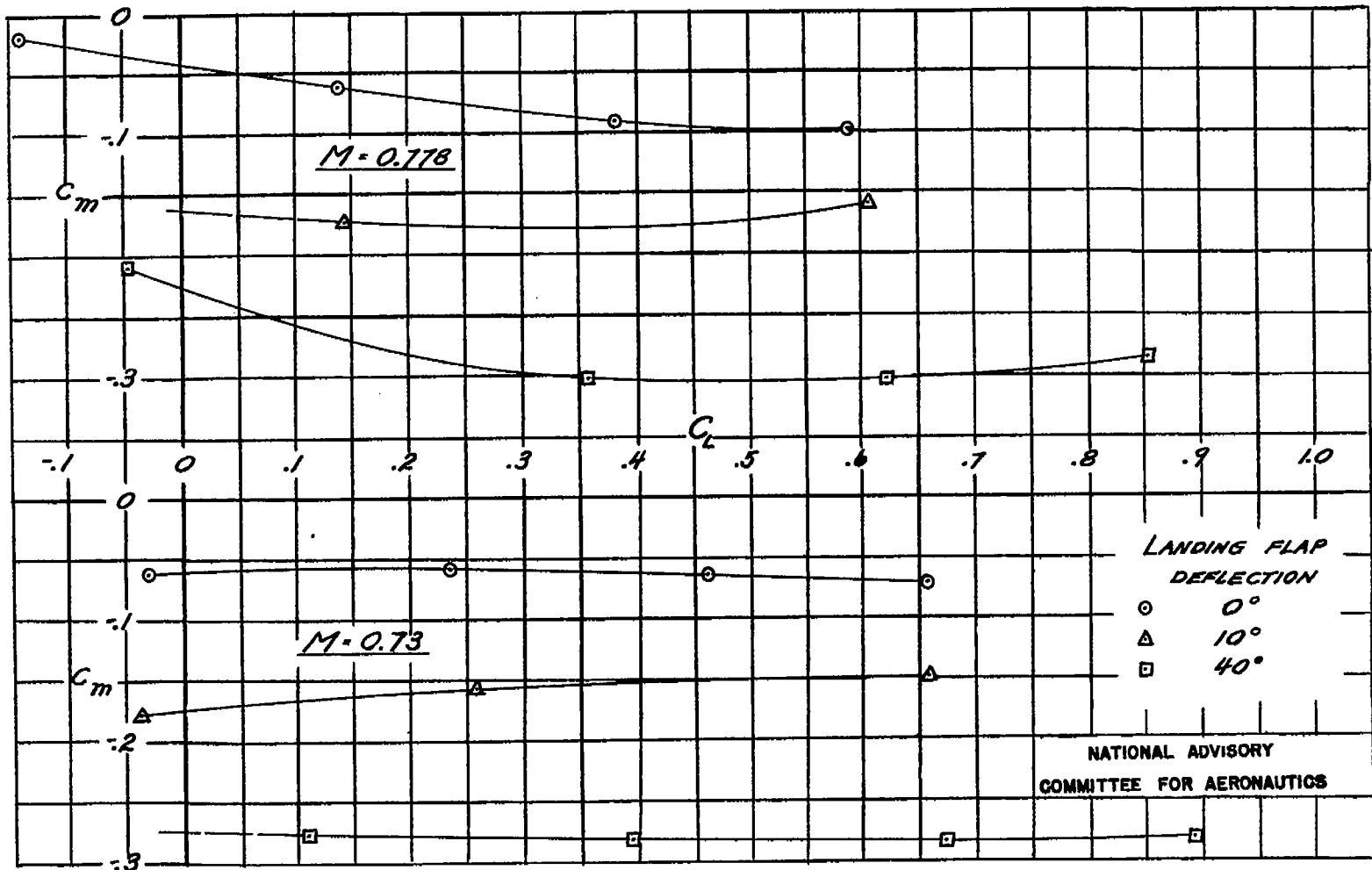
(a)  $M = 0.296, 0.494, 0.591, 0.638$ , AND  $0.685$   
 FIGURE 17.- VARIATION OF SECTION PITCHING-MOMENT COEFFICIENT AT STATION  
 77.500 WITH TAIL-OFF LIFT COEFFICIENT. MOMENT AXIS AT 25.4 PERCENT CHORD.

NATIONAL ADVISORY

COMMITTEE FOR AERONAUTICS

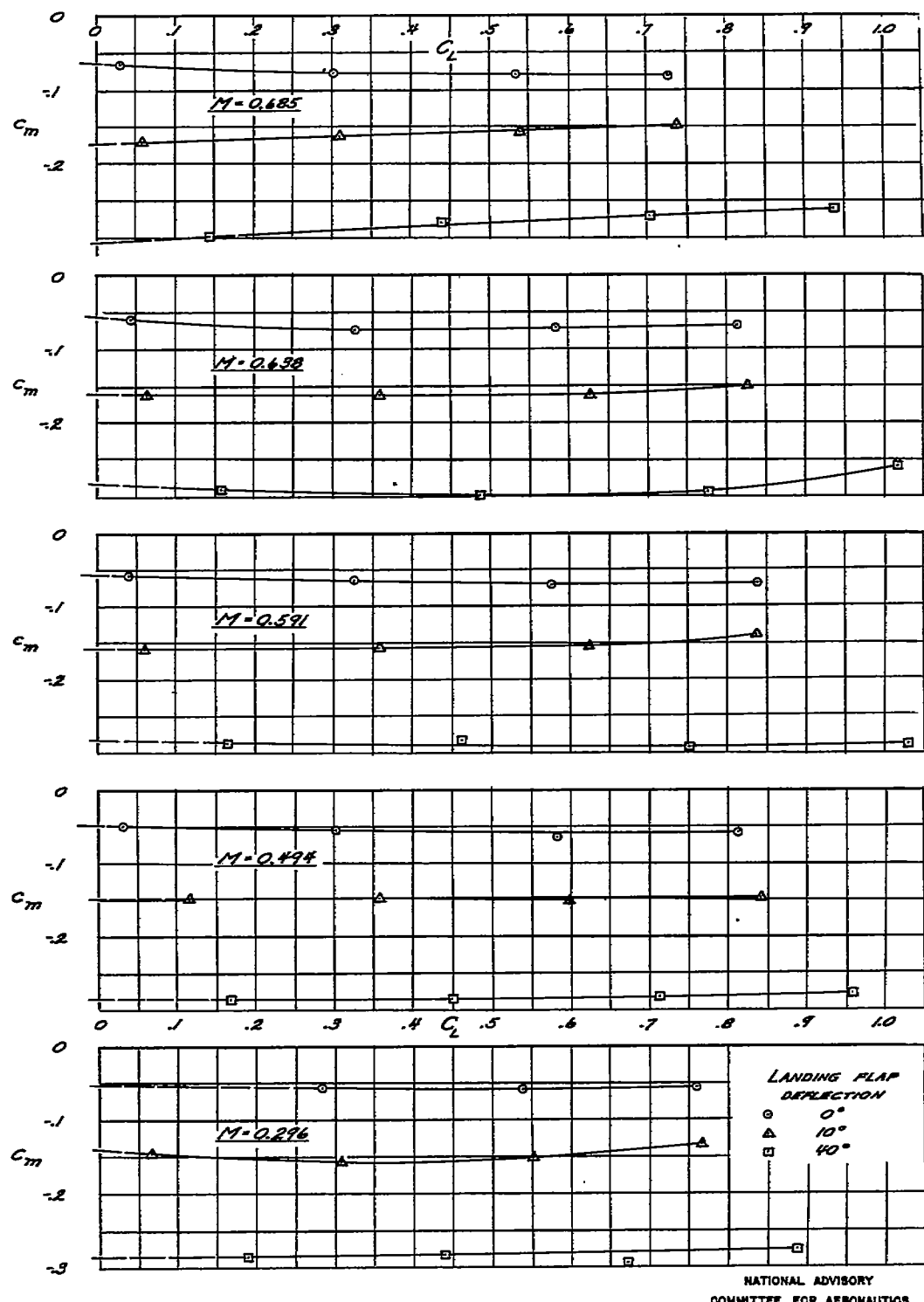
Fig. 17b

NACA RM No. A7D23



(b)  $M = 0.73$  AND  $0.778$

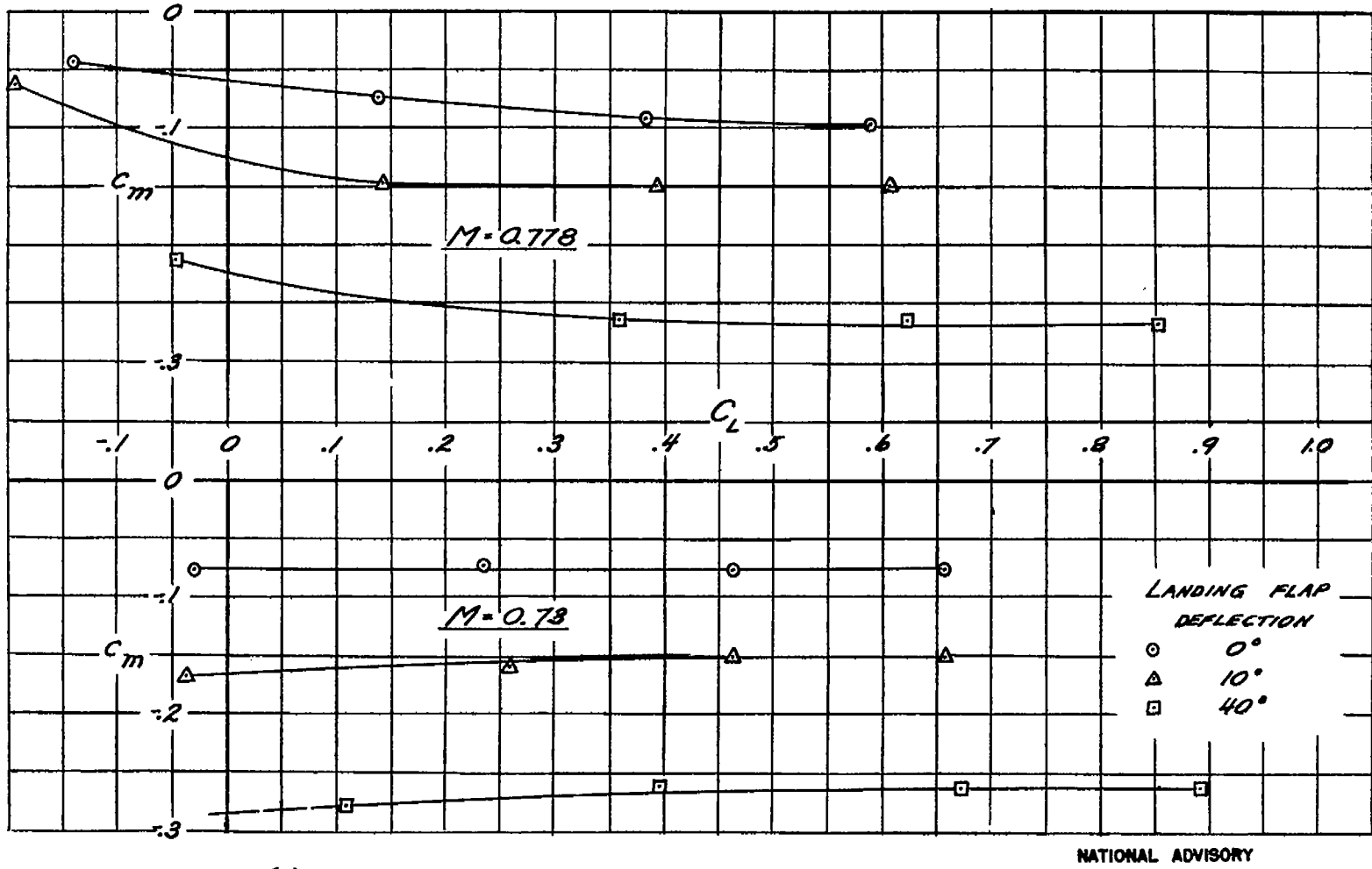
FIGURE 17.- CONCLUDED



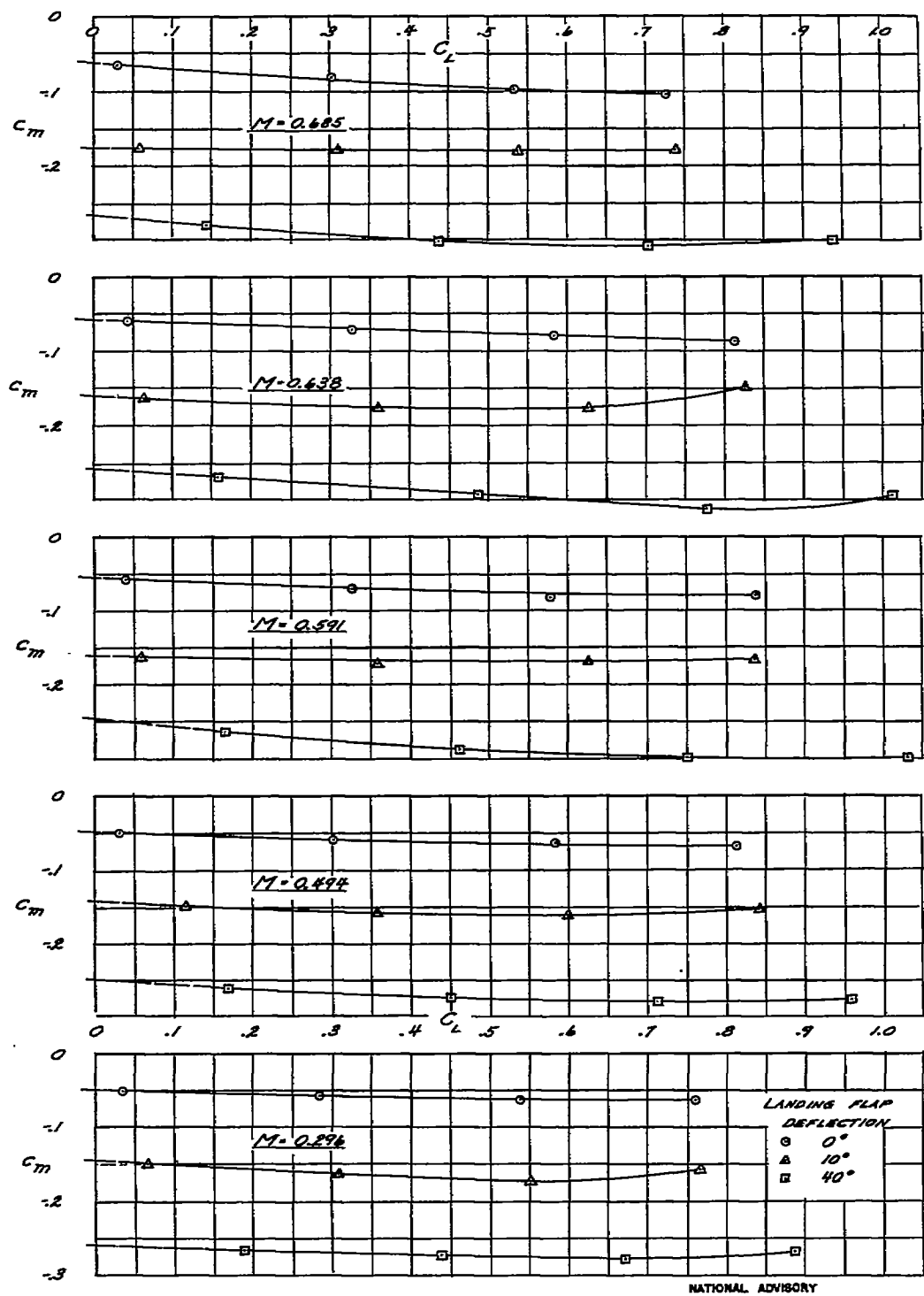
(a)  $M = 0.296, 0.494, 0.591, 0.638$ , AND  $0.685$   
 FIGURE 18.- VARIATION OF SECTION PITCHING MOMENT COEFFICIENT AT STATION 110.000  
 WITH TAIL-OFF LIFT COEFFICIENT. MOMENT AXIS AT 25.1 PERCENT CHORD.

Fig. 18b

NACA RM No. A7D23



(b)  $M = 0.73$  AND  $0.778$   
FIGURE 18.- CONCLUDED

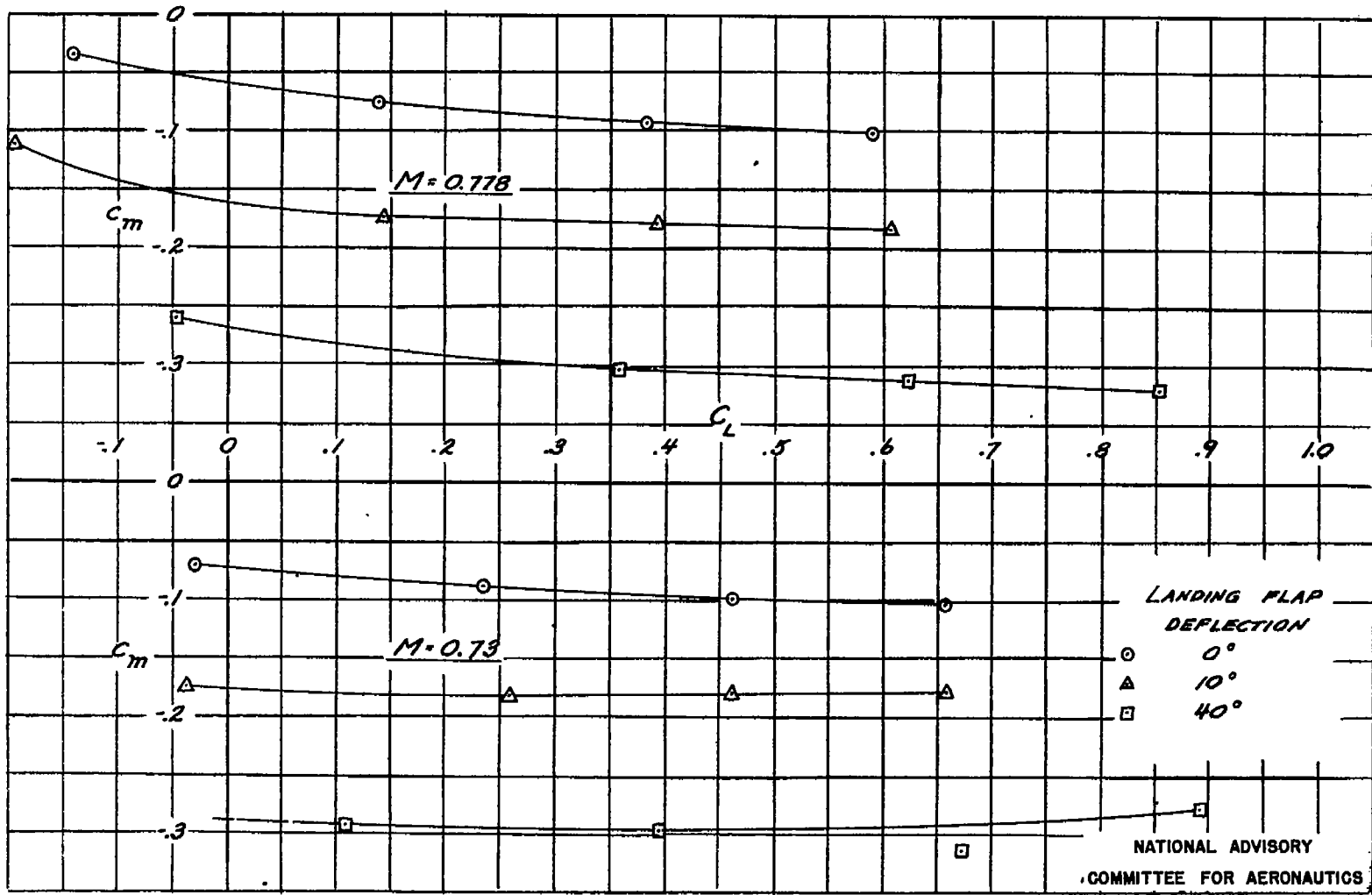


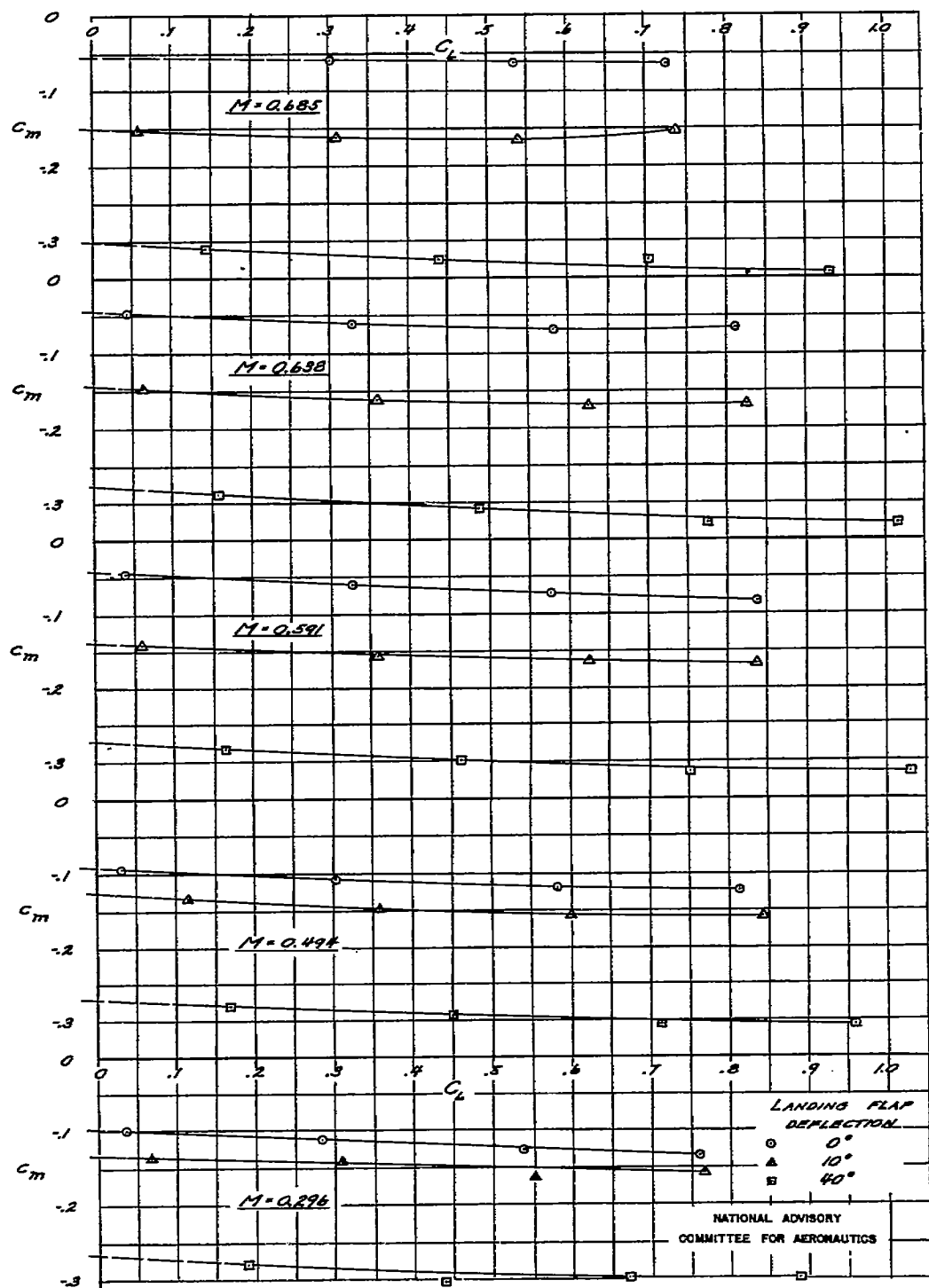
(a)  $M = 0.296, 0.494, 0.591, 0.638$ , AND  $0.685$   
 FIGURE 19. - VARIATION OF SECTION PITCHING MOMENT COEFFICIENT AT STATION  
 140.000 WITH TAIL-OFF LIFT COEFFICIENT. MOMENT AXIS AT 24.7 PERCENT CHORD.

NATIONAL ADVISORY  
COMMITTEE FOR AERONAUTICS

FIG. 19b

NACA RM No. A7D23

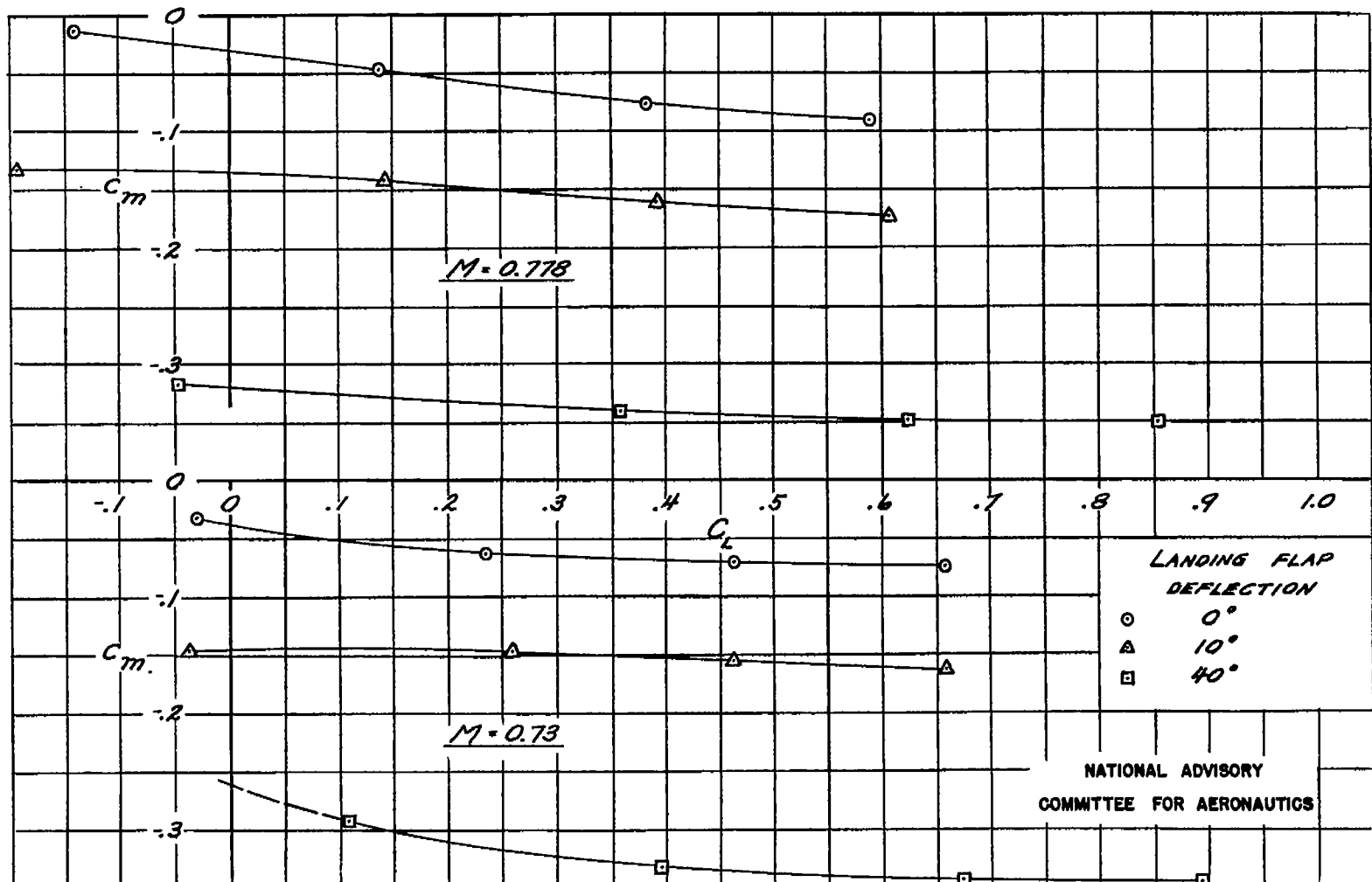
(b)  $M = 0.73$  AND  $0.778$   
FIGURE 19.- CONCLUDED.



(a)  $M = 0.296, 0.494, 0.591, 0.685$   
 FIGURE 20.-VARIATION OF SECTION PITCHING-MOMENT COEFFICIENT AT STATION  
 170.334 WITH TAIL-OFF LIFT COEFFICIENT. MOMENT AXIS AT 24.3 PERCENT CHORD.

Fig. 20b

NACA RM No. A7D23



(b)  $M = 0.73$  AND  $0.778$   
FIGURE 20.- CONCLUDED

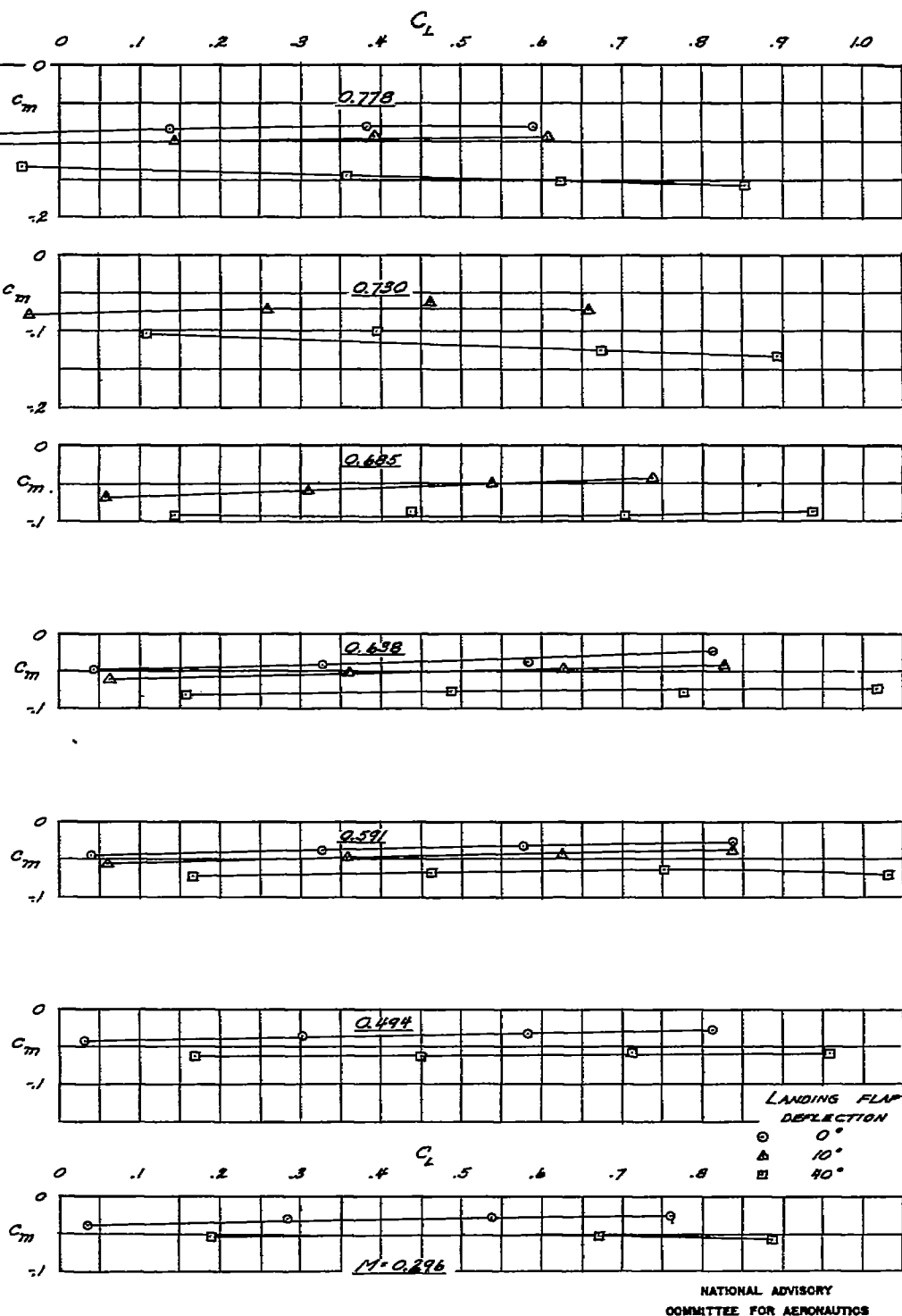


FIGURE 21.- VARIATION OF SECTION PITCHING-MOMENT COEFFICIENT AT STATION 219.093 WITH TAIL-OFF LIFT COEFFICIENT. MOMENT AXIS AT 23.5 PERCENT CHORD.

Fig. 22

NACA RM No. A7D23

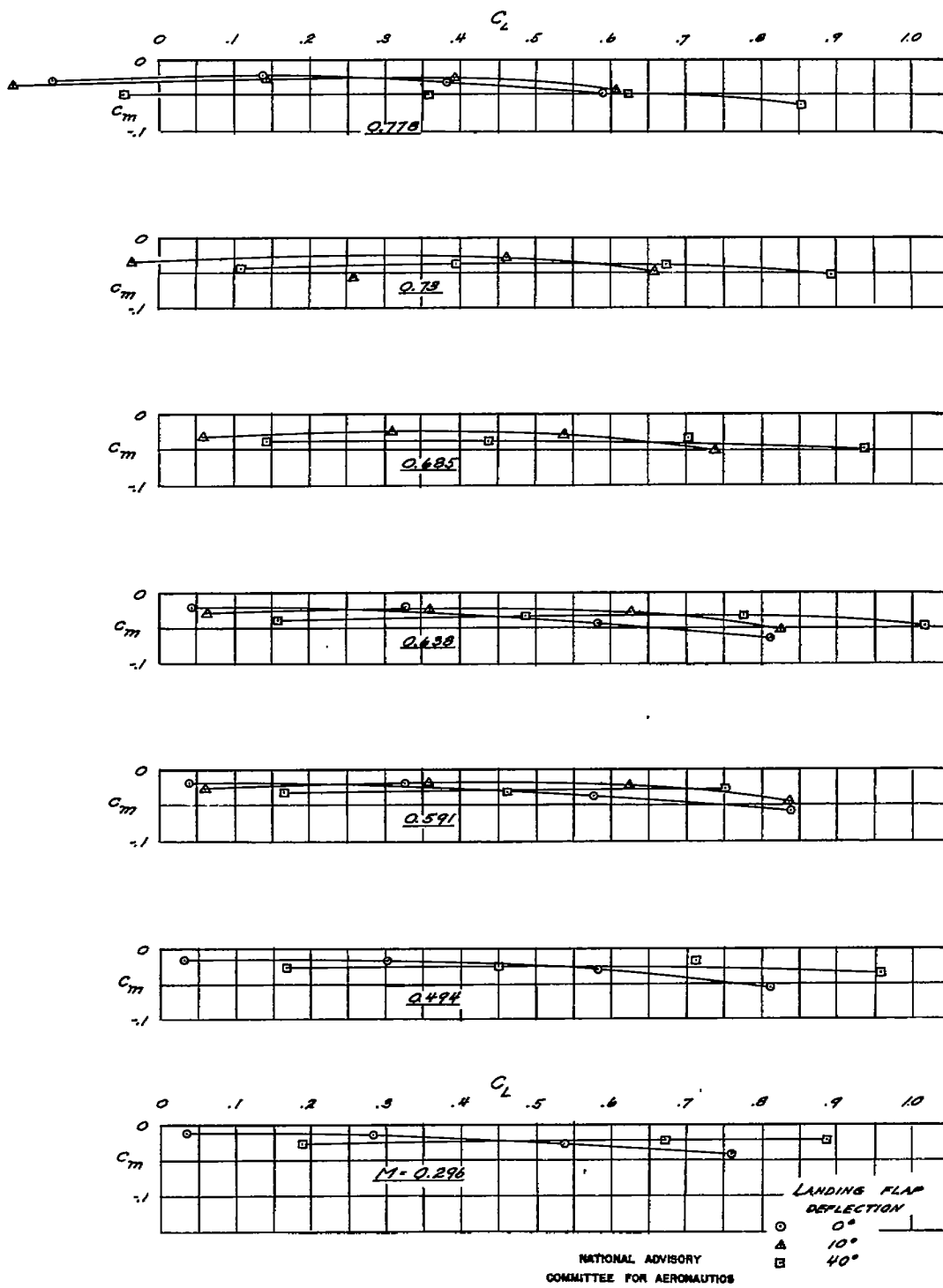


FIGURE 22.- VARIATION OF SECTION PITCHING-MOMENT COEFFICIENT AT STATION 266.334 WITH TAIL-OFF LIFT COEFFICIENT. MOMENT AXIS AT 22.5 PERCENT CHORD.

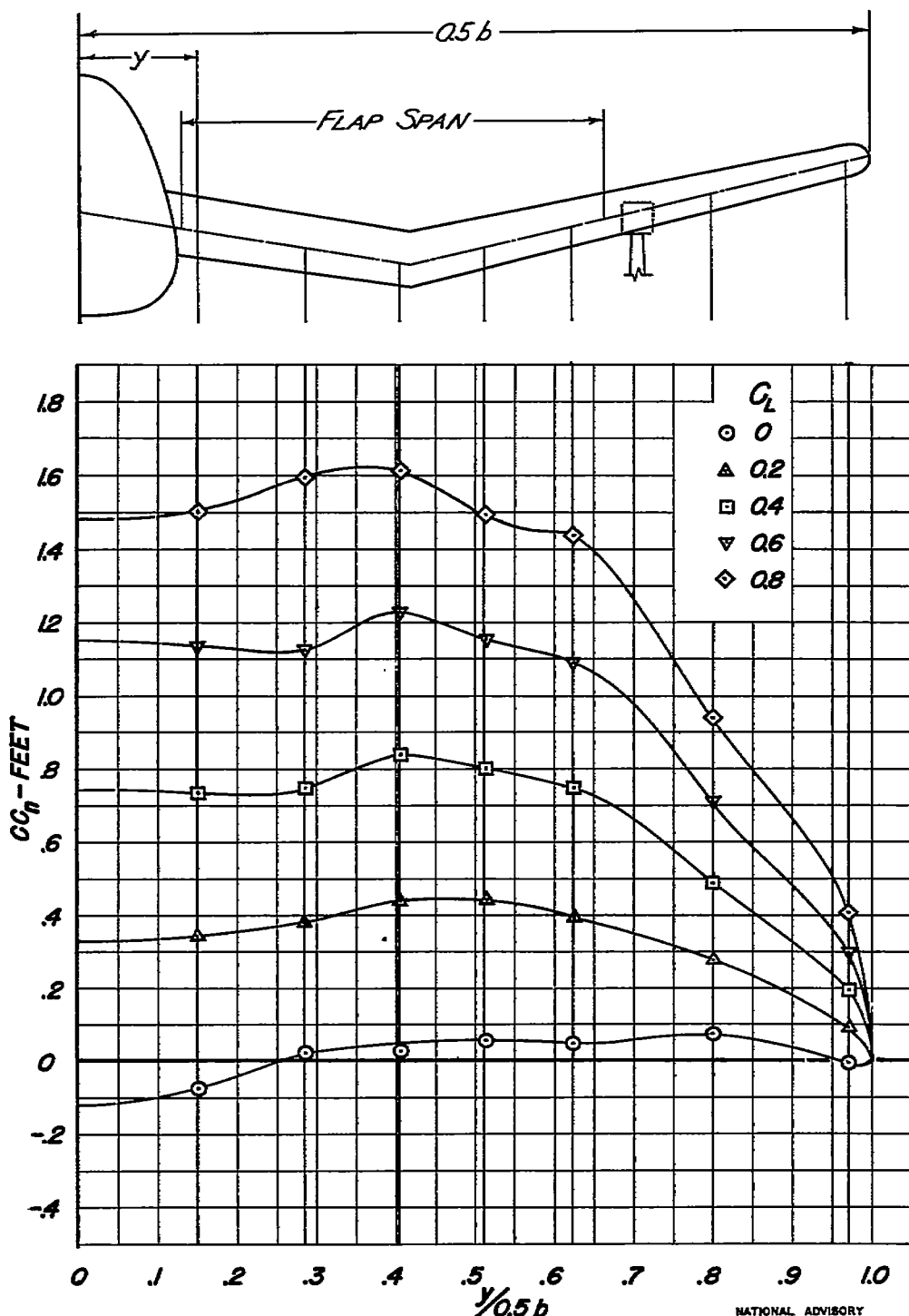
(a)  $M = 0.296$ NATIONAL ADVISORY  
COMMITTEE FOR AERONAUTICSFIGURE 23.- SPANWISE VARIATION OF THE NORMAL FORCE WITH  
LANDING FLAPS NEUTRAL.

Fig. 23b

NACA RM No. A7D23

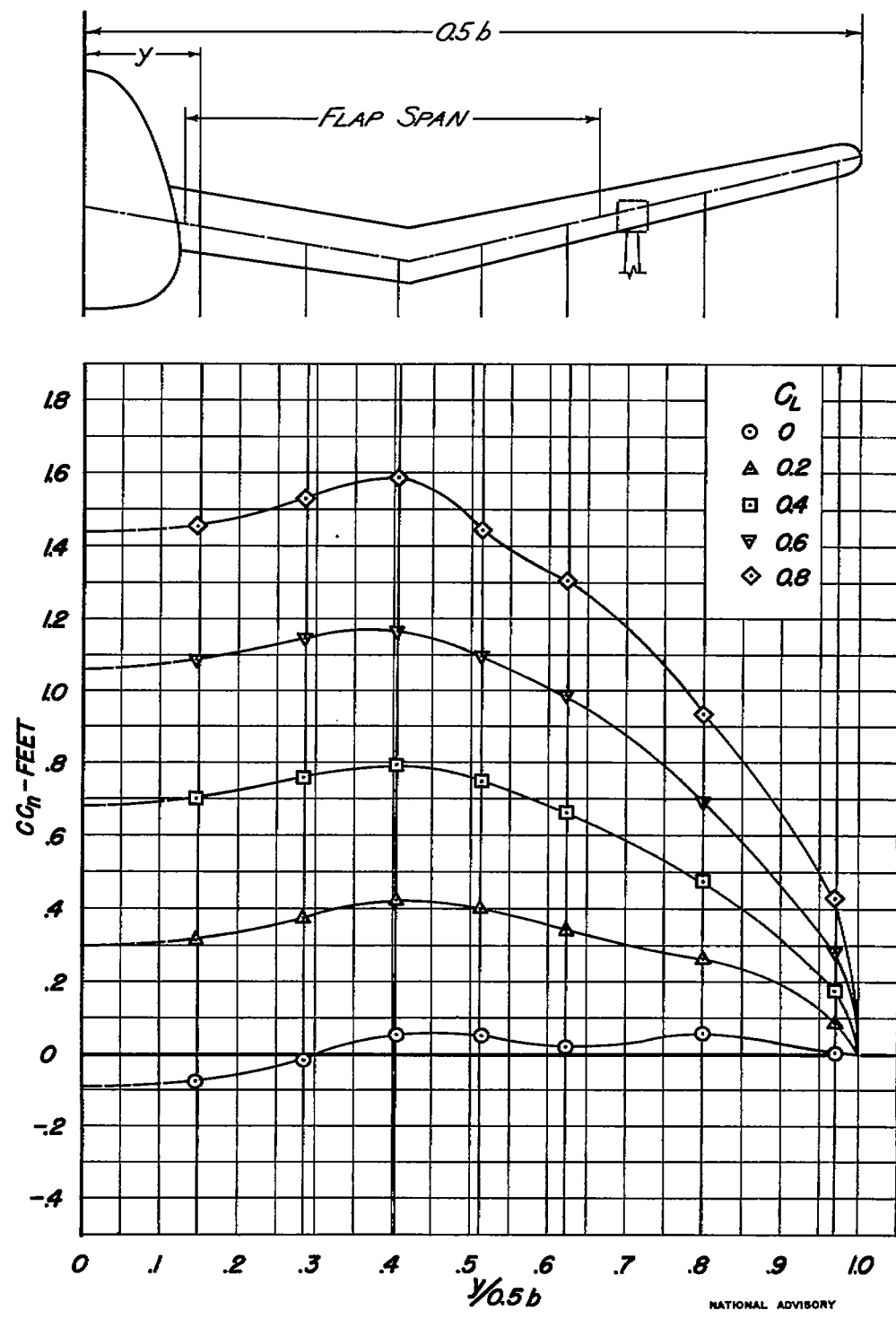
(b)  $M=0.494$ 

FIGURE 23.-CONTINUED.

NATIONAL ADVISORY  
COMMITTEE FOR AERONAUTICS

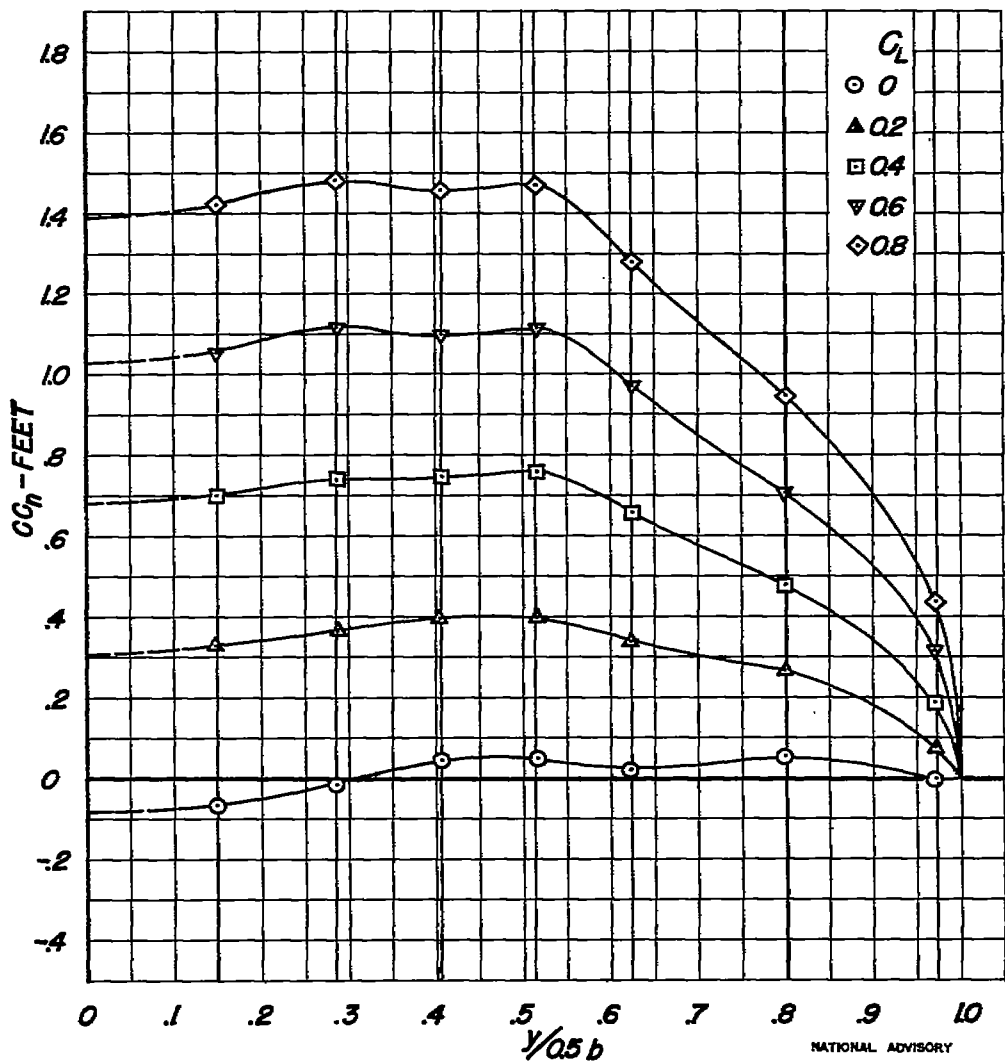
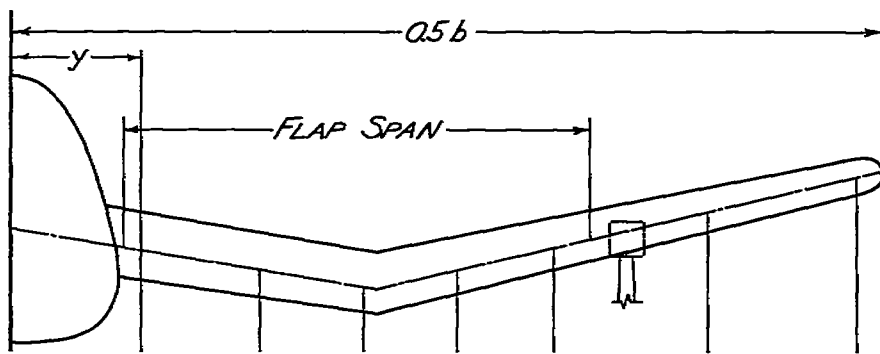
(c)  $M = 0.591$ 

FIGURE 23.- CONTINUED.

NATIONAL ADVISORY  
COMMITTEE FOR AERONAUTICS

Fig. 23d

NACA RM No. A7D23

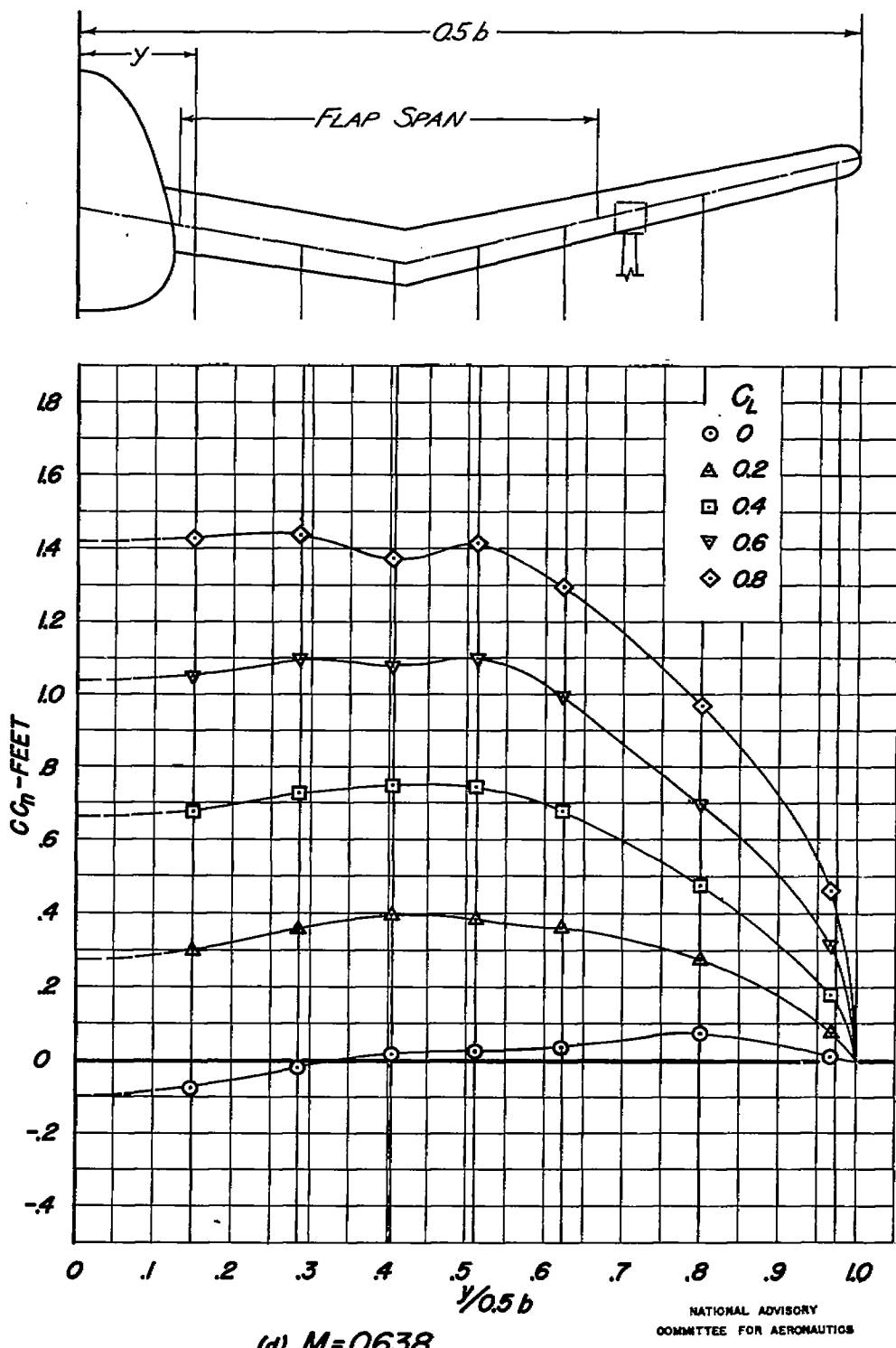


FIGURE 23.- CONTINUED.

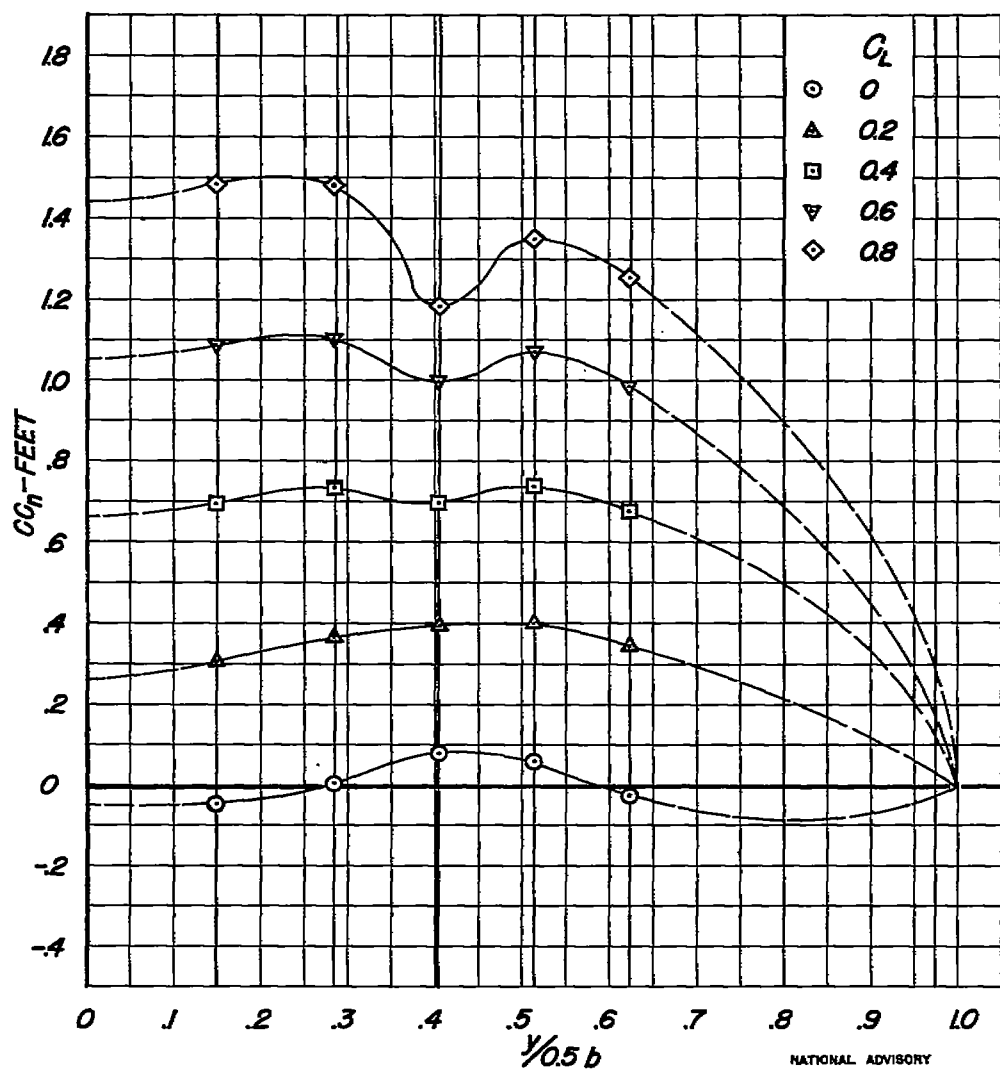
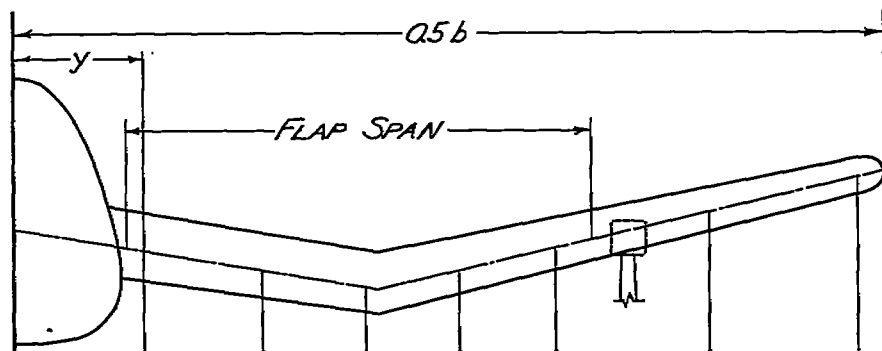
(e)  $M=0.685$ NATIONAL ADVISORY  
COMMITTEE FOR AERONAUTICS

FIGURE 23. - CONTINUED.

Fig. 23f

NACA RM No. A7D23

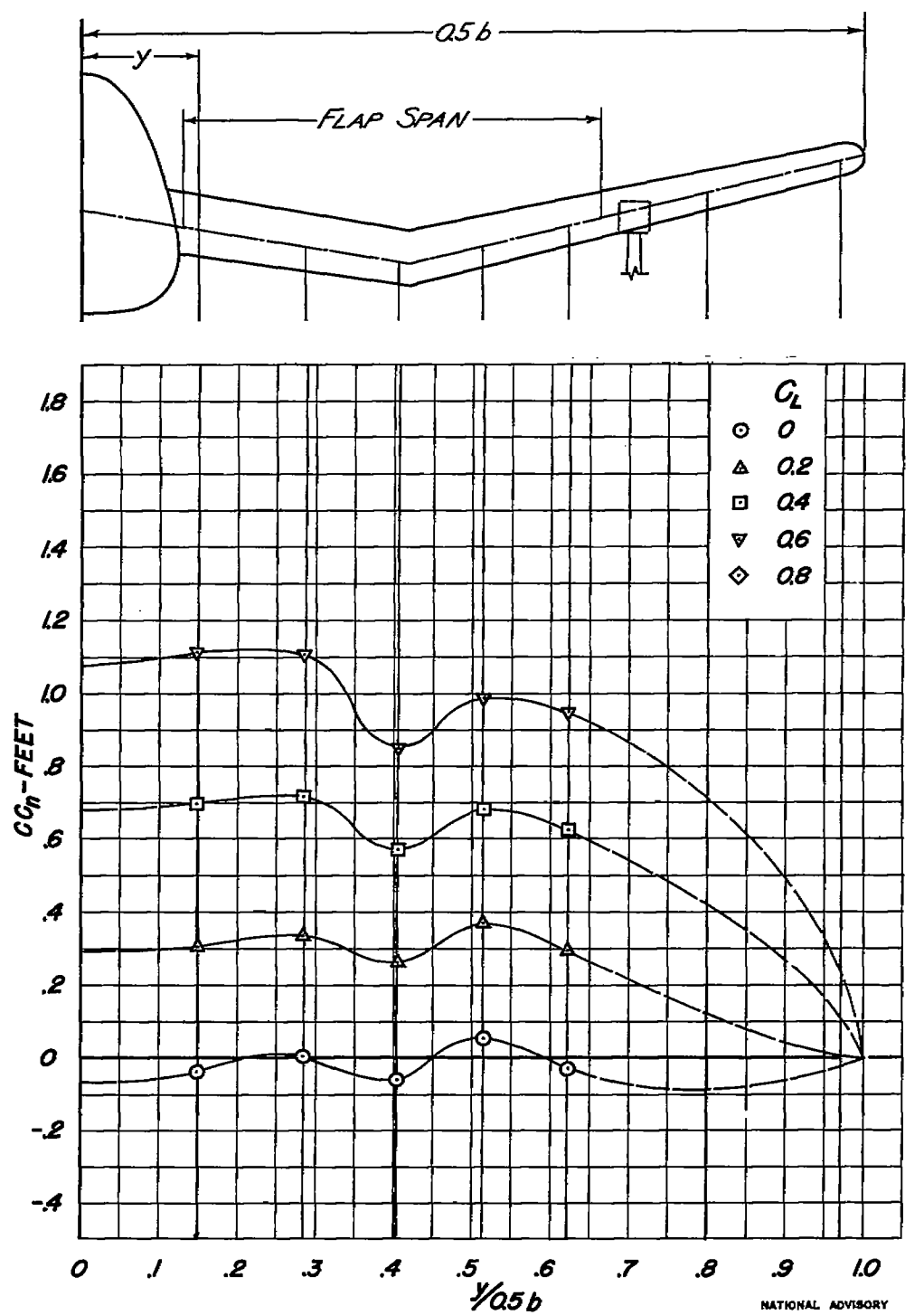
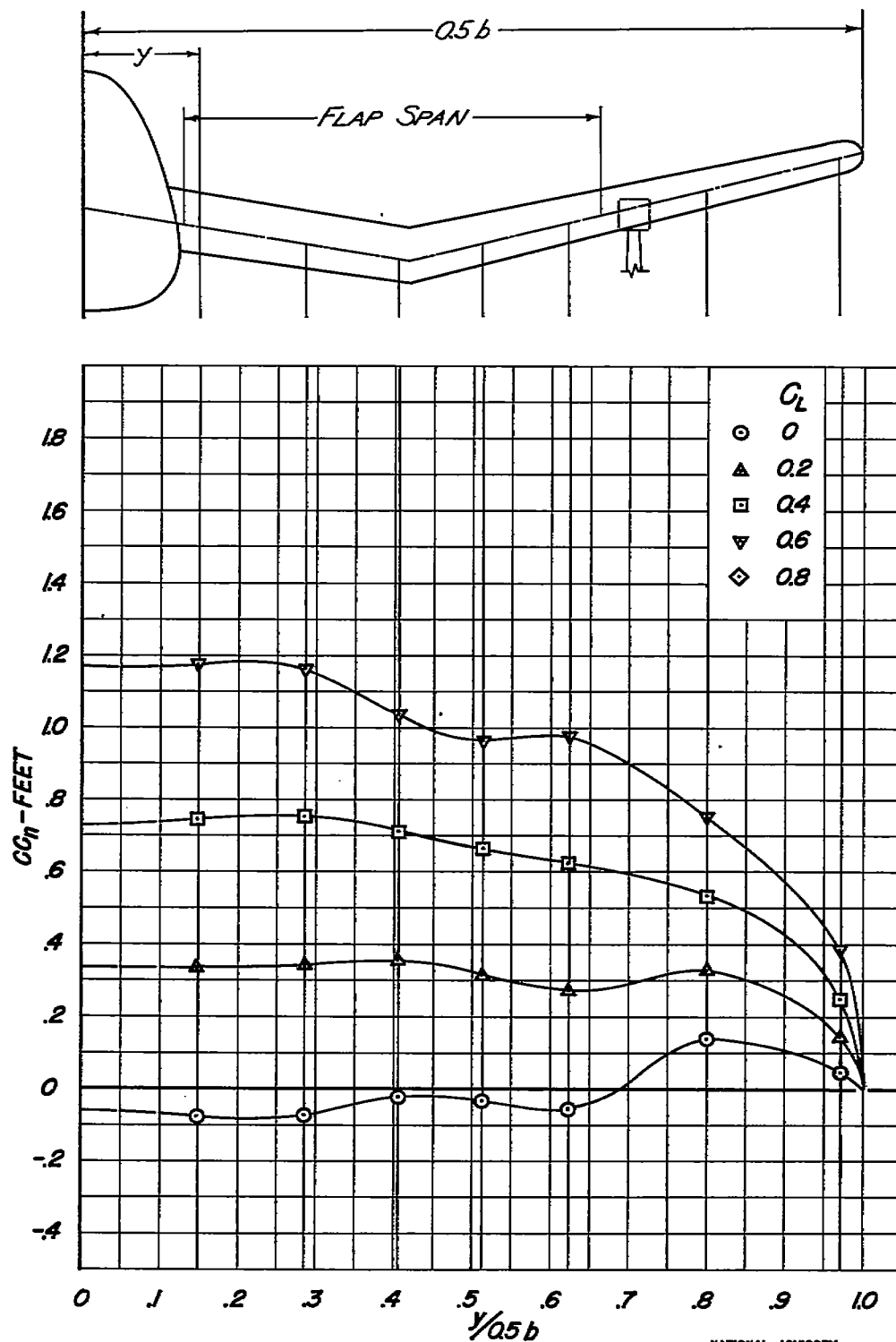
(i)  $M=0.73$ NATIONAL ADVISORY  
COMMITTEE FOR AERONAUTICS

FIGURE 23.- CONTINUED.

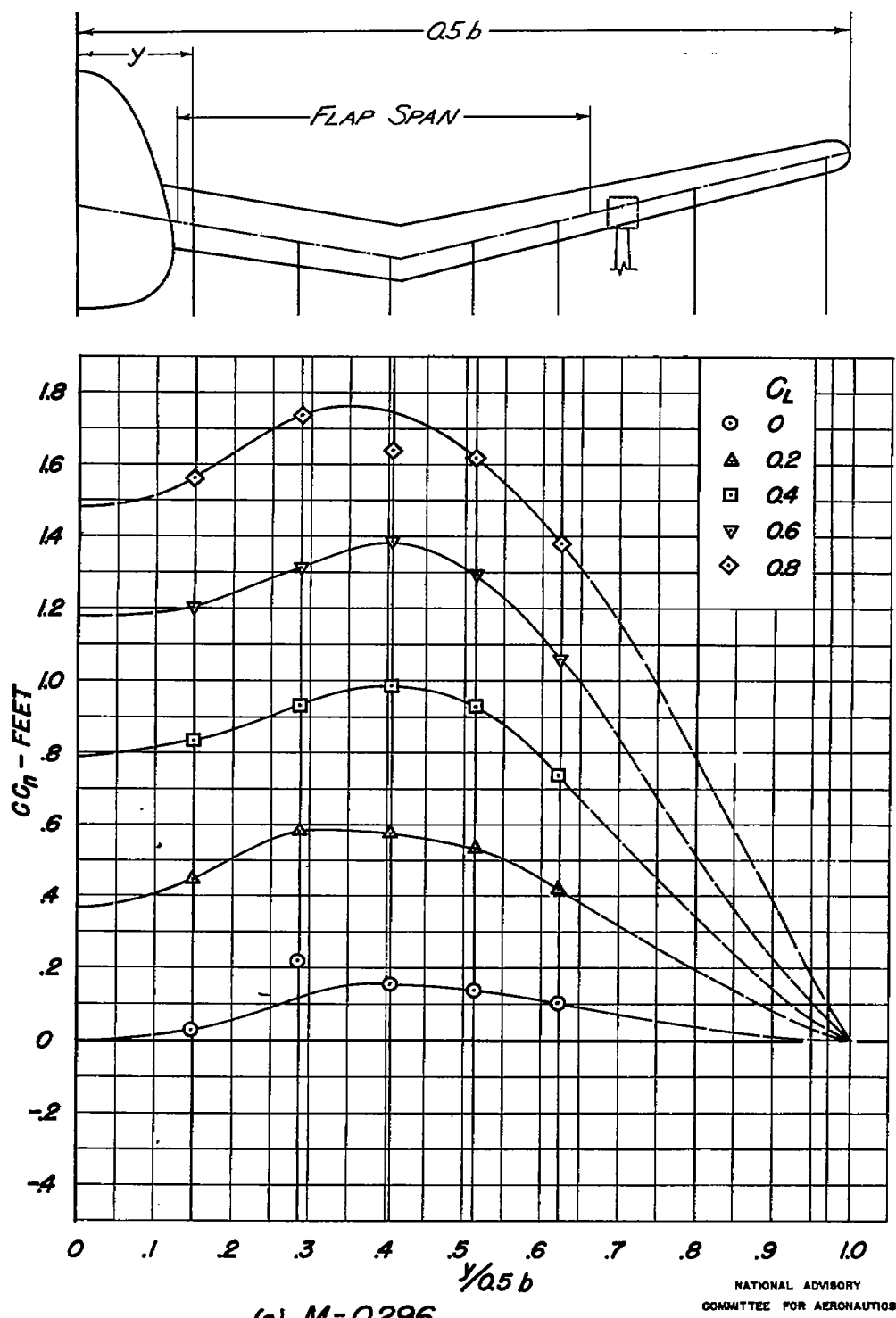
(g)  $M = 0.778$ 

NATIONAL ADVISORY  
COMMITTEE FOR AERONAUTICS

FIGURE 23. - CONCLUDED.

Fig. 24a

NACA RM No. A7D23

(a)  $M = 0.296$ FIGURE 24.- SPANWISE VARIATION OF THE NORMAL FORCE WITH  
LANDING FLAPS DEFLECTED  $10^\circ$ .

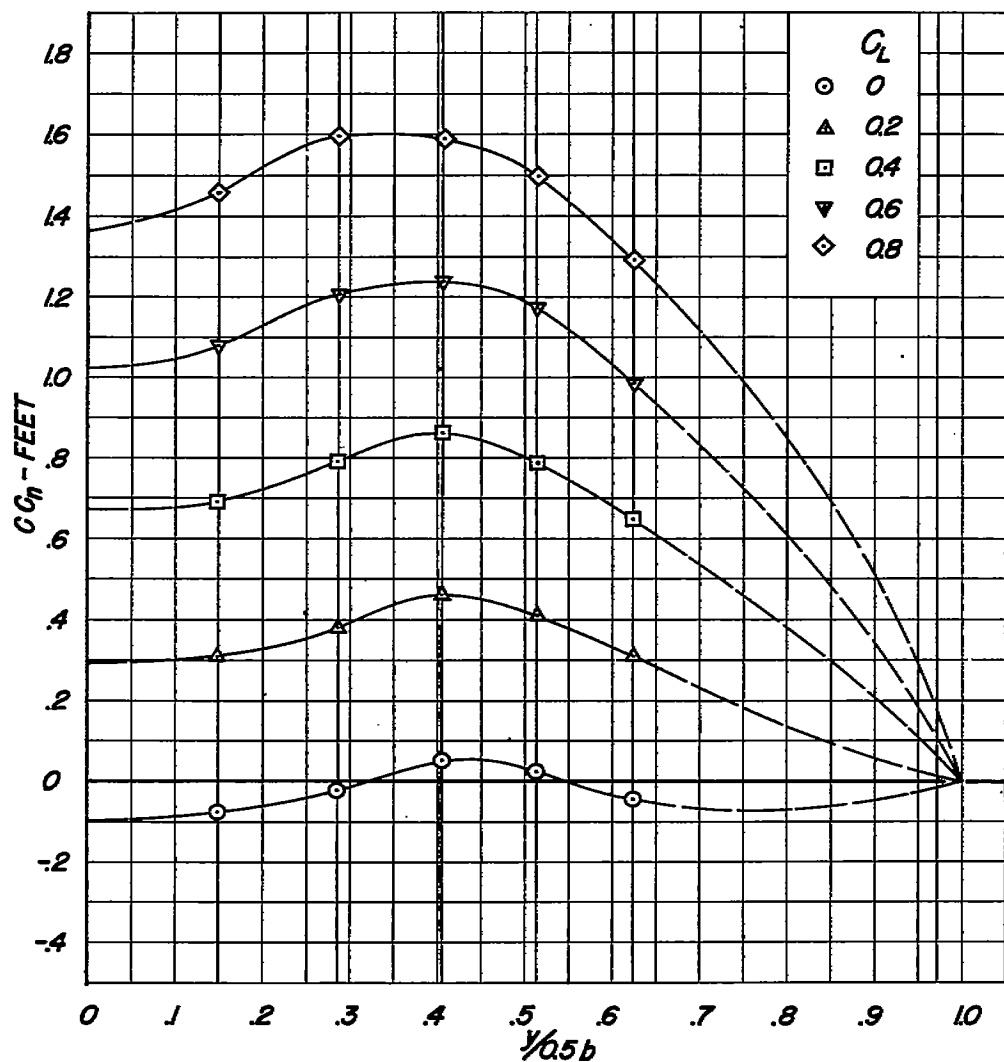
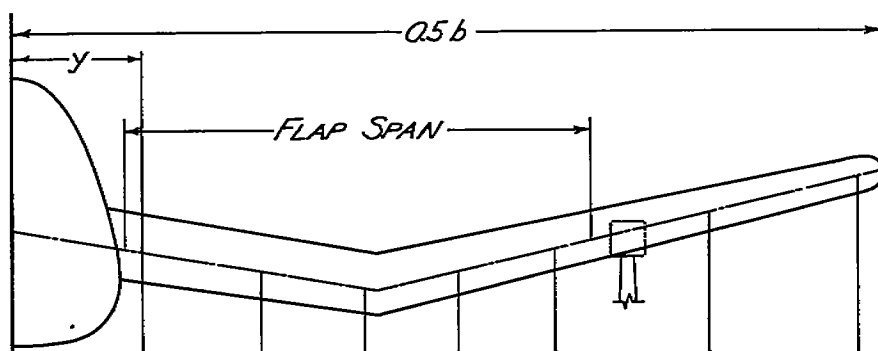
(b)  $M = 0.494$ NATIONAL ADVISORY  
COMMITTEE FOR AERONAUTICS

FIGURE 24.-CONTINUED

Fig. 24c

NACA RM No. A7D23

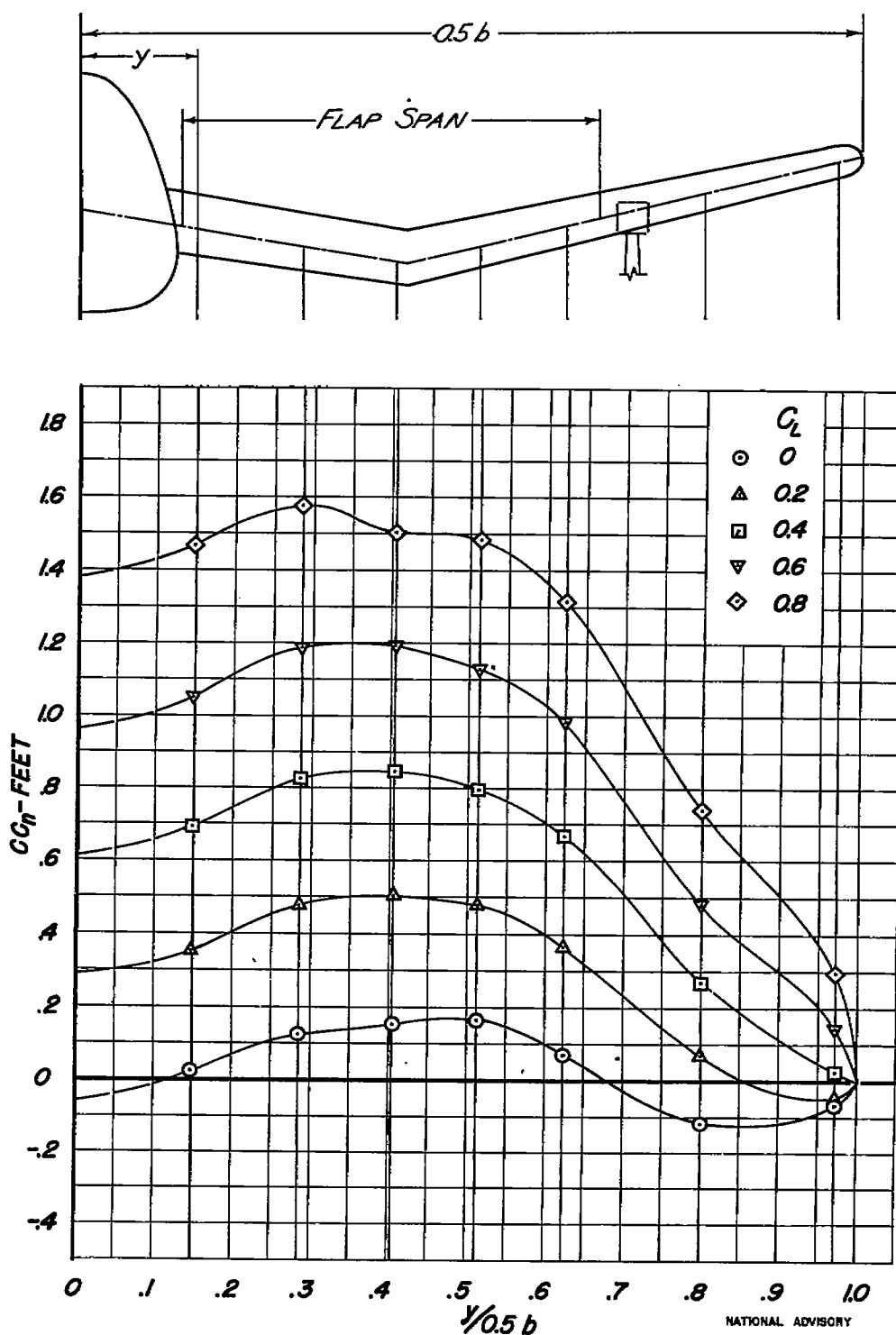
(c)  $M=0.591$ 

FIGURE 24.- CONTINUED.

NATIONAL ADVISORY  
COMMITTEE FOR AERONAUTICS

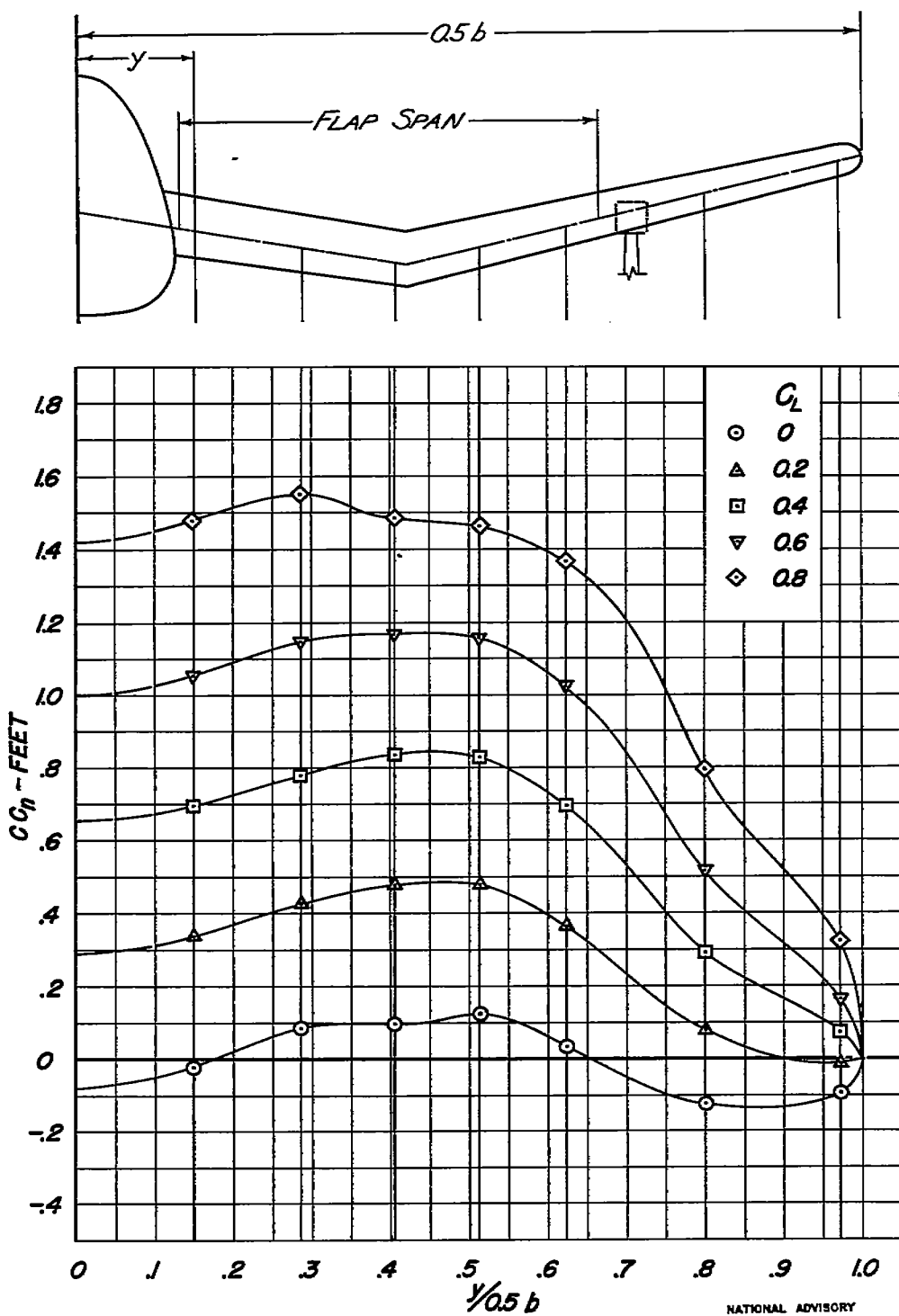
(d)  $M = 0.638$ NATIONAL ADVISORY  
COMMITTEE FOR AERONAUTICS

FIGURE 24. - CONTINUED.

Fig. 24e

NACA RM No. A7D23

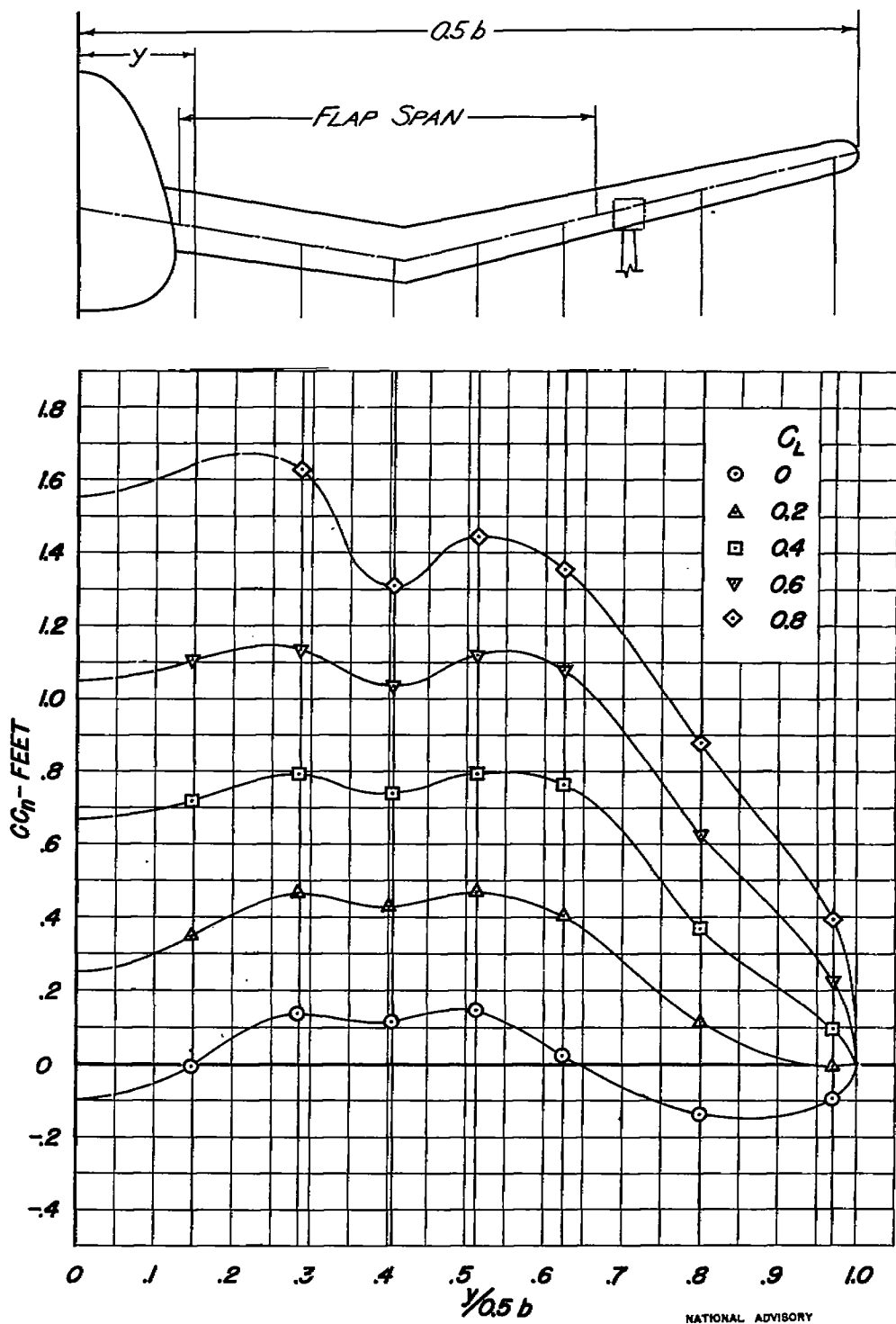
(e)  $M = 0.685$ 

FIGURE 24. - CONTINUED.

NATIONAL ADVISORY  
COMMITTEE FOR AERONAUTICS

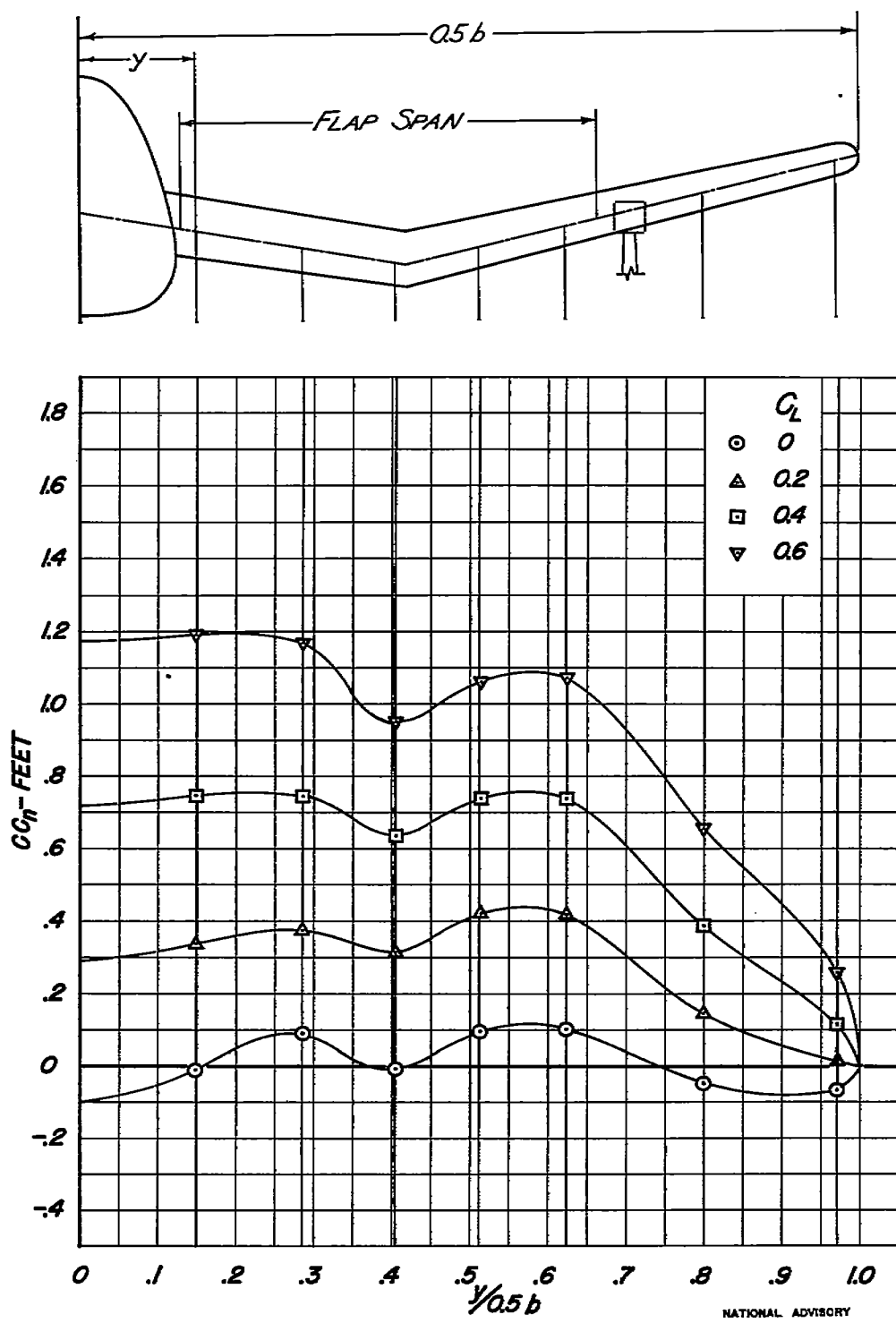
(f)  $M = 0.73$ NATIONAL ADVISORY  
COMMITTEE FOR AERONAUTICS

FIGURE 24.-CONTINUED.

Fig. 24g

NACA RM No. A7D23

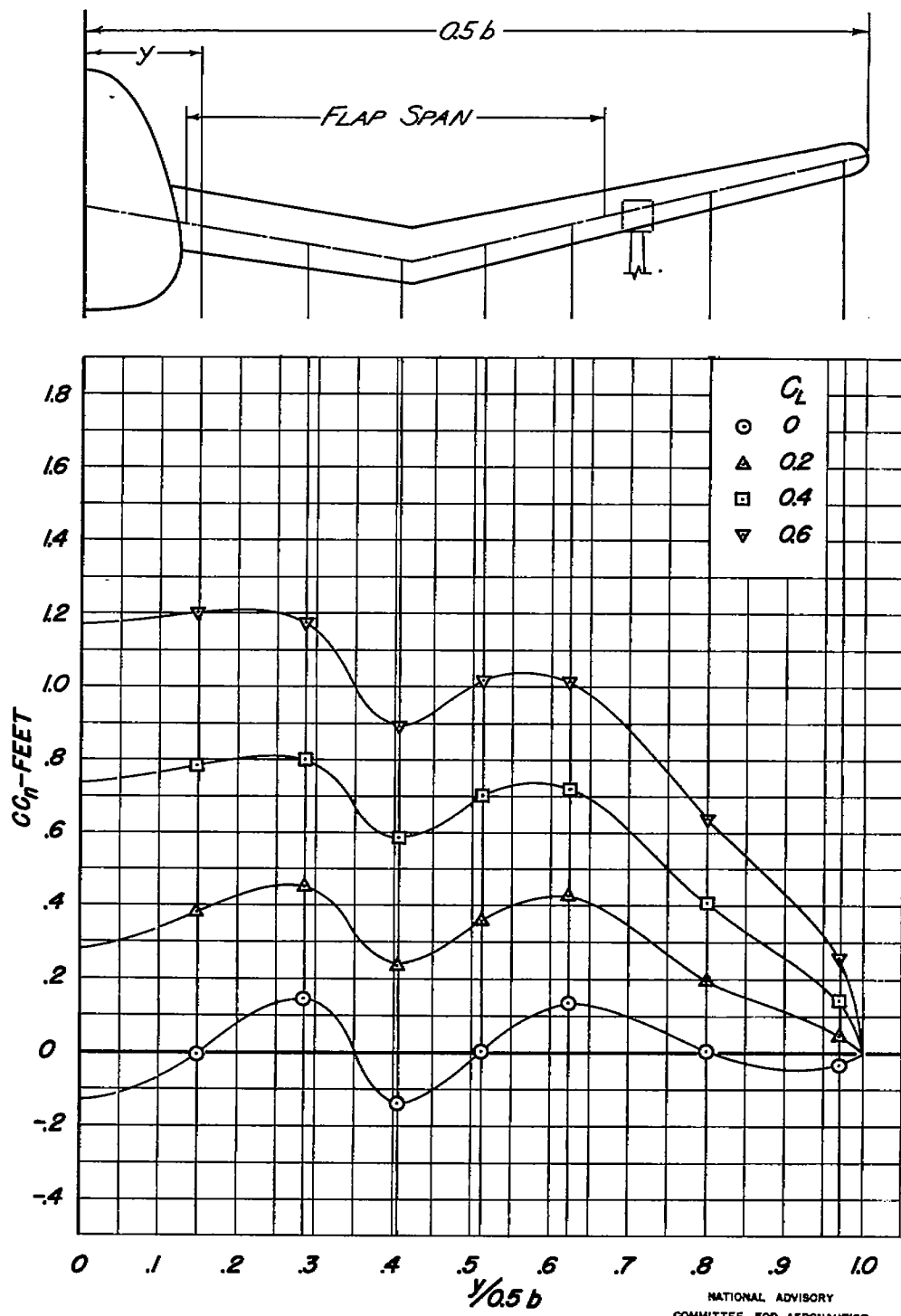
(g)  $M = 0.778$ NATIONAL ADVISORY  
COMMITTEE FOR AERONAUTICS

FIGURE 24.-CONCLUDED.

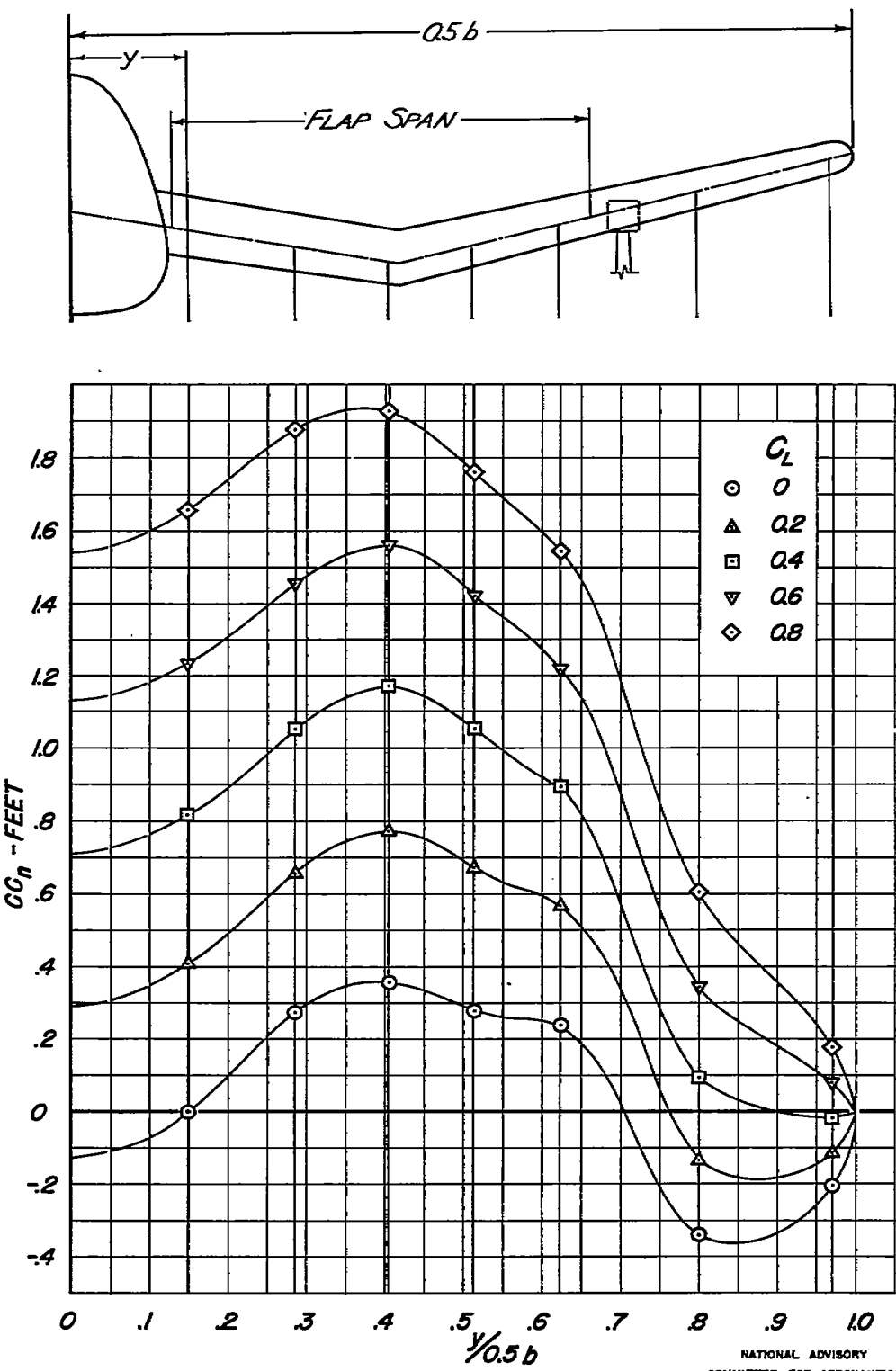
(a)  $M = 0.296$ 

FIGURE 25.- SPANWISE VARIATION OF THE NORMAL FORCE WITH  
LANDING FLAPS DEFLECTED 40°.

NATIONAL ADVISORY  
COMMITTEE FOR AERONAUTICS

Fig. 25b

NACA RM No. A7D23

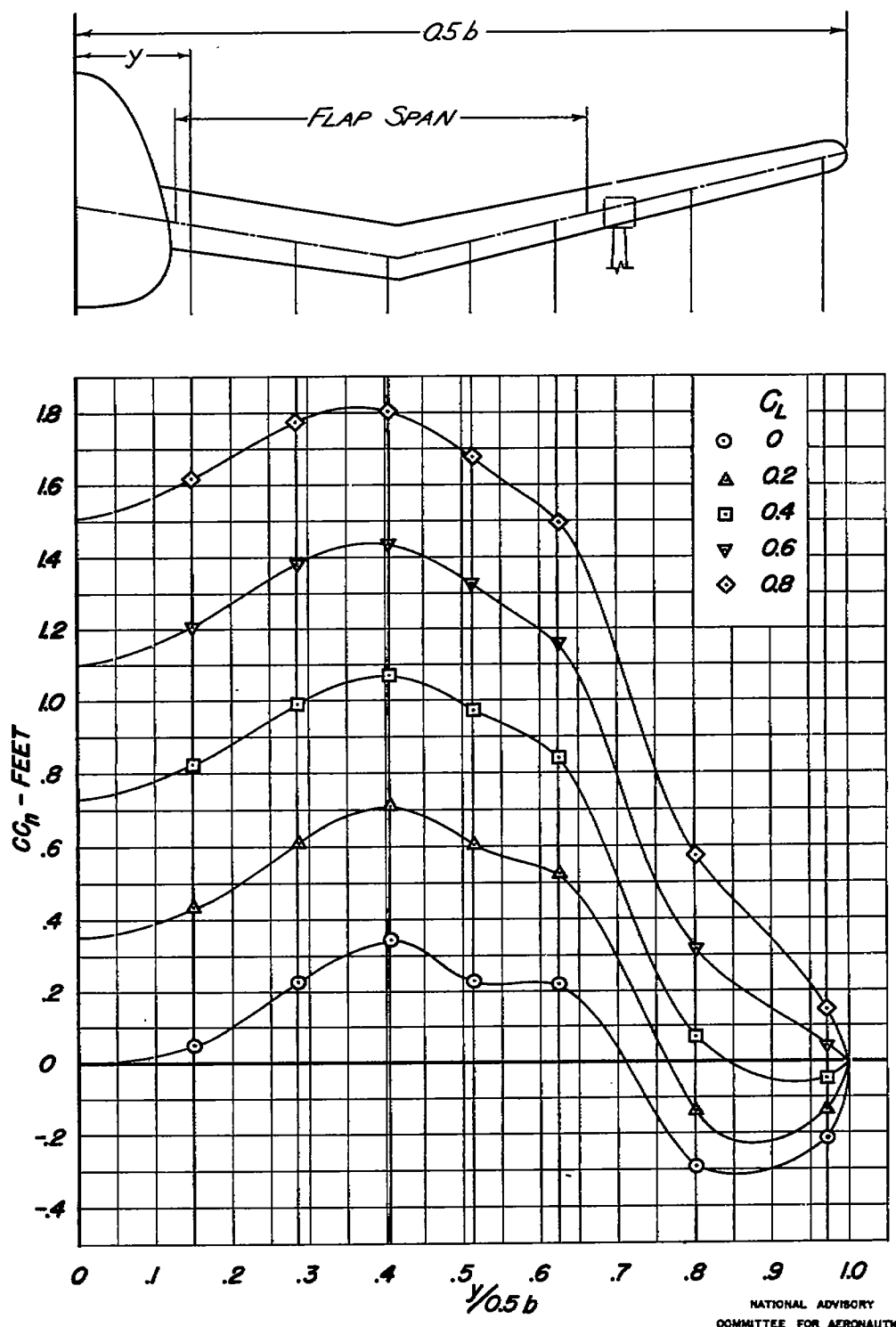
(b)  $M = 0.494$ 

FIGURE 25.- CONTINUED

NATIONAL ADVISORY  
COMMITTEE FOR AERONAUTICS

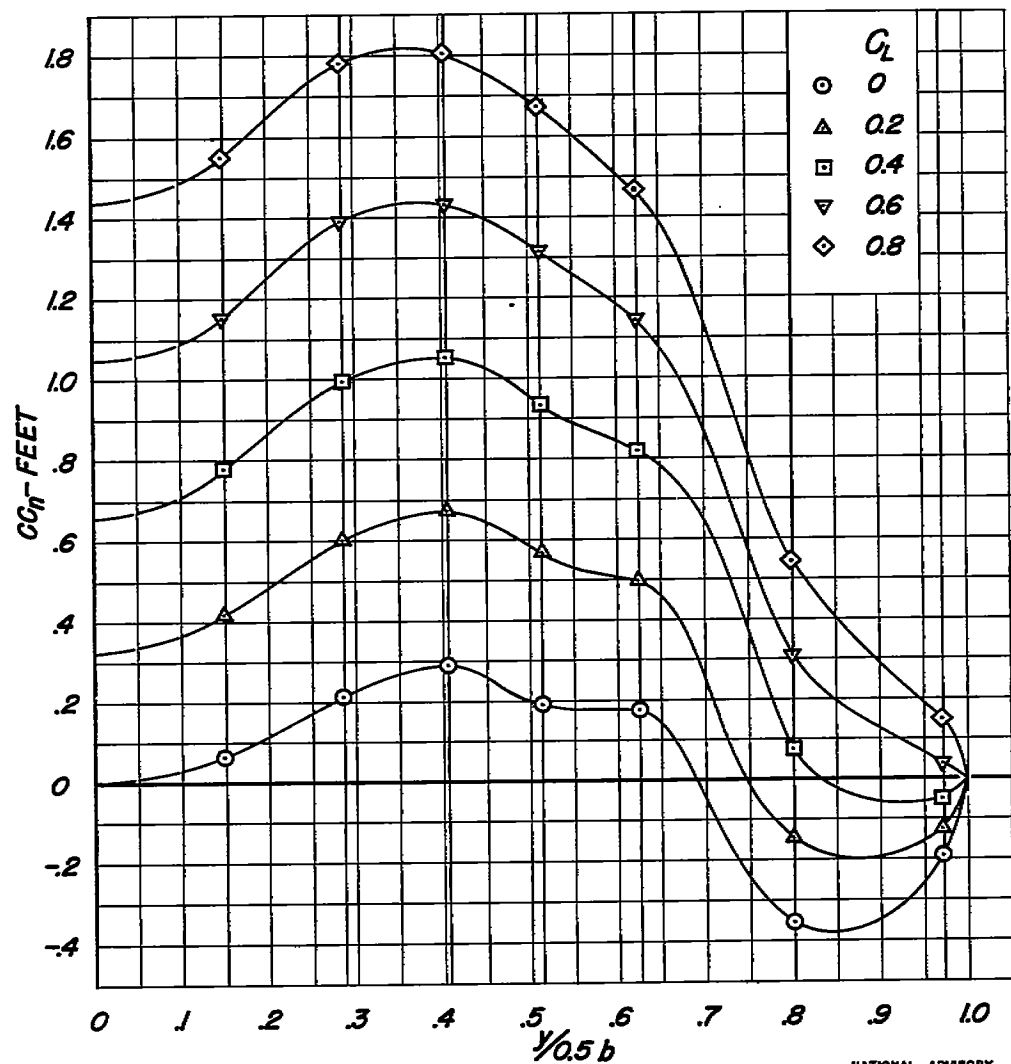
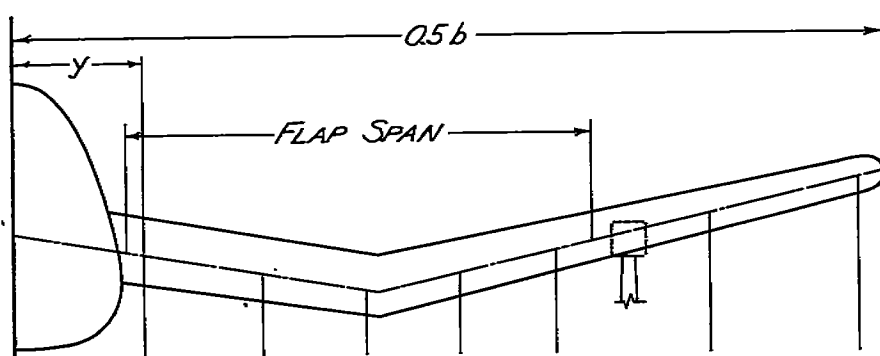
(c)  $M = 0.591$ NATIONAL ADVISORY  
COMMITTEE FOR AERONAUTICS

FIGURE 25. - CONTINUED.

Fig. 25d

NACA RM No. A7D23

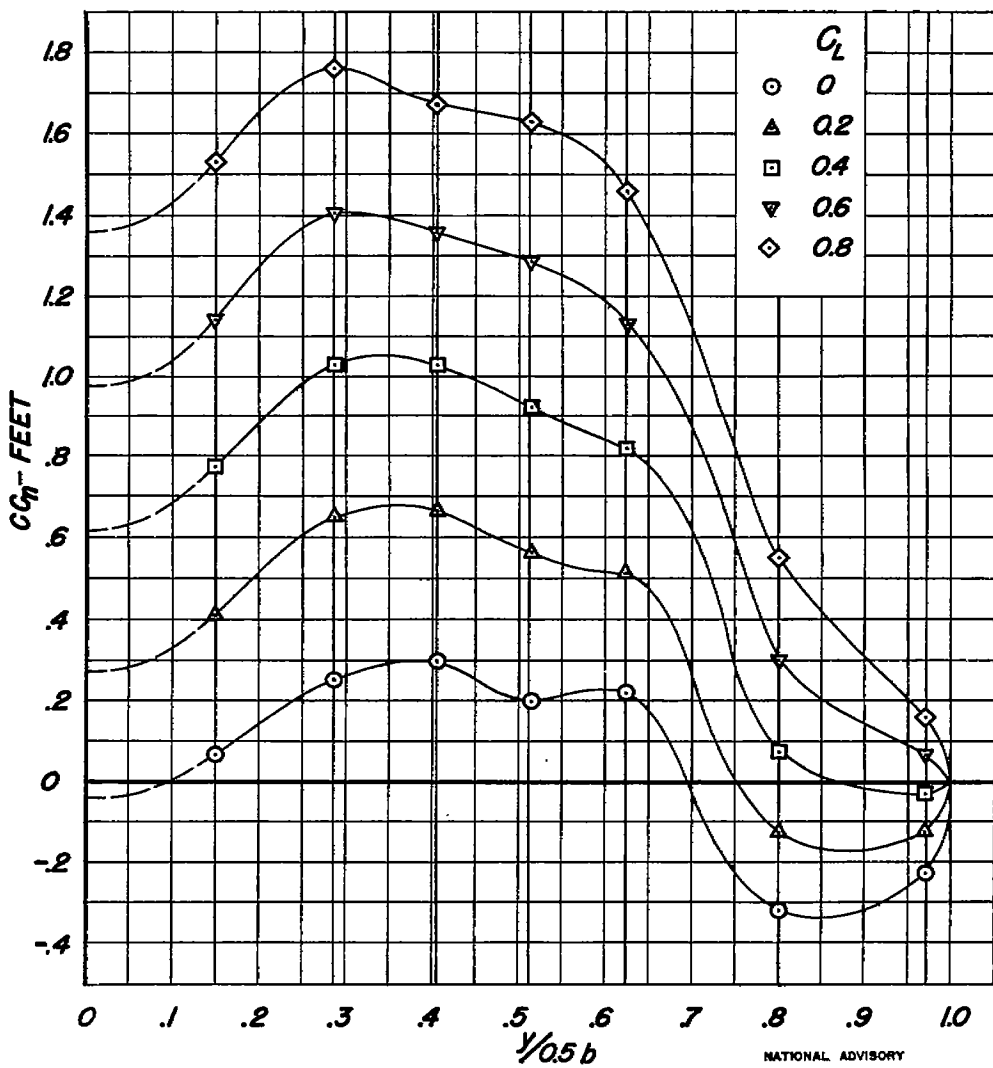
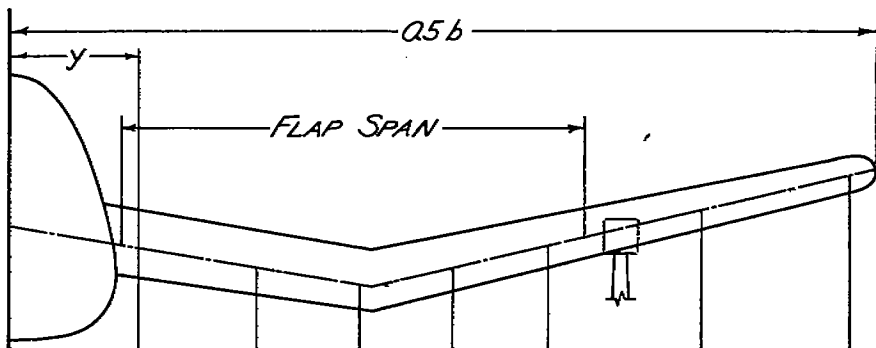
(d)  $M = 0.638$ 

FIGURE 25.- CONTINUED.

NATIONAL ADVISORY  
COMMITTEE FOR AERONAUTICS

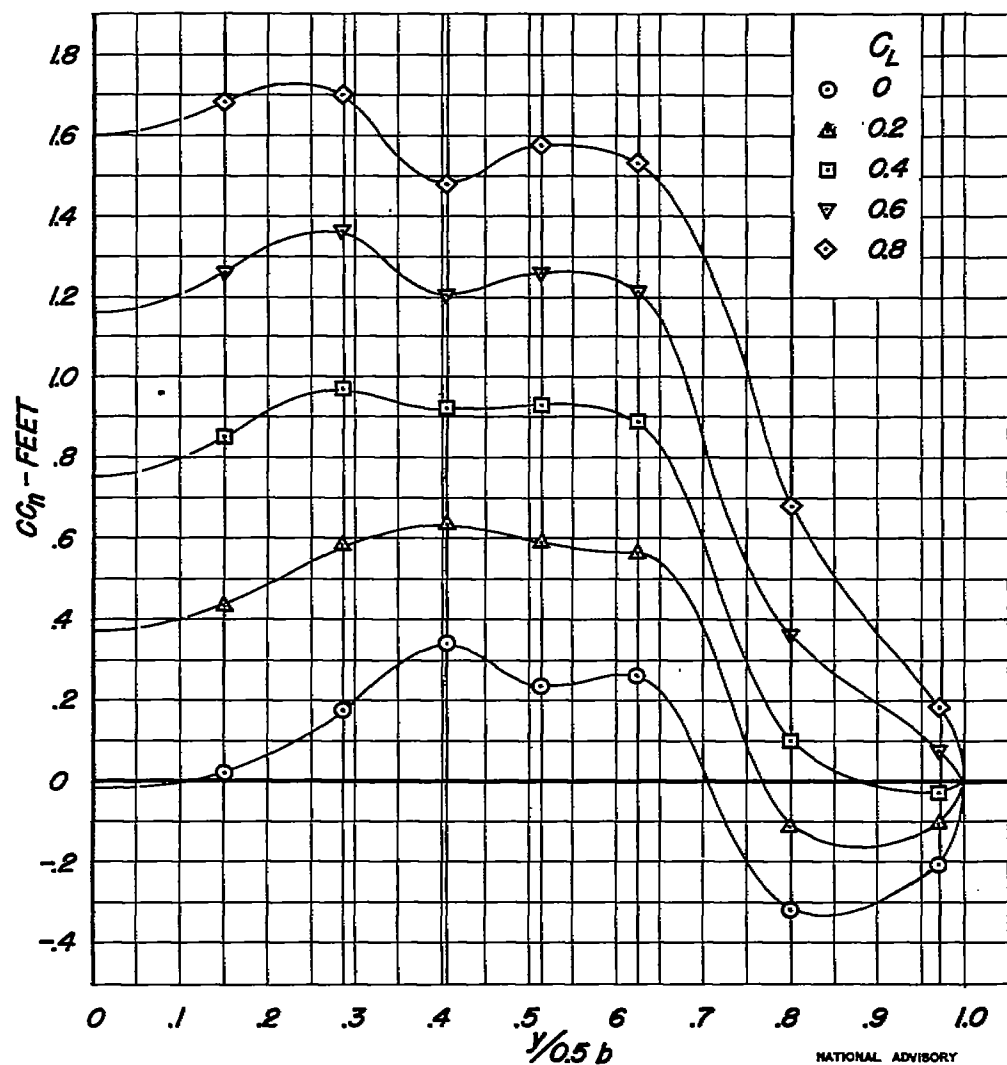
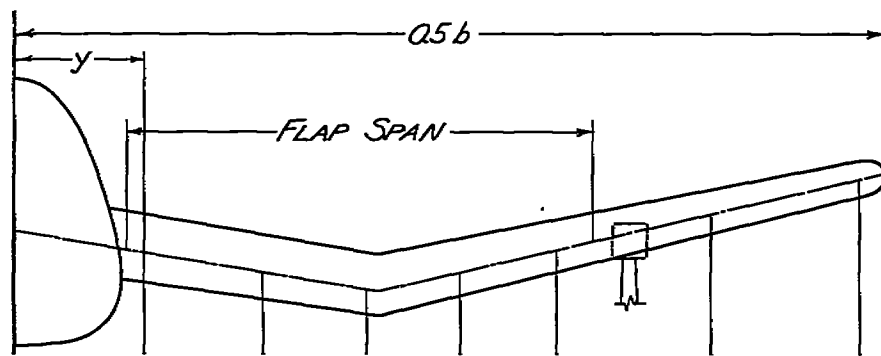
(e)  $M = 0.685$ NATIONAL ADVISORY  
COMMITTEE FOR AERONAUTICS

FIGURE 25. - CONTINUED.

Fig. 25f

NACA RM No. A7D23

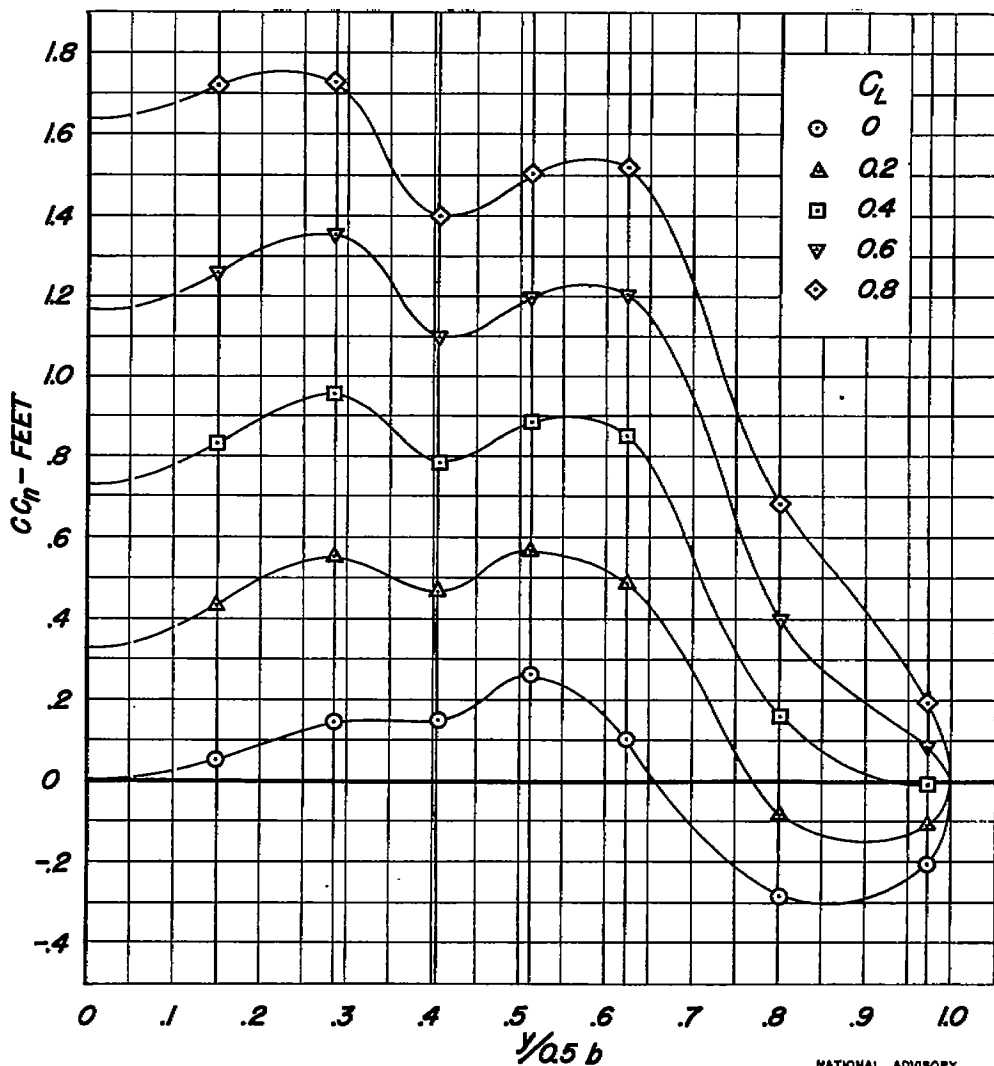
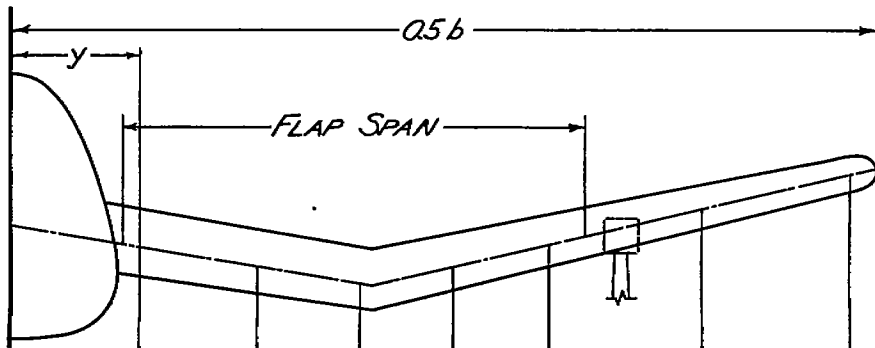
(f)  $M = 0.73$ NATIONAL ADVISORY  
COMMITTEE FOR AERONAUTICS

FIGURE 25. - CONTINUED.

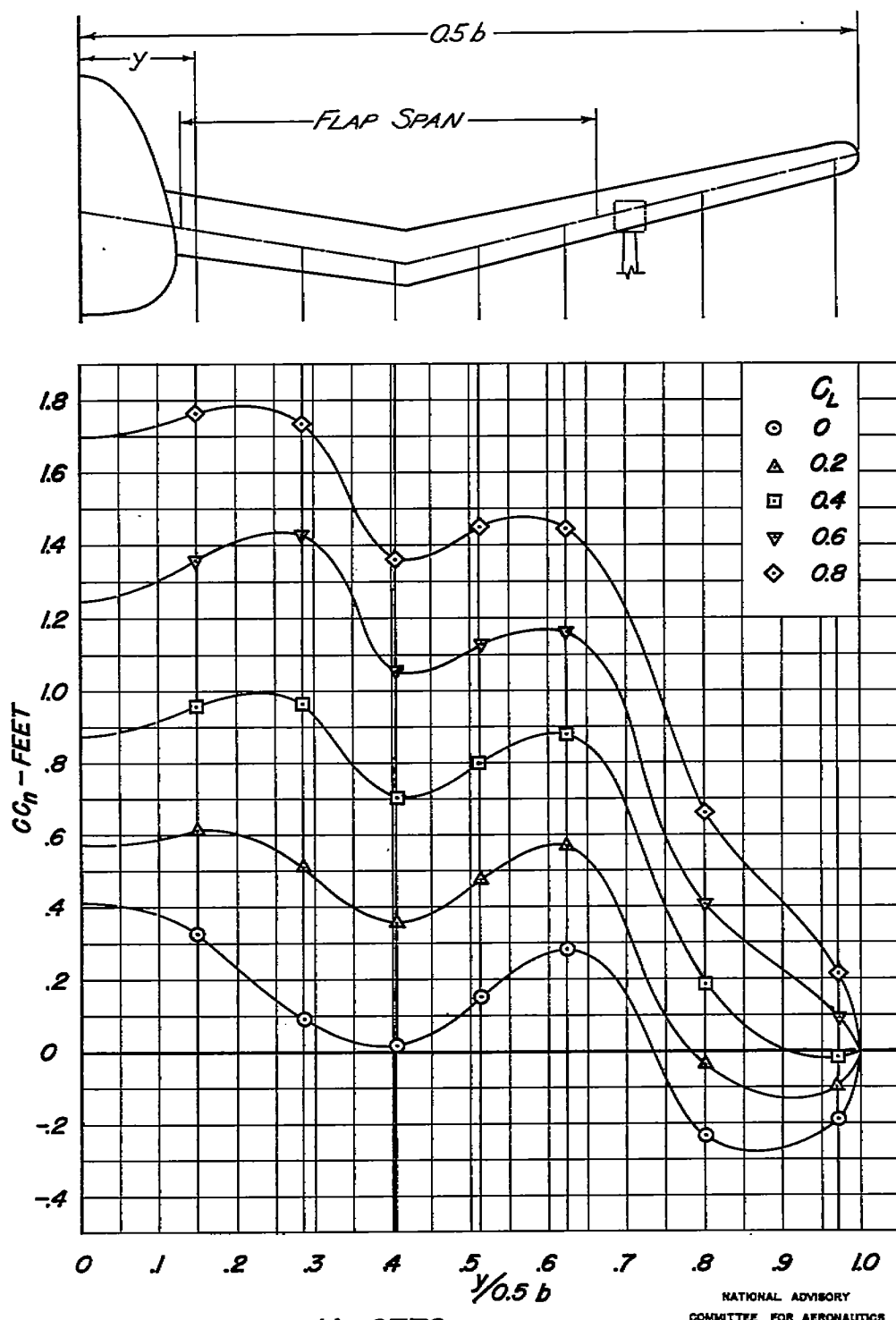
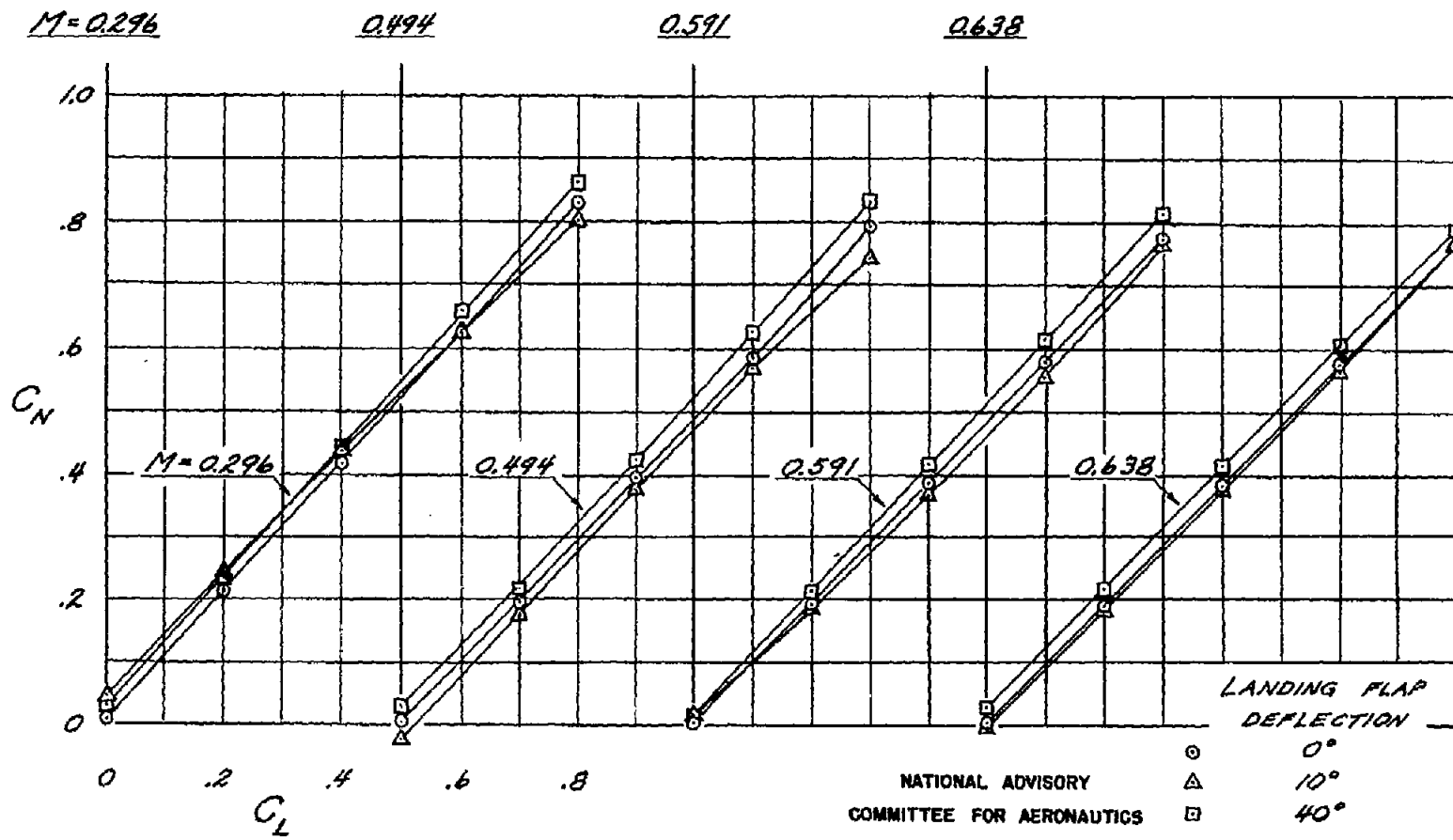
(g)  $M = 0.778$ 

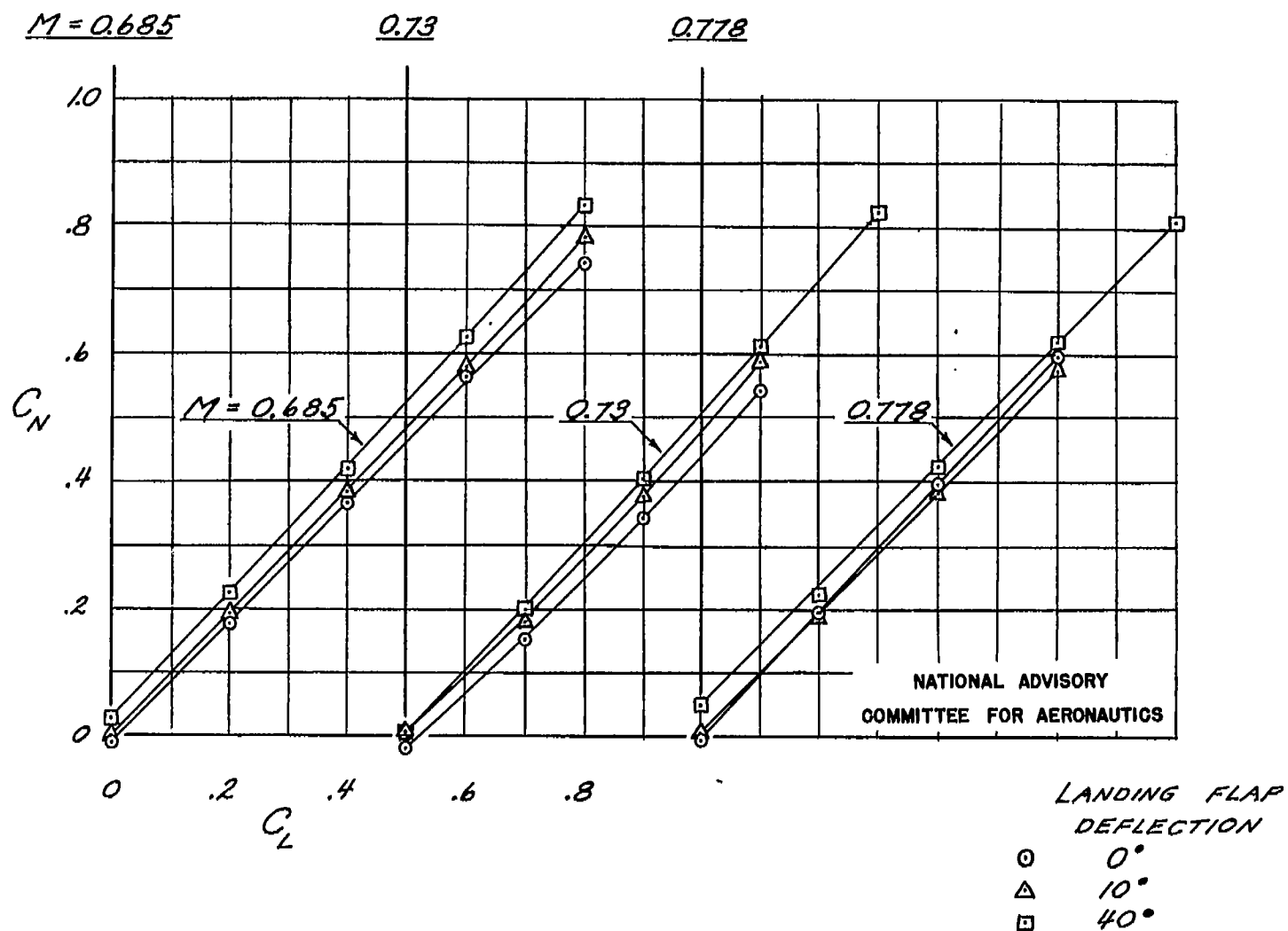
FIGURE 25. - CONCLUDED.

FIG. 26a

NACA RM No. A7D23



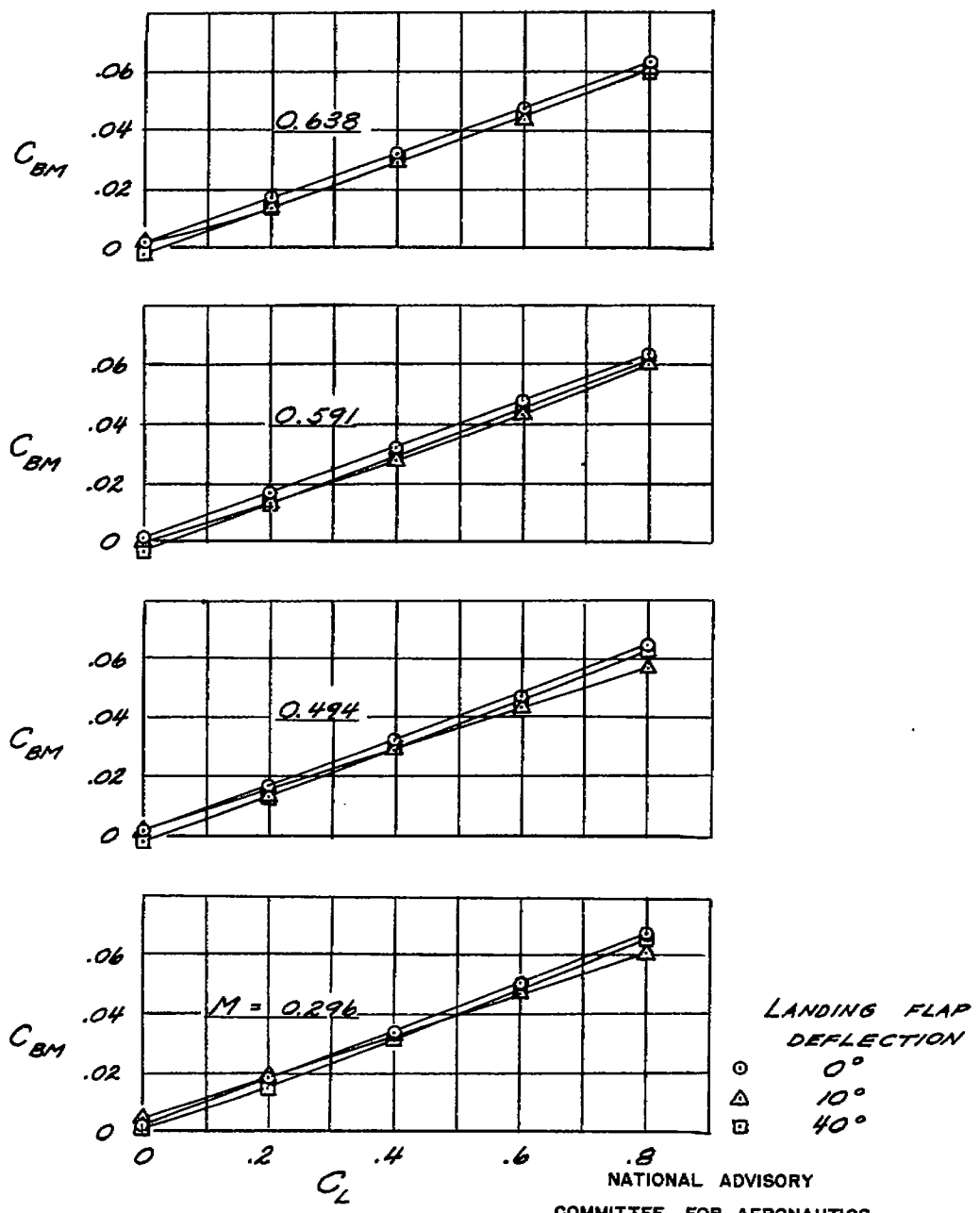
(a)  $M = 0.296, 0.494, 0.591$ , AND  $0.638$   
 FIGURE 26.- VARIATION OF THE WING NORMAL-FORCE COEFFICIENT WITH TAIL-OFF LIFT  
 COEFFICIENT FOR THREE LANDING-FLAP DEFLECTIONS.



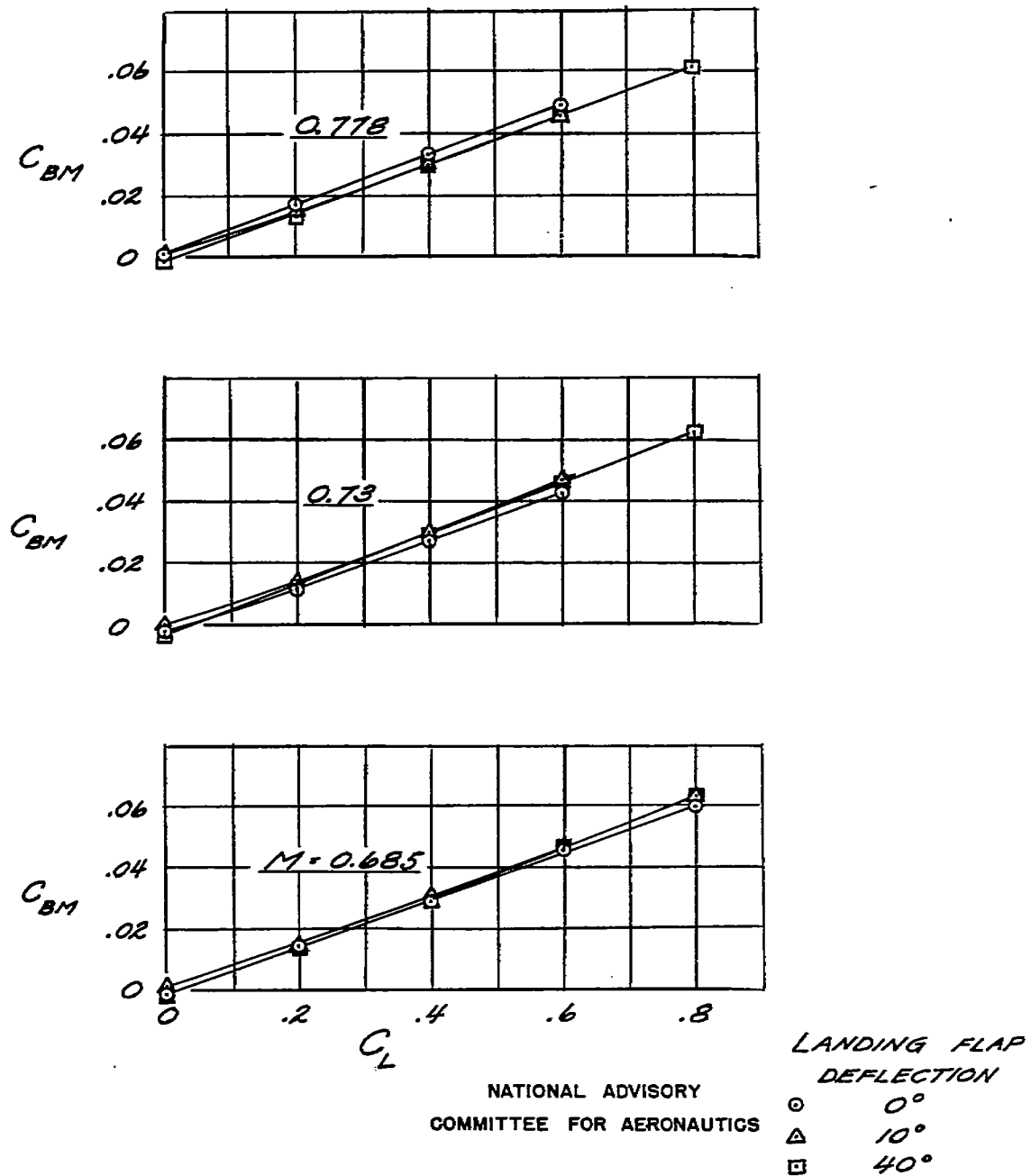
(b)  $M = 0.685, 0.73$ , AND  $0.778$   
FIGURE 26 .- CONCLUDED

Fig. 27a

NACA RM No. A7D23



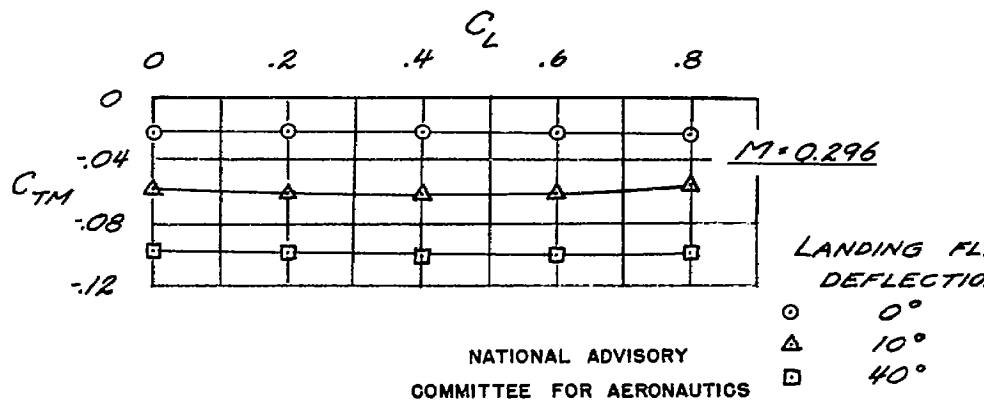
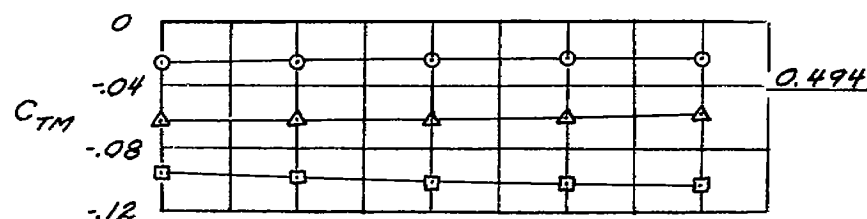
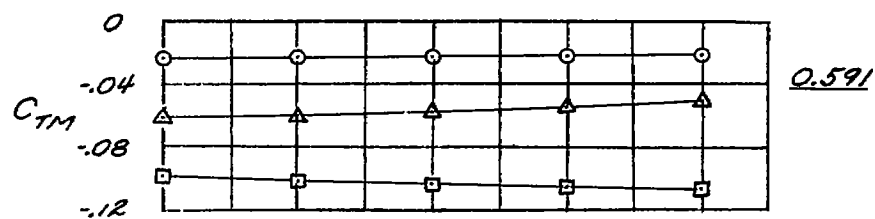
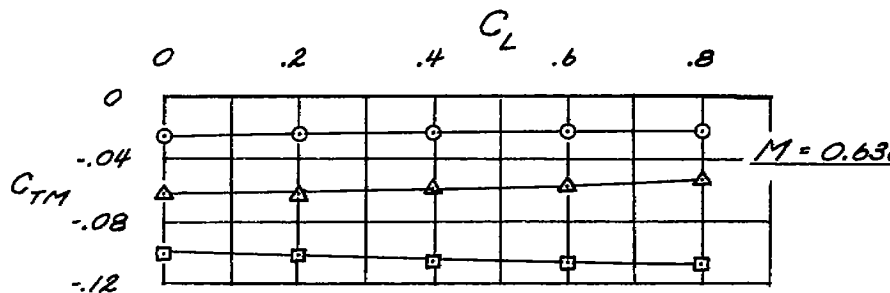
(a)  $M = 0.296, 0.494, 0.591$ , AND  $0.638$   
**FIGURE 27.- VARIATION OF THE ROOT BENDING-MOMENT COEFFICIENT WITH THE TAIL-OFF LIFT COEFFICIENT FOR THREE LANDING -FLAP DEFLECTIONS.**



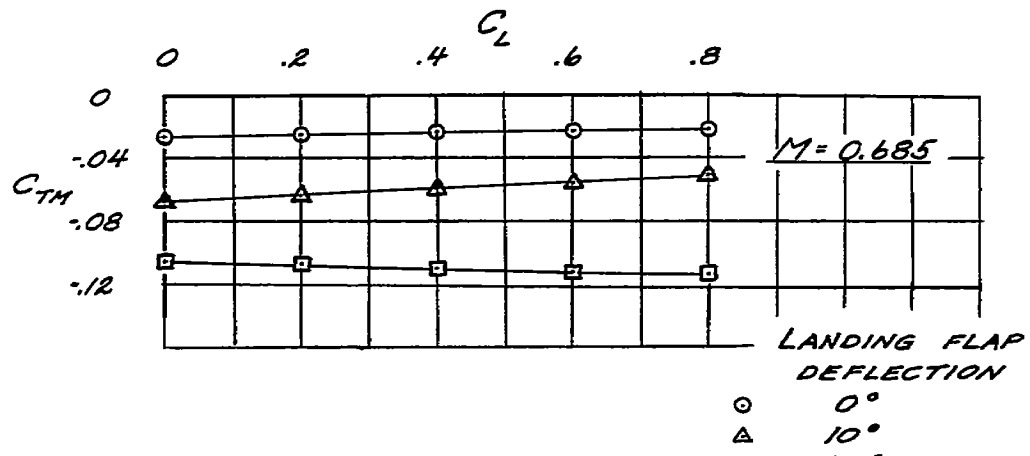
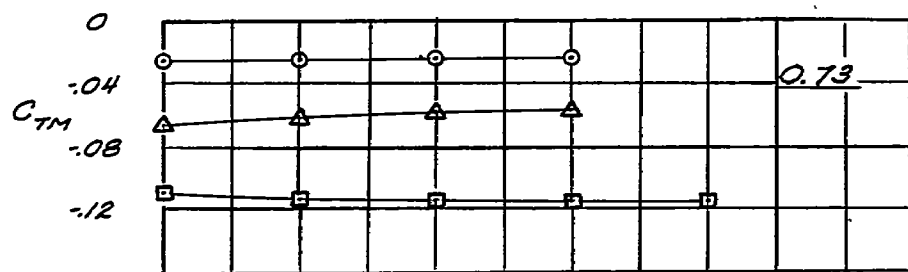
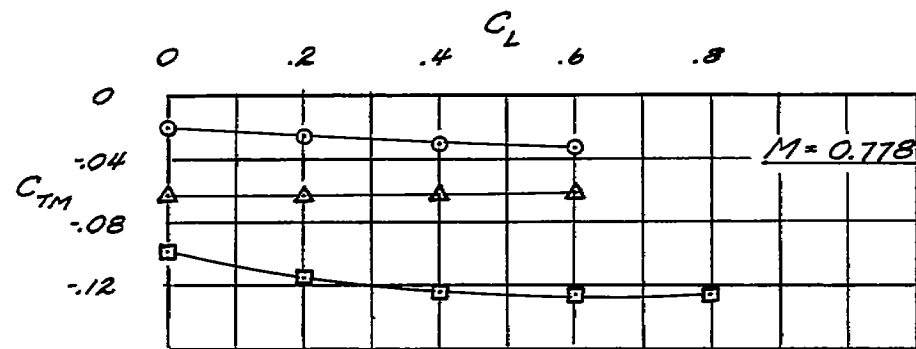
(b)  $M = 0.685, 0.73, \text{ and } 0.778$   
FIGURE 27. - CONCLUDED

Fig. 28a

NACA RM No. A7D23

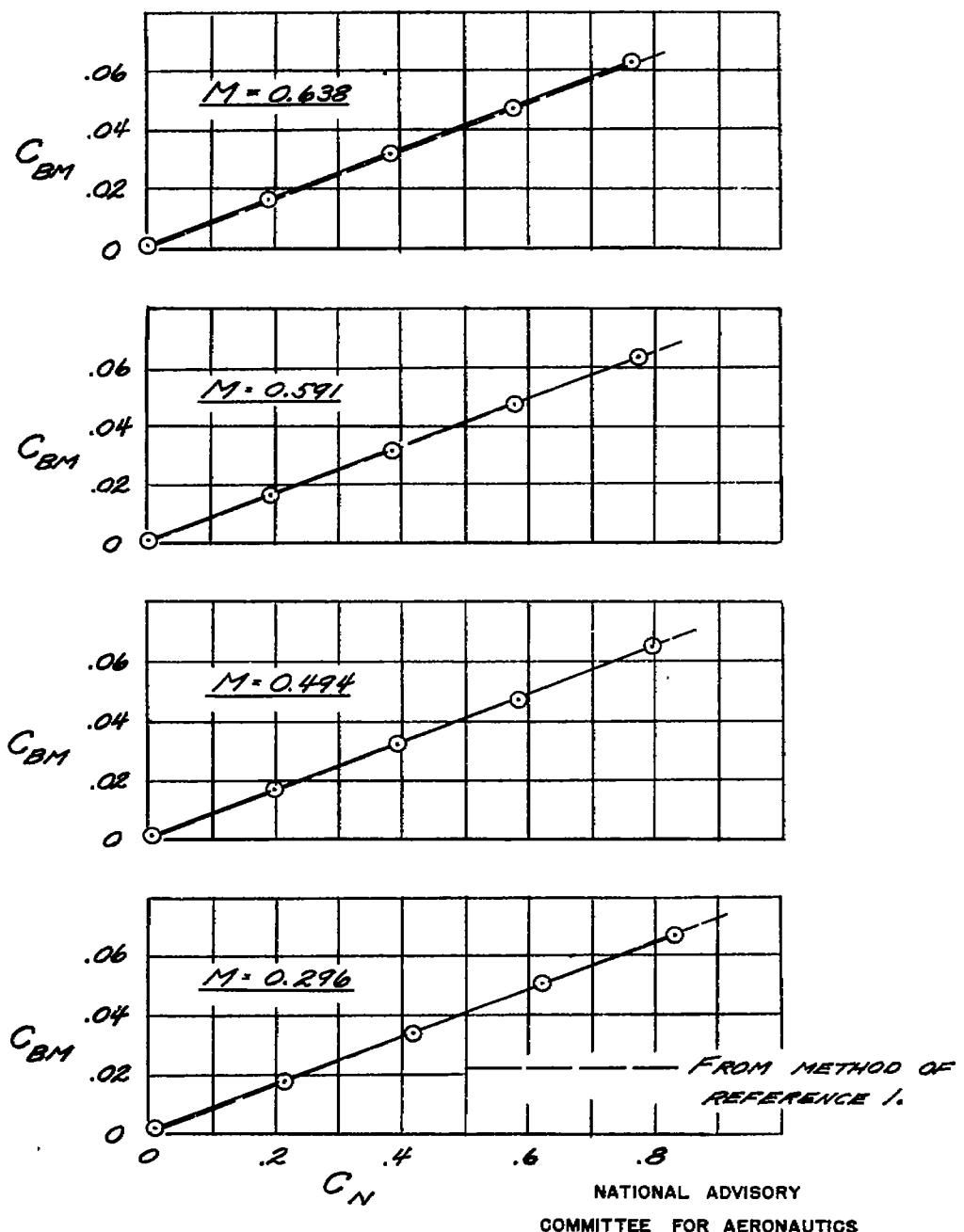


(a)  $M = 0.296, 0.494, 0.591$ , AND  $0.638$   
**FIGURE 28.- VARIATION OF THE ROOT TORSIONAL-MOMENT COEFFICIENT WITH THE TAIL-OFF LIFT COEFFICIENT FOR THREE LANDING-FLAP DEFLECTIONS.**

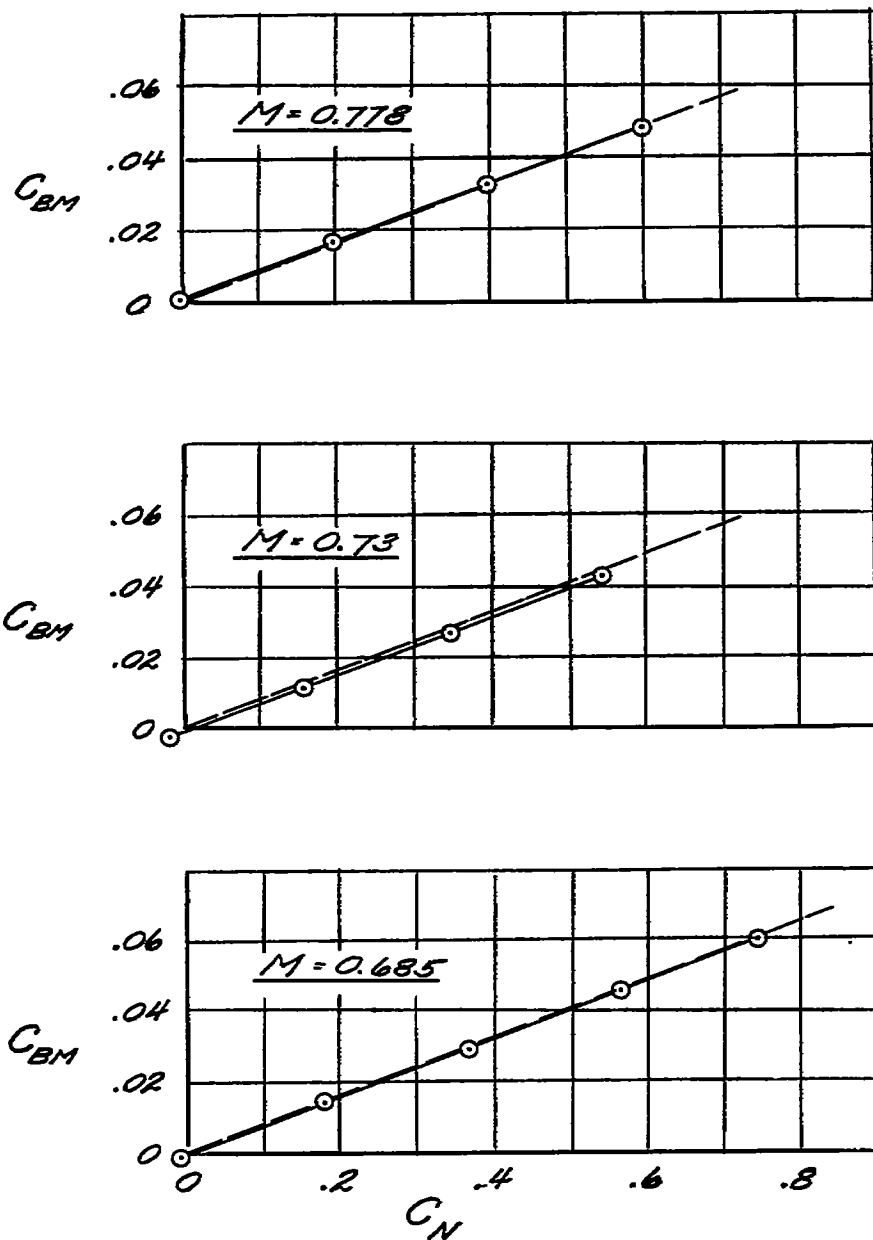


NATIONAL ADVISORY  
COMMITTEE FOR AERONAUTICS

(b) -  $M = 0.685, 0.73, \text{ AND } 0.778$   
FIGURE 28.- (CONCLUDED)



(a)  $M = 0.296, 0.494, 0.591$ , AND  $0.638$   
**FIGURE 29. - COMPARISON OF THE VARIATION OF ROOT BENDING-MOMENT COEFFICIENT WITH NORMAL-FORCE COEFFICIENT AS DETERMINED EXPERIMENTALLY AND BY THE METHOD OF REFERENCE 1. LANDING FLAPS NEUTRAL.**

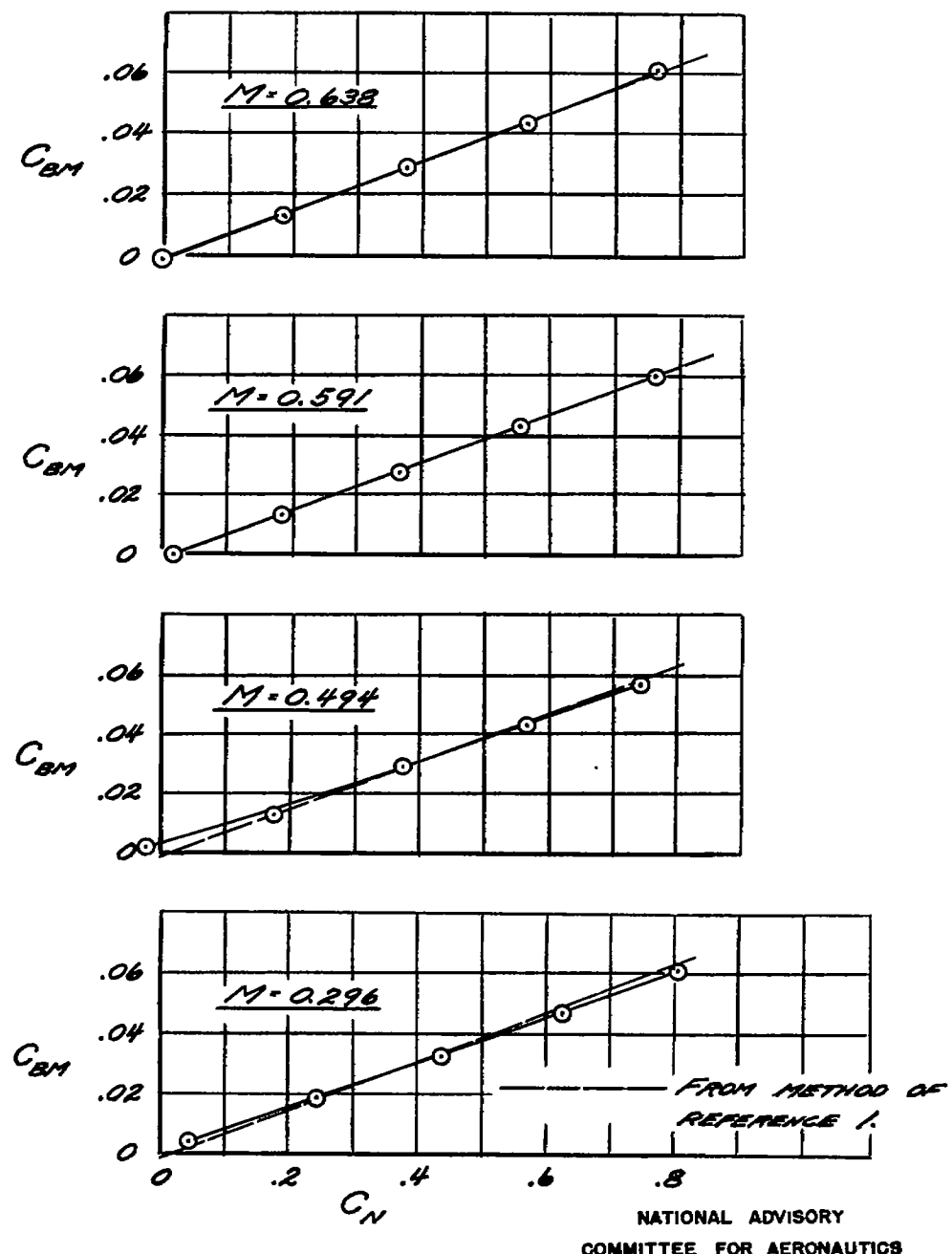


— — — — — FROM METHOD OF REFERENCE!

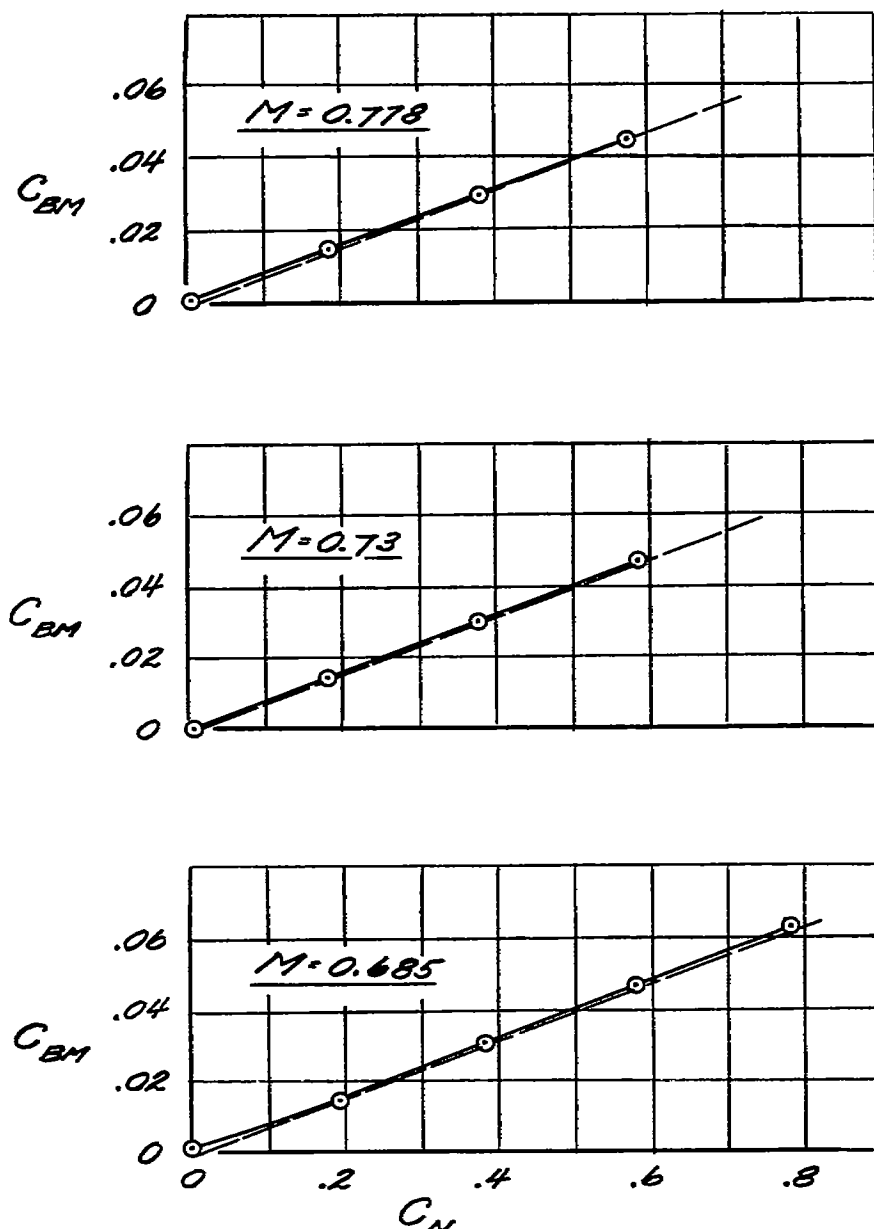
NATIONAL ADVISORY  
COMMITTEE FOR AERONAUTICS

(b)  $M = 0.685, 0.73$ , AND  $0.778$

FIGURE 29.- CONCLUDED



(a)  $M = 0.296, 0.494, 0.591$ , AND  $0.638$   
 FIGURE 30.- COMPARISON OF THE VARIATION OF ROOT BENDING-MOMENT COEFFICIENT WITH NORMAL-FORCE COEFFICIENT AS DETERMINED EXPERIMENTALLY AND BY THE METHOD OF REFERENCE 1. LANDING FLAPS DEFLECTED  $10^\circ$ .



— — — FROM METHOD OF REFERENCE 1.

NATIONAL ADVISORY  
COMMITTEE FOR AERONAUTICS

(b)  $M = 0.685, 0.73, \text{ AND } 0.778$

FIGURE 30 . - CONCLUDED

Fig. 31a

NACA RM No. A7D23

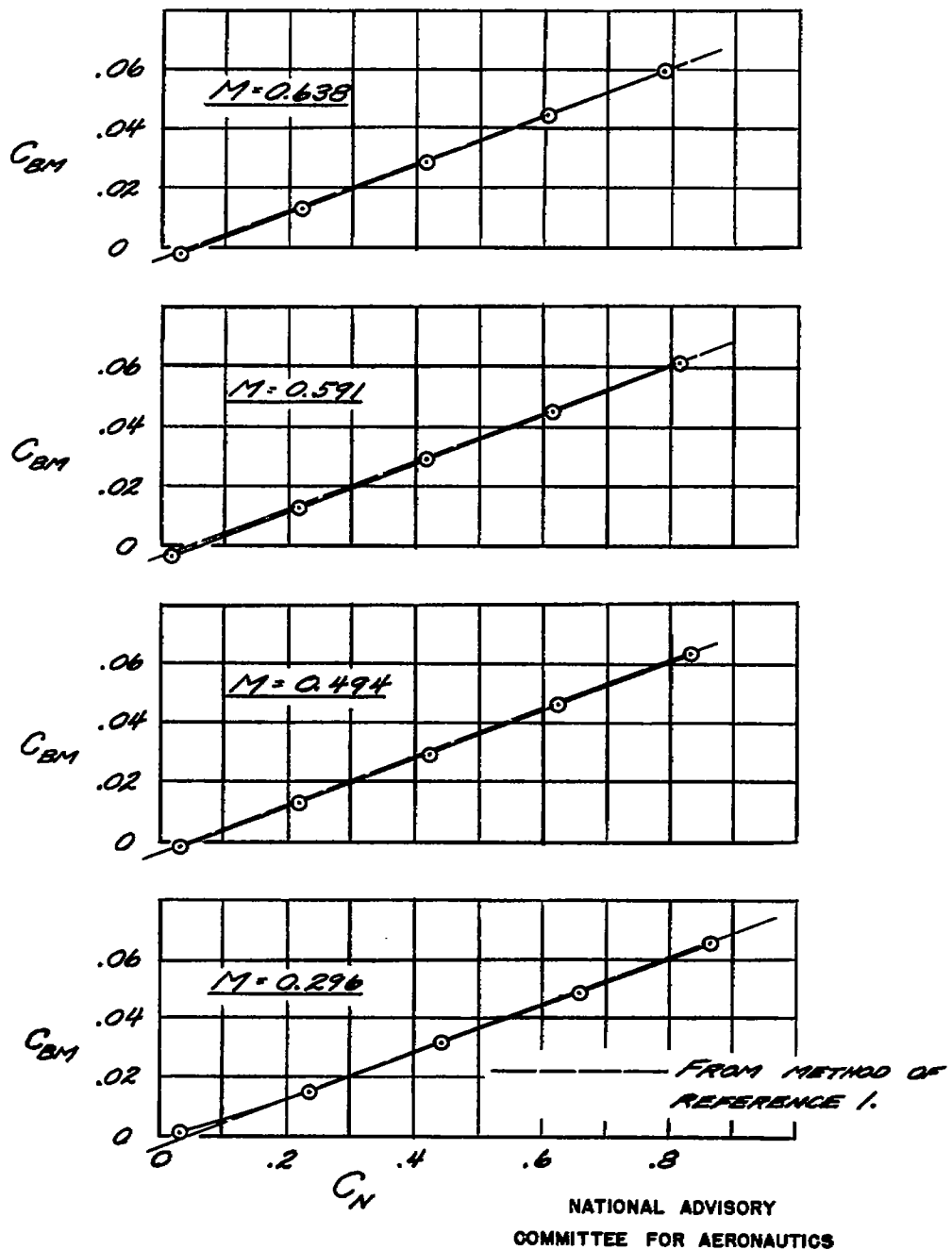
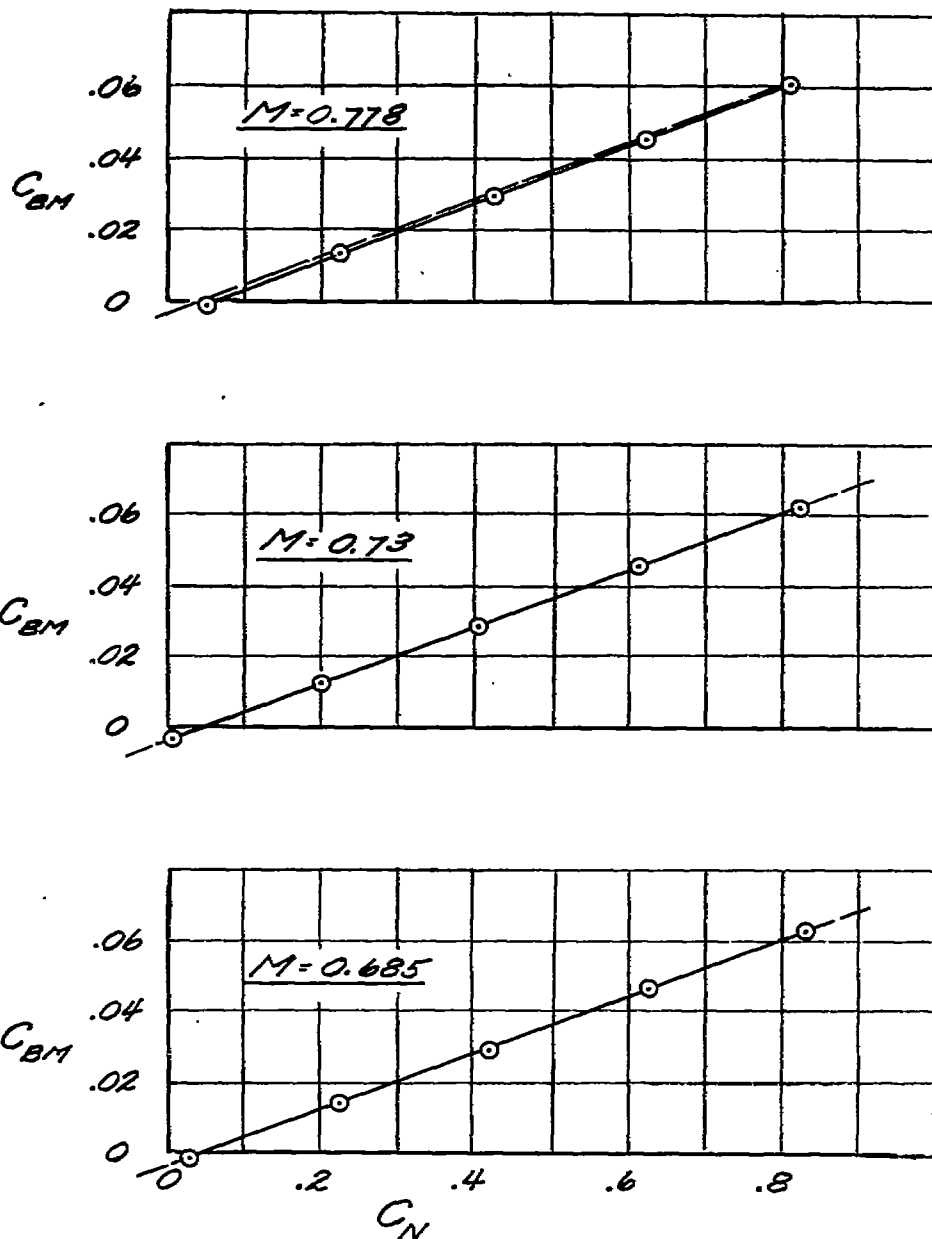
(a)  $M = 0.296, 0.494, 0.591$ , AND  $0.638$ 

FIGURE 31.- COMPARISON OF THE VARIATION OF ROOT BENDING-MOMENT COEFFICIENT WITH NORMAL-FORCE COEFFICIENT AS DETERMINED EXPERIMENTALLY AND BY THE METHOD OF REFERENCE 1. LANDING FLAPS DEFLECTED  $40^\circ$ .



— FROM METHOD OF REFERENCE I.

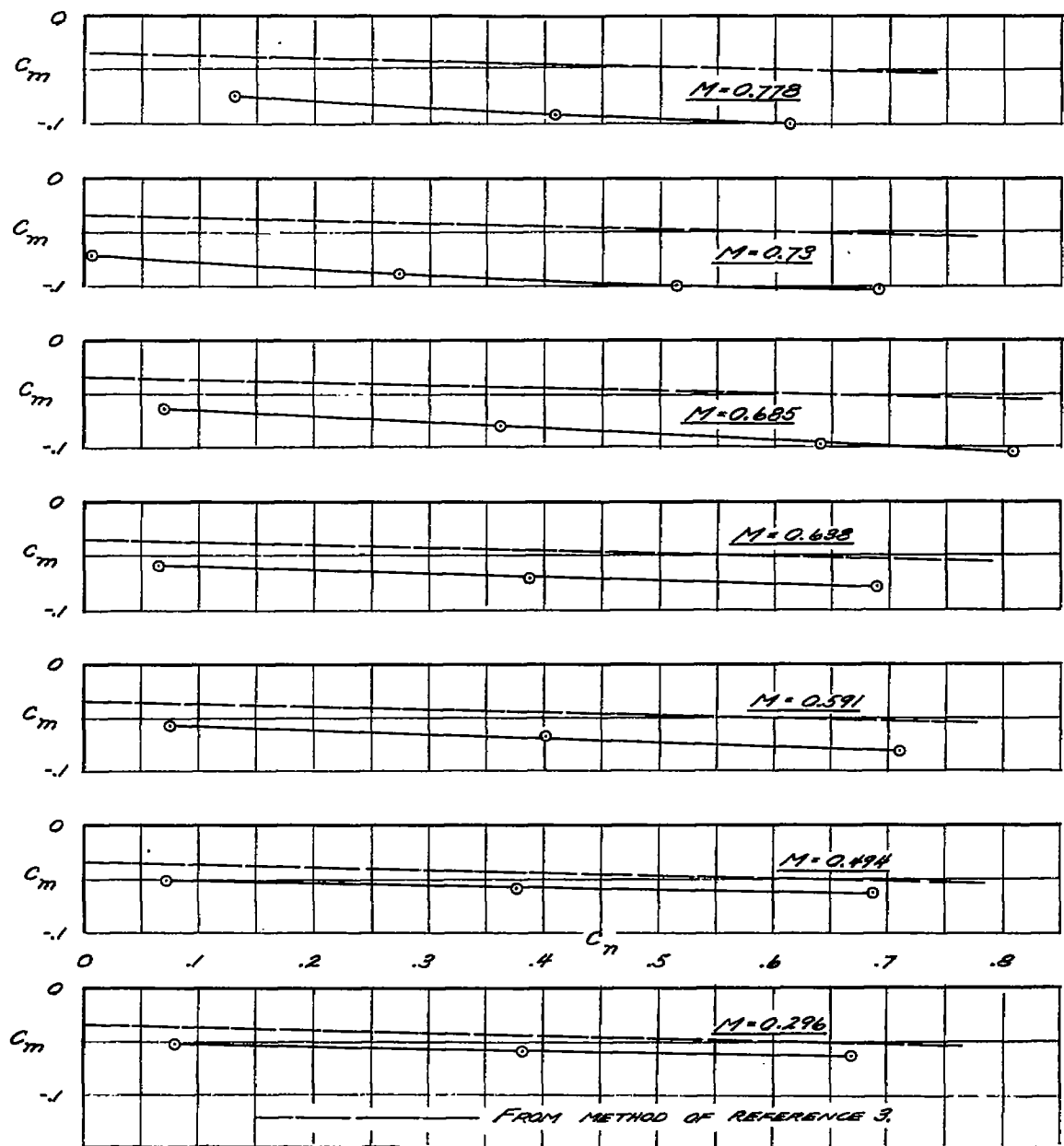
NATIONAL ADVISORY  
COMMITTEE FOR AERONAUTICS

(b)  $M = 0.685, 0.73, \text{ AND } 0.778$

FIGURE 31 .- CONCLUDED

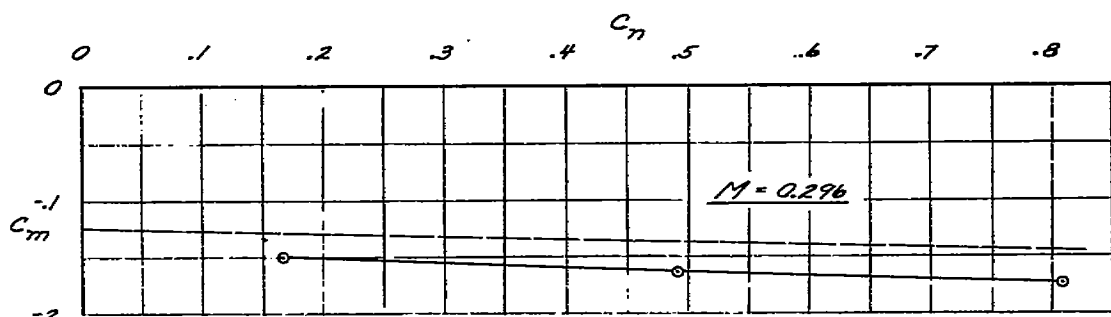
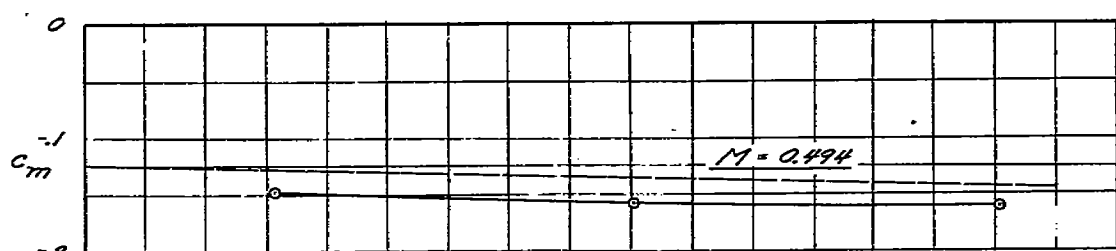
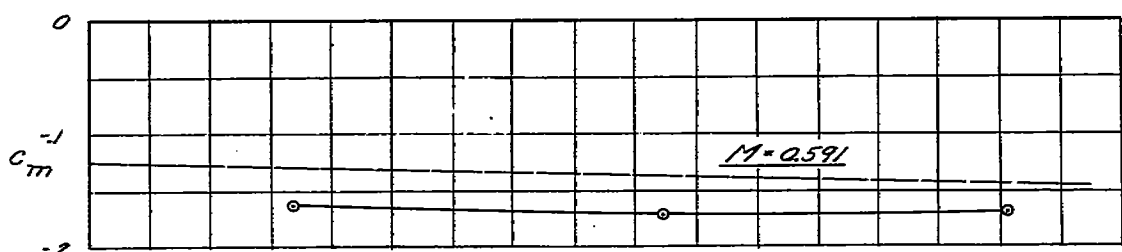
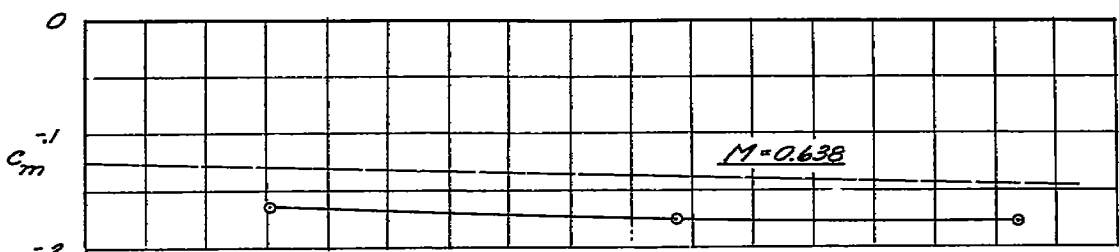
Fig. 32

NACA RM No. A7D23



NATIONAL ADVISORY  
COMMITTEE FOR AERONAUTICS

FIGURE 32.- COMPARISON OF THE VARIATION OF SECTION PITCHING-MOMENT COEFFICIENT WITH SECTION NORMAL-FORCE COEFFICIENT WITH LANDING FLAPS NEUTRAL AS DETERMINED EXPERIMENTALLY AND BY THE METHOD OF REFERENCE 3. STATION 140.000; MOMENT AXIS AT 24.7 PERCENT CHORD.



— — — — — FROM METHOD OF REFERENCE 3.

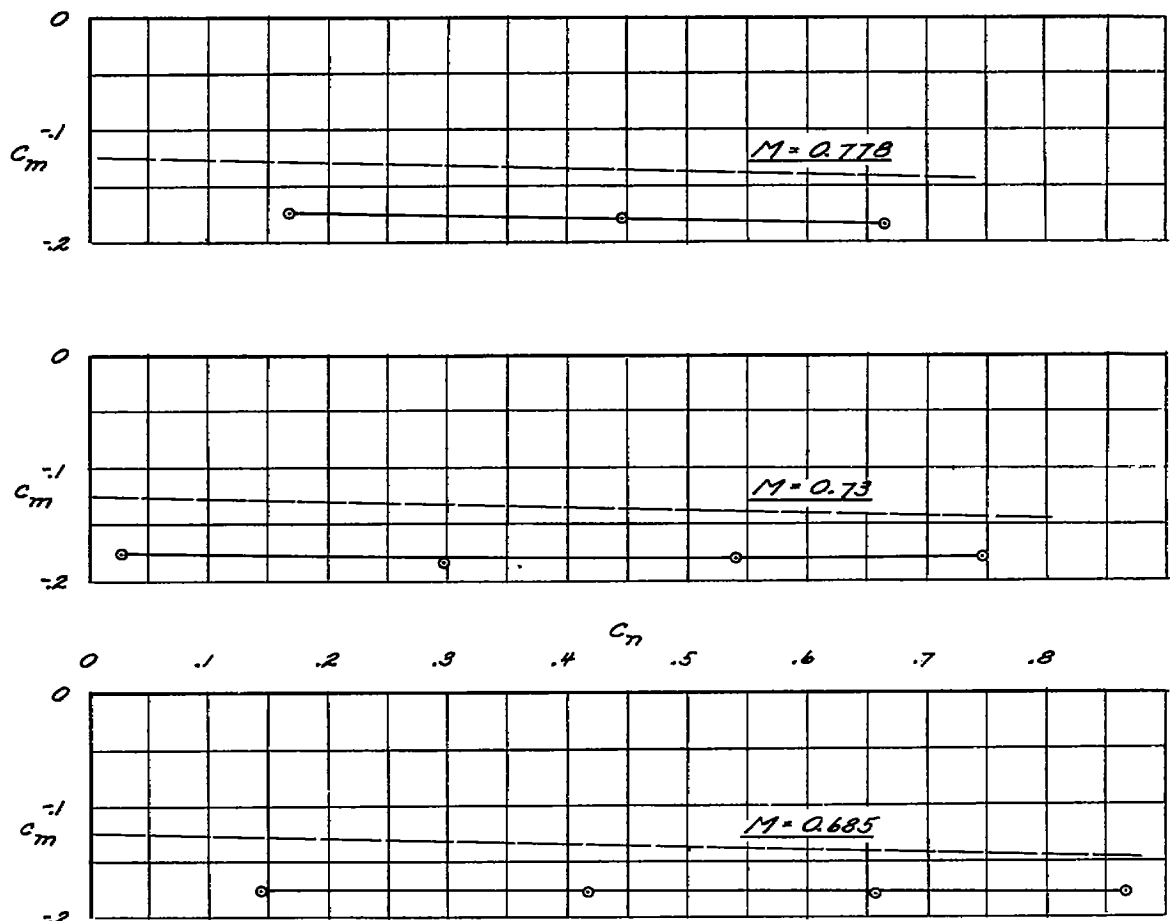
NATIONAL ADVISORY  
COMMITTEE FOR AERONAUTICS

(a)  $M = 0.296, 0.494, 0.591$ , AND  $0.638$

FIGURE 33.— COMPARISON OF THE VARIATION OF SECTION PITCHING-MOMENT COEFFICIENT WITH SECTION NORMAL-FORCE COEFFICIENT FOR A LANDING FLAP DEFLECTION OF  $10^\circ$  AS DETERMINED EXPERIMENTALLY AND BY THE METHOD OF REFERENCE 3. STATION 140.000; MOMENT AXIS AT 24.7 PERCENT CHORD.

Fig. 33b

NACA RM No. A7D23



NATIONAL ADVISORY  
COMMITTEE FOR AERONAUTICS

— — — — — FROM METHOD OF REFERENCE 3.

(b)  $M = 0.685, 0.73,$  AND  $0.778$   
FIGURE 33.— CONCLUDED

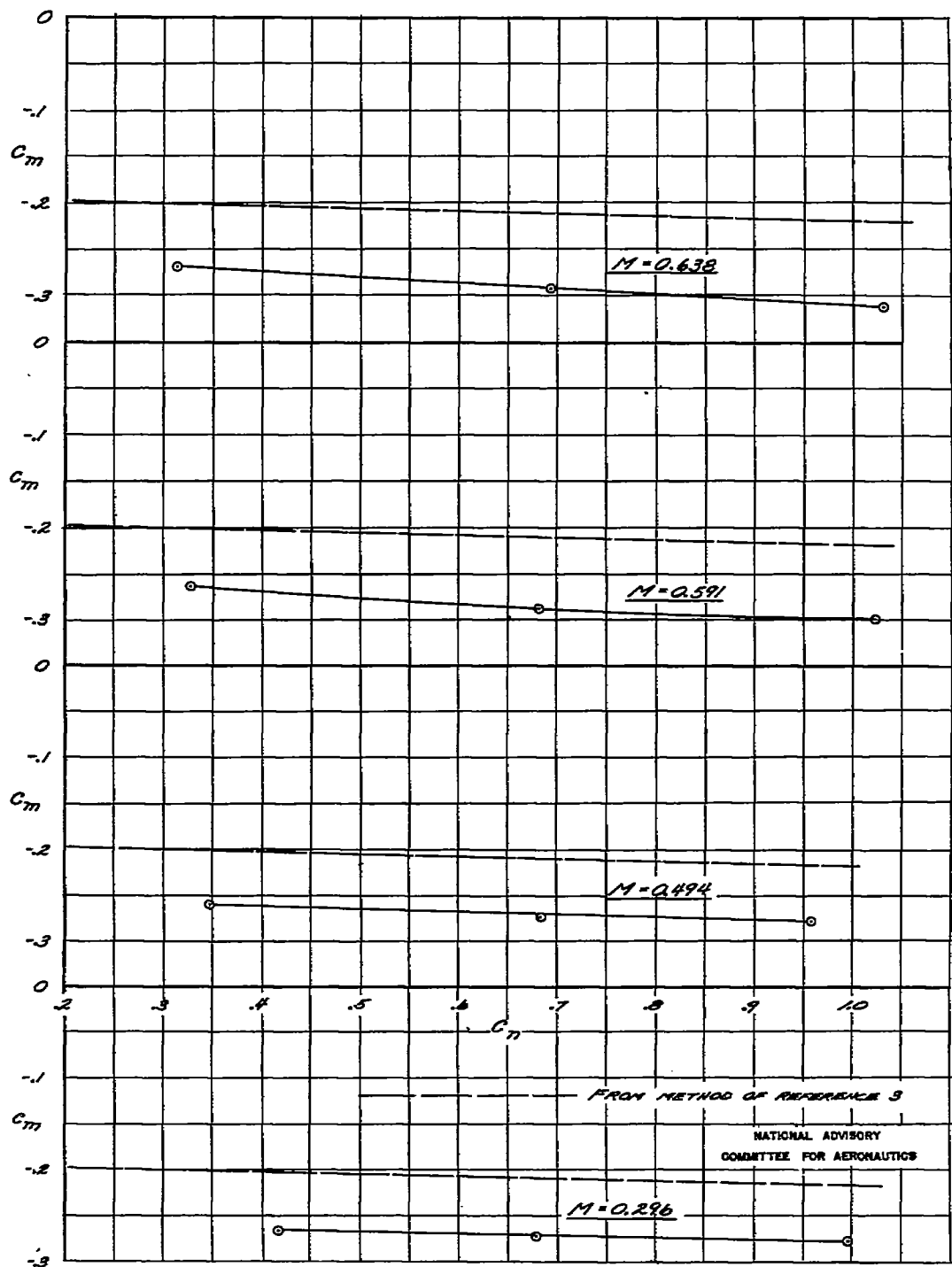
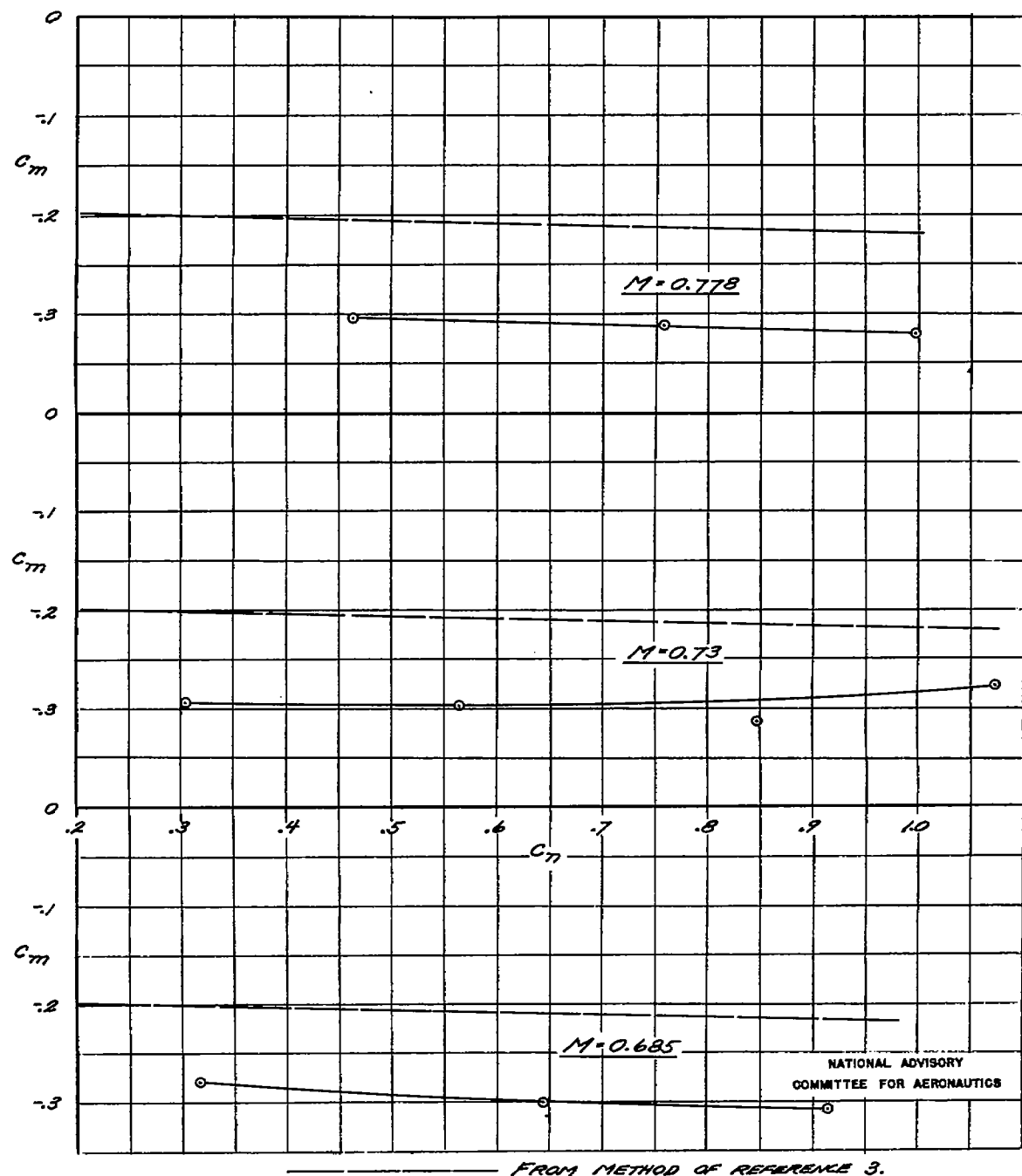


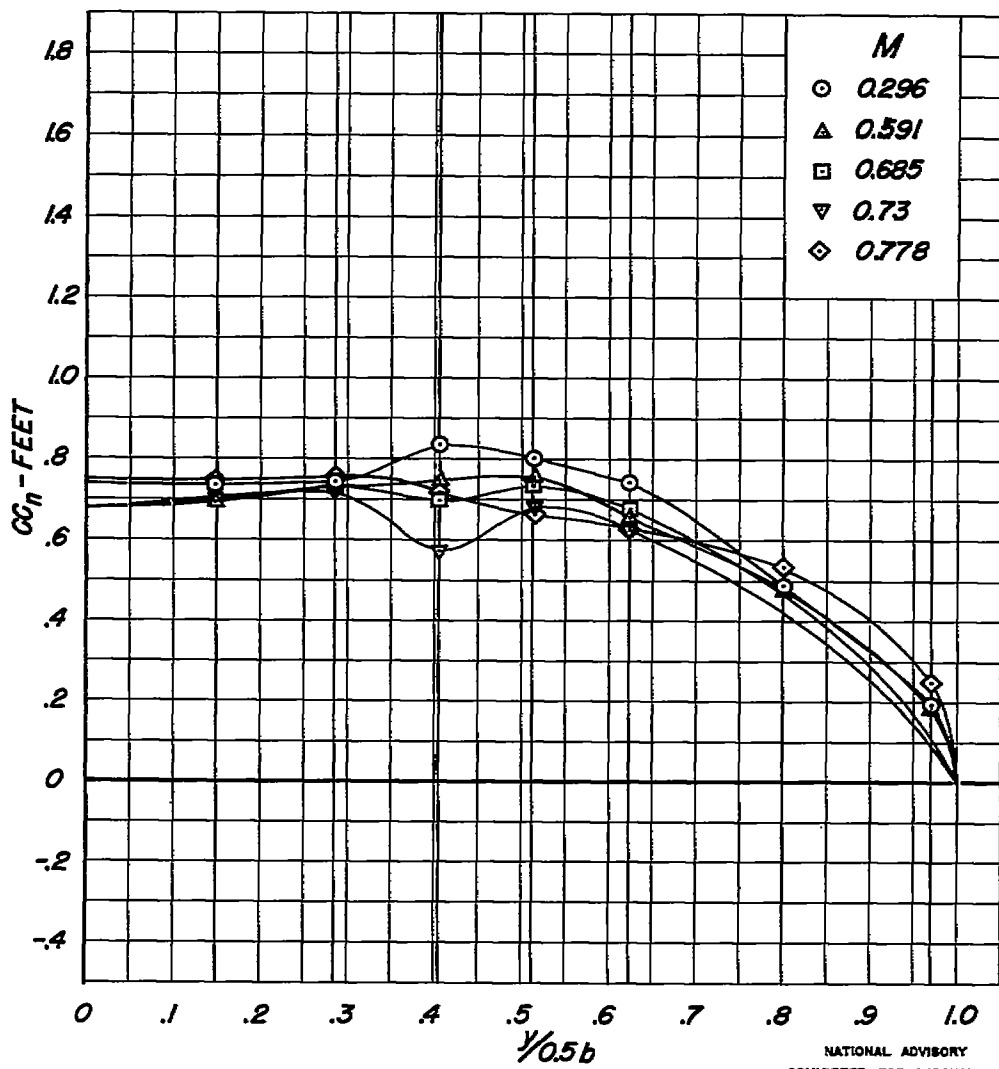
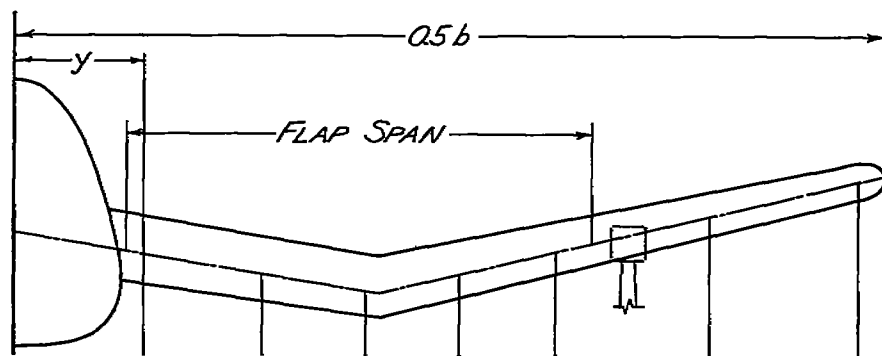
FIGURE 34.-COMPARISON OF THE VARIATION OF SECTION PITCHING-MOMENT COEFFICIENT WITH SECTION NORMAL-FORCE COEFFICIENT FOR A LANDING FLAP DEFLECTION OF  $40^\circ$  AS DETERMINED EXPERIMENTALLY AND BY THE METHOD OF REFERENCE 3. STATION 140,000; MOMENT AXIS AT 24.7 PERCENT CHORD.

Fig. 34b

NACA RM No. A7D23

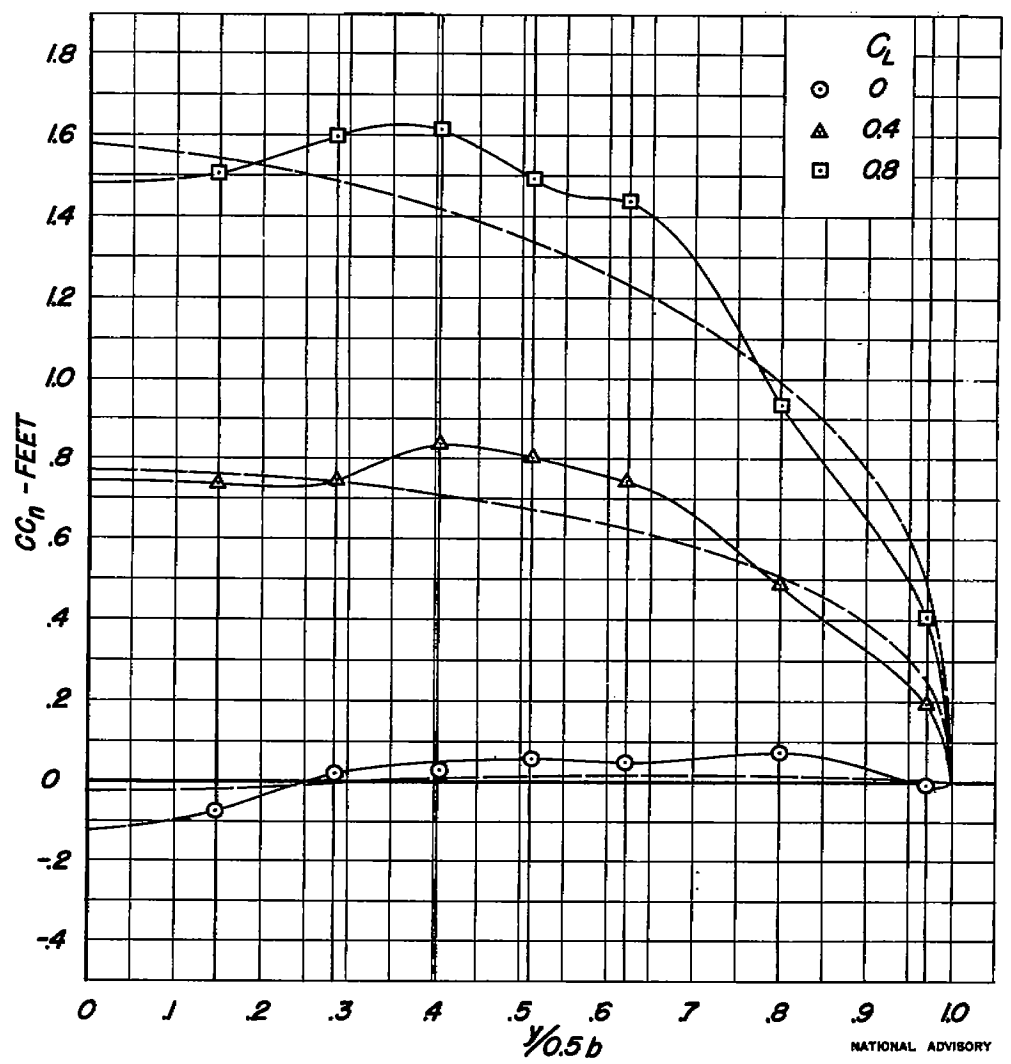
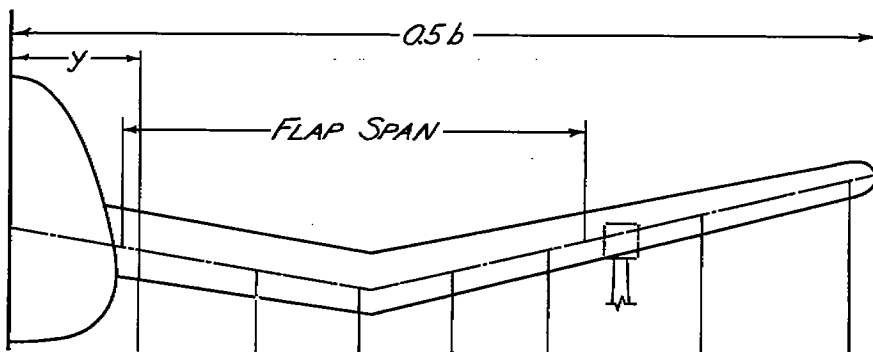


(B)  $M = 0.685, 0.73, \text{ AND } 0.778$   
FIGURE 34. - CONCLUDED.



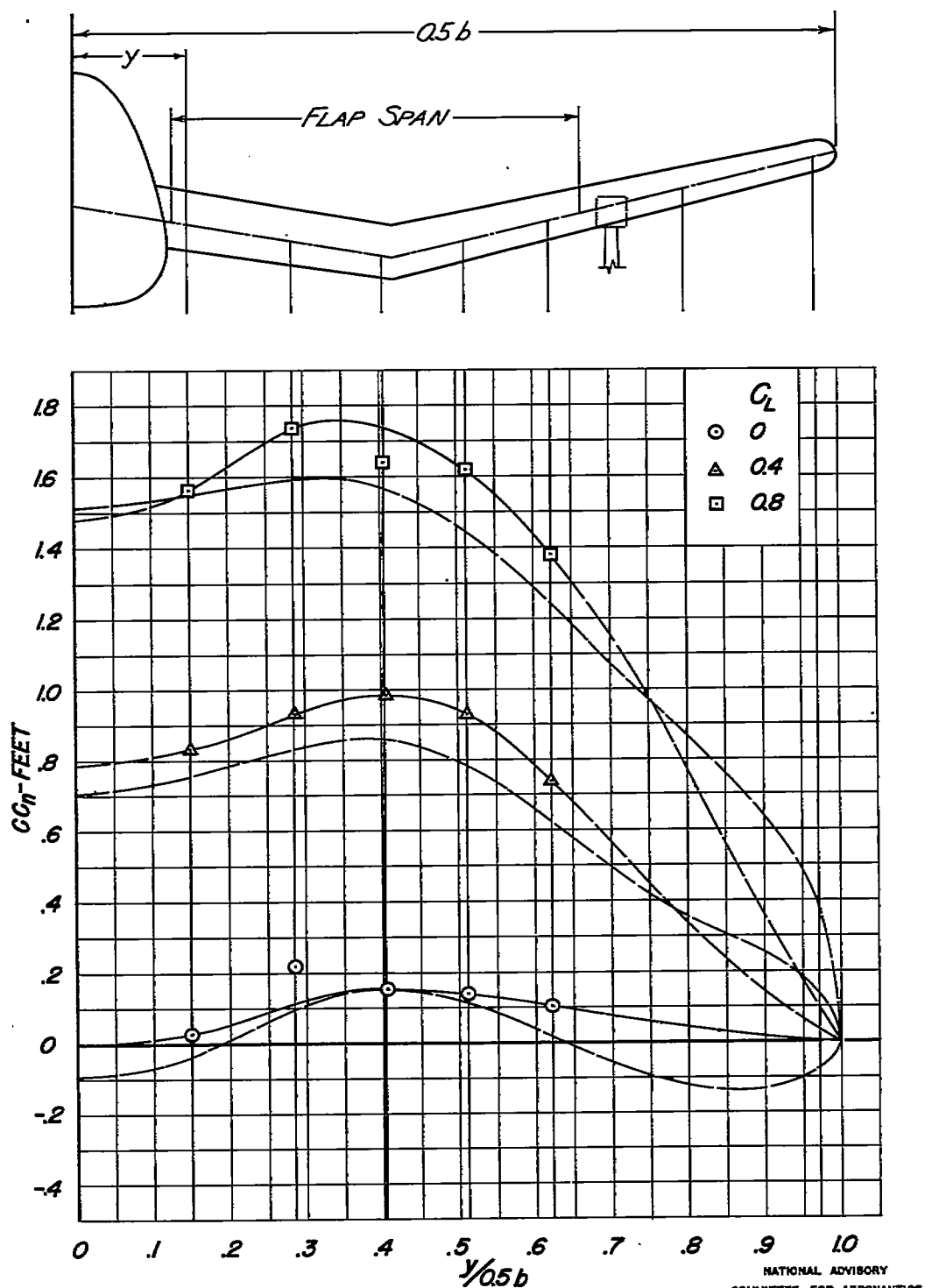
NATIONAL ADVISORY  
COMMITTEE FOR AERONAUTICS

FIGURE 35.—EFFECTS OF MACH NUMBER ON THE SPANWISE  
NORMAL-FORCE DISTRIBUTION WITH FLAPS NEUTRAL.  $C_L = 0.4$



(a) LANDING FLAPS NEUTRAL

FIGURE 36.-COMPARISON OF SPANWISE NORMAL-FORCE DISTRIBUTION AS DETERMINED EXPERIMENTALLY AND BY METHOD OF REFERENCE I.  $M=0.296$

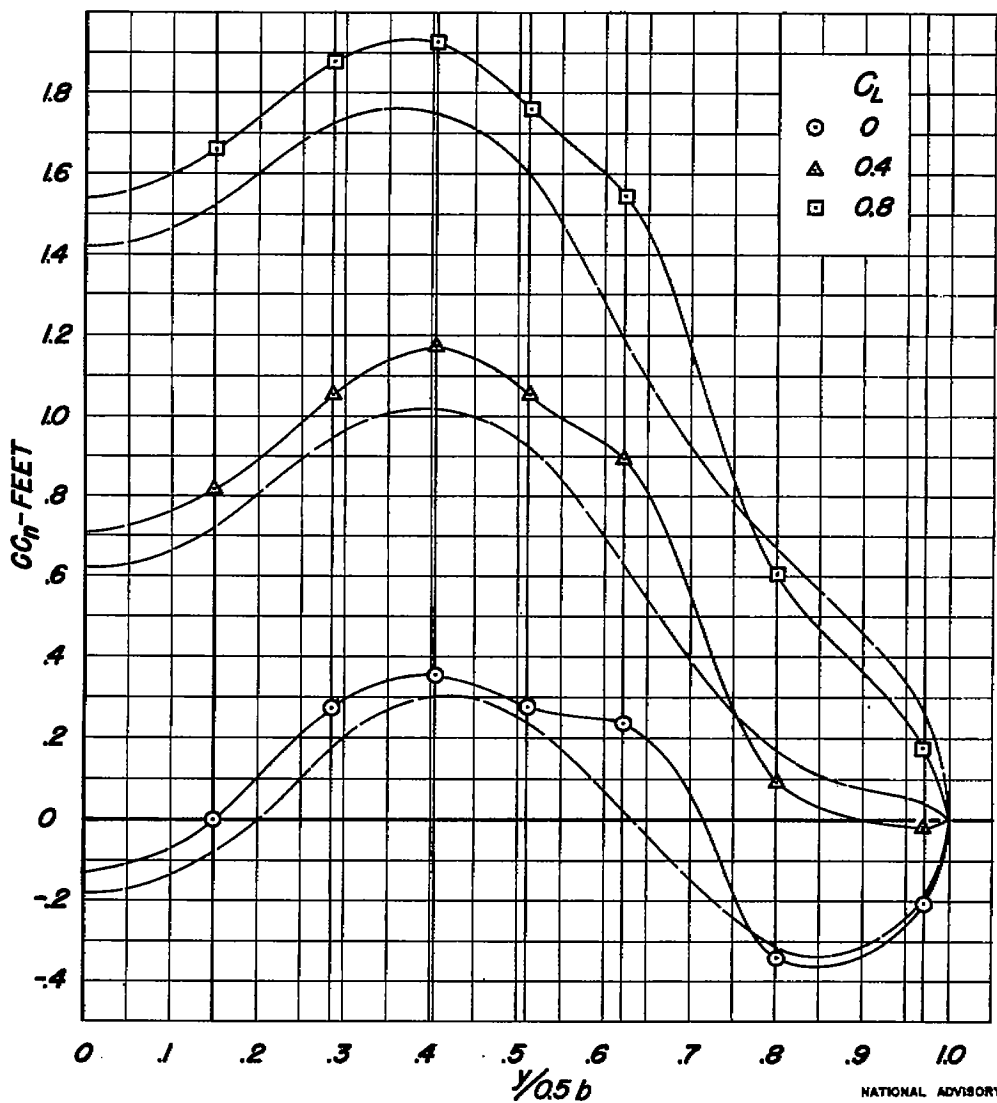
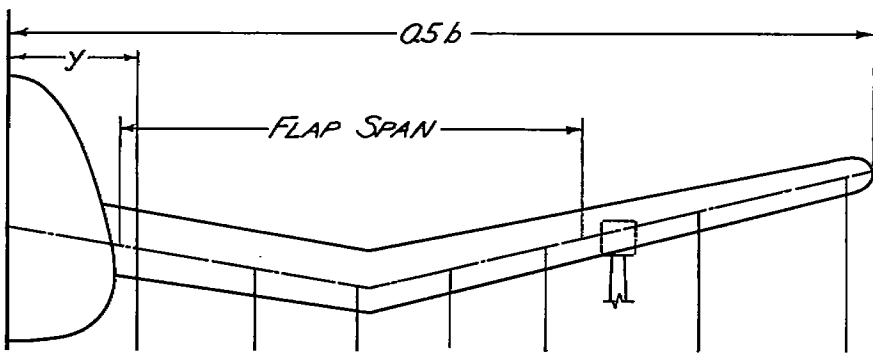


(b) LANDING FLAPS DEFLECTED 10°

FIGURE 36.- CONTINUED.

Fig. 36c

NACA RM No. A7D23

NATIONAL ADVISORY  
COMMITTEE FOR AERONAUTICS

(c) LANDING FLAPS DEFLECTED 40°

FIGURE 36.- CONCLUDED.

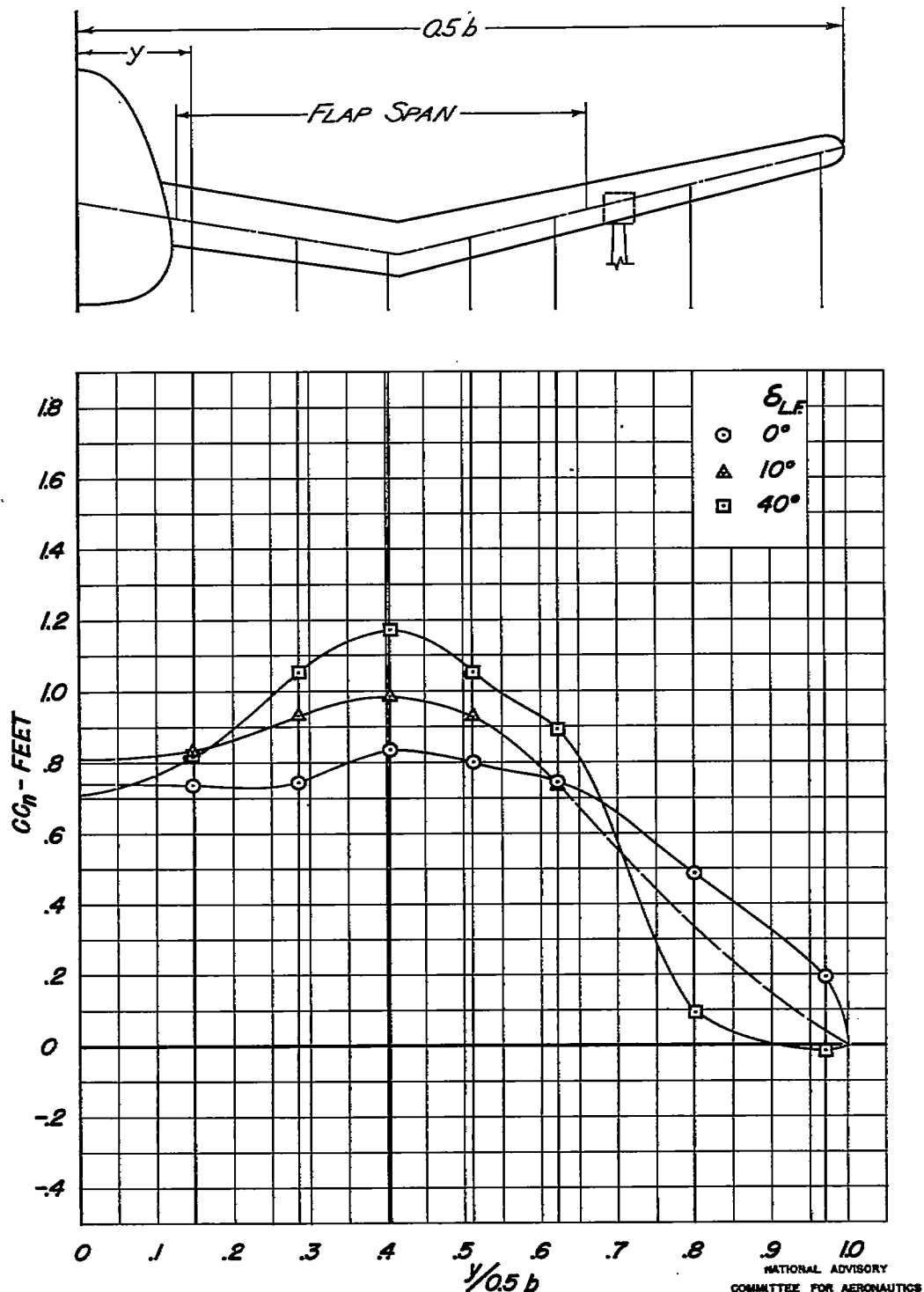


FIGURE 37 - TYPICAL EFFECTS OF LANDING-FLAP DEFLECTION  
ON THE SPANWISE NORMAL-FORCE DISTRIBUTION.  
 $M=0.296$ ;  $C_L=0.4$ .

NASA Technical Library



3 1176 01434 4189

